

TUM-HEP-878/13

TTK-13-04

SFB/CPP-13-15

IFIC/13-05

February 24, 2022

# Non-relativistic pair annihilation of nearly mass degenerate neutralinos and charginos II. P-wave and next-to-next-to-leading order S-wave coefficients

C. HELLMANN<sup>a,b</sup> and P. RUIZ-FEMENÍA<sup>c</sup>

<sup>a</sup>*Physik Department T31,  
James-Franck-Straße, Technische Universität München,  
D-85748 Garching, Germany*

<sup>b</sup>*Institut für Theoretische Teilchenphysik und Kosmologie,  
RWTH Aachen University, D-52056 Aachen, Germany*

<sup>c</sup>*Instituto de Física Corpuscular (IFIC), CSIC-Universitat de València  
Apdo. Correos 22085, E-46071 Valencia, Spain*

## Abstract

This paper is a continuation of an earlier work (arXiv:1210.7928) which computed analytically the tree-level annihilation rates of a collection of non-relativistic neutralino and chargino two-particle states in the general MSSM. Here we extend the results by providing the next-to-next-to-leading order corrections to the rates in the non-relativistic expansion in momenta and mass differences, which include leading  $P$ -wave effects, in analytic form. The results are a necessary input for the calculation of the Sommerfeld-enhanced dark matter annihilation rates including short-distance corrections at next-to-next-to-leading order in the non-relativistic expansion in the general MSSM with neutralino LSP.

# 1 Introduction

The increasing precision on the experimental determination of the dark matter (DM) density, which is expected to be further improved by the data from the PLANCK satellite, has brought a renewed interest in the impact of radiative corrections to the annihilation cross section of dark matter candidates of particle nature. Particles with weak interaction strength and masses around the TeV scale that dropped out of thermal equilibrium in the Early Universe yield the correct order of magnitude for the relic density. An example of the latter is provided by the lightest neutralino of the minimal supersymmetric extension of the standard model (MSSM), perhaps the most promising candidate for such weakly interacting dark matter. The potential to set stringent constraints on the parameter space of the MSSM using the high precision measurements of the dark matter density crucially depends on having an accurate calculation of the neutralino relic abundance.

A necessary input for this calculation is the annihilation cross section of the lightest neutralino, and of all possible co-annihilation processes. While programs exist that provide the tree-level results numerically [1, 2], at the one-loop level such calculations are not available for a generic MSSM model, although they have been performed for some scenarios [3–7], or under certain approximations [8–10].

There is however a certain class of radiative corrections where higher-order loop diagrams contributing to the DM annihilation amplitude are not necessarily suppressed. At the temperatures where freeze-out of the relic particle abundance takes place, the dark matter particles are non-relativistic, with typical velocities of order  $v \sim 0.2c$ . Quantum loop corrections due to the exchange of light particles between the non-relativistic DM particles before annihilation can become more and more important in situations where the force coupling strength is larger than the DM velocity and the mass of the force carrier is much lighter than the DM mass, eventually requiring a resummation of the terms in the perturbative expansion to all loop orders. This phenomenon has been termed as “Sommerfeld effect”, and can lead to a significant enhancement of the DM annihilation rates, also of relevance for the calculation of primary decay spectra in the present Universe. In the MSSM, Sommerfeld corrections may constitute the dominant radiative correction when the lightest neutralino is much heavier than the electroweak gauge bosons and the Yukawa potential generated by their exchange becomes long-range. For such heavy neutralinos mixing effects are suppressed by  $\mathcal{O}(M_Z/m_{\text{LSP}})$  and thus mass degeneracies arise in the neutralino-chargino sector, making necessary to account for co-annihilation processes in the relic density calculation. Two prominent examples of this scenario are the MSSM wino- and Higgsino-limit, for which the impact of the Sommerfeld effect has been extensively studied [11–15].

The tree-level DM annihilation cross section can be expanded in the relative velocity  $v_{\text{rel}}$  of the two annihilating particles ( $v_{\text{rel}} = |\mathbf{v}_1 - \mathbf{v}_2|$ ),

$$\sigma_{\text{ann}} v_{\text{rel}} = a + b v_{\text{rel}}^2 + \mathcal{O}(v_{\text{rel}}^4), \quad (1)$$

for non-relativistic  $v_{\text{rel}}$ . In a previous work [16] (referred to as paper I in the following) the calculation of the leading-order coefficient  $a$  in (1) was presented in analytic form for

the general MSSM with neutralino LSP, including results for all co-annihilation processes with nearly mass-degenerate neutralinos and charginos. In this paper we complete the calculation by providing analytic results for the subleading term in this expansion, the coefficient  $b$ . In the non-relativistic effective theory (EFT) framework devised in paper I, the coefficients  $a$ ,  $b$  account for the short-distance part of the neutralino and chargino pair-annihilation processes and are written as a combination of the absorptive parts of Wilson coefficients of local four-fermion operators. The absorptive part of the EFT matrix element of these four-fermion operators then gives the full neutralino and chargino pair-annihilation rates, including the long-range Sommerfeld effect.

While the leading-order term  $a$  in (1) receives contributions only from  $S$ -wave annihilations, the subleading term  $b$  encodes both  $S$ - and  $P$ -wave annihilation contributions, which we provide separately. This is required for a correct implementation of the Sommerfeld correction factors, that depend on the spin and partial-wave configuration of the annihilating state. In recent literature which addresses the Sommerfeld effect including the  $\mathcal{O}(v_{\text{rel}}^2)$  terms in the annihilation cross section, only the  $P$ -wave contributions to the coefficient  $b$  have been computed approximately using numerical routines at the amplitude level [10], or it has been assumed that  $b$  is entirely  $P$ -wave [17].

The results presented in I (and complemented in this work) also extend those from previous approaches in another relevant aspect. The knowledge of the tree-level annihilation cross section (1) for all nearly mass-degenerate neutralino and chargino two-particle states is not sufficient for the calculation of the Sommerfeld corrected (co-)annihilation rates. As described in paper I, a contribution to the full annihilation rate of an incoming  $\chi_i\chi_j$  state is given by the imaginary part of the amplitude for the process

$$\chi_i\chi_j \rightarrow \dots \rightarrow \chi_{e_1}\chi_{e_2} \rightarrow X_A X_B \rightarrow \chi_{e_4}\chi_{e_3} \rightarrow \dots \rightarrow \chi_i\chi_j, \quad (2)$$

where the transitions among the  $\chi\chi$  states are mediated by long-range potential interactions and the short-distance annihilation into SM and light Higgs particles ( $X_A X_B$ ) involves the two-particle states  $\chi_{e_1}\chi_{e_2}$  and  $\chi_{e_4}\chi_{e_3}$ . The case when  $\chi_{e_1}\chi_{e_2}$  and  $\chi_{e_4}\chi_{e_3}$  are different states corresponds to an off-diagonal short-distance annihilation rate. In our EFT approach the diagonal and the off-diagonal (tree-level) short-distance rates are encoded in the absorptive part of local four-fermion operators' Wilson coefficients, that are obtained from matching the EFT tree-level matrix elements of the four-fermion operators to the absorptive part of the hard (1-loop) MSSM amplitudes for the  $\chi_{e_1}\chi_{e_2} \rightarrow X_A X_B \rightarrow \chi_{e_4}\chi_{e_3}$  scattering reactions. The off-diagonal terms have not been taken into account in the Sommerfeld-enhanced neutralino relic abundance calculations aside from the wino- and Higgsino-limits [11–13, 15], and their implementation using the numerical packages that provide the tree-level annihilation rates has not yet been attempted. In contrast, the analytic results presented in this work allow for a systematic treatment of all diagonal and off-diagonal short-distance annihilation rates at next-to-next-to-leading order in the non-relativistic expansion in Sommerfeld-enhanced annihilation reactions.

The contents of this paper are the following: In Sec. 2 we briefly review the effective Lagrangian framework introduced in paper I and recollect the essential notation. We then introduce the dimension-8 four-fermion operators that encode the next-to-next-to-

leading non-relativistic corrections to the short-distance annihilation of neutralino and chargino particle pairs. As for the case of the (leading-order) dimension-6 operators discussed in paper I, the analytic results for the absorptive part of the Wilson coefficients can be obtained as the product of kinematic and coupling factors. In the Appendix A we recall the master formula to write down the Wilson coefficients and the rules for its implementation. While we rely on paper I for the extraction of coupling factors also for the Wilson coefficients presented in this work, explicit expressions for the  $P$ -wave kinematic factors are given in the Appendix A. The expressions for the (rather lengthy) next-to-next-to-leading  $S$ -wave Wilson coefficients are collected in a `Mathematica` package attached to this paper [18], which also includes the  $P$ -wave kinematic factors and those from the leading-order operators that were written explicitly in the appendix of paper I. Appendix B explains the notation used in this electronic supplement. In Sec. 3 we generalise the formula for the tree-level annihilation rates to the case of off-diagonal annihilation processes, which is needed in order to analyse the size of next-to-next-to-leading corrections in an off-diagonal transition used as a case example in Sec. 4. Apart from the latter, Sec. 4 also discusses three selected (diagonal) processes where the role of the next-to-next-to-leading corrections from our analytic calculation of the annihilation cross section is markedly different. Through these examples we illustrate the importance of separating the different partial-wave contributions to the short-distance annihilation for the computation of the Sommerfeld-corrected cross sections. Our results for the diagonal annihilation rates for these examples are checked against the corresponding unexpanded cross sections computed with a numerical code. To serve as an example of how to use the results presented in this work, we have included in Appendix C a step-by-step calculation of the non-relativistic  $\chi_1^+ \chi_1^- \rightarrow W^+ W^-$  annihilation cross section including up to  $\mathcal{O}(v_{\text{rel}}^2)$  effects for the case of pure-wino neutralino dark matter. Analytic results for the Wilson coefficients needed to determine the exclusive (off-)diagonal (co-)annihilation rates  $\chi_{e_1} \chi_{e_2} \rightarrow X_A X_B \rightarrow \chi_{e_4} \chi_{e_3}$  in the decoupling limit of the pure-wino scenario are also provided in that appendix. Finally, we summarise our findings in Sec. 5.

## 2 Basis of the dimension-8 operators in $\delta\mathcal{L}_{\text{ann}}$

The non-relativistic MSSM (NRMSSM) effective theory set-up of paper I is built out of  $n_0 \leq 4$  nearly on-shell non-relativistic neutralino ( $\chi_i^0, i = 1, \dots, n_0$ ) and  $n_+ \leq 2$  nearly on-shell non-relativistic chargino ( $\chi_j^\pm, j = 1, \dots, n_+$ ) modes whose masses are nearly degenerate with the mass  $m_{\text{LSP}}$  of the lightest neutralino  $\chi_1^0$ . As pair-annihilation reactions of these neutralino and chargino species into (not non-relativistic) SM and light Higgs-particle final states take place at distances of the order  $\mathcal{O}(1/m_{\text{LSP}})$ , much smaller than the characteristic range of potential interactions between the incoming  $\chi\chi$  two-particle states, we can incorporate the actual annihilation rates in the effective theory through the absorptive part of Wilson coefficients of local four-fermion operators ( $\delta\mathcal{L}_{\text{ann}}$ ), in analogy to the treatment of quarkonium annihilation in NRQCD [19]. In contrast to the  $Q\bar{Q}$  case, here the long-range potential interactions can lead to transitions

among different two-particle states before the short-distance annihilation takes place: the initially incoming  $\chi_i\chi_j$  particle pair can scatter to any accessible (nearly on-shell)  $\chi_{e_a}\chi_{e_b}$  particle pair prior to the annihilation into SM and light Higgs two-particle final states  $X_AX_B$ . Therefore we have to account for absorptive parts of generic  $\chi_{e_1}\chi_{e_2} \rightarrow X_AX_B \rightarrow \chi_{e_4}\chi_{e_3}$  amplitudes, where  $\chi_{e_1}\chi_{e_2}$  and  $\chi_{e_4}\chi_{e_3}$  can be different states (see Fig. 1 in paper I).

At  $\mathcal{O}(\alpha_2^2)$ , where  $\alpha_2 = g_2^2/4\pi$  with  $g_2$  the  $SU(2)_L$  gauge coupling in the MSSM, the absorptive part of the four-fermion operators' Wilson coefficients are obtained by matching the absorptive part of  $\chi_{e_1}\chi_{e_2} \rightarrow \chi_{e_4}\chi_{e_3}$  1-loop scattering amplitudes evaluated in the MSSM with the tree-level matrix element of four-fermion operators contained in  $\delta\mathcal{L}_{\text{ann}}$  in the effective theory. At the 1-loop level, the contribution to the absorptive part from every individual final state  $X_AX_B$  is free from infrared divergences, and can be given separately. At higher orders the absorptive part of the Wilson coefficients refers to the inclusive case, *i.e.* summed over all accessible final states.

The leading-order contributions to  $\delta\mathcal{L}_{\text{ann}}$  are given by dimension-6 four-fermion operators, encoding leading-order  $S$ -wave scattering reactions. The corresponding operators have been given in paper I. At next-to-next-to-leading order in the non-relativistic expansion in momenta and mass differences, dimension-8 four-fermion operators contribute.<sup>1</sup> Here we adopt the same notation used for  $\delta\mathcal{L}_{\text{ann}}^{d=6}$  in I in order to write the dimension-8 four-fermion operators in  $\delta\mathcal{L}_{\text{ann}}^{d=8}$  as

$$\begin{aligned} \delta\mathcal{L}_{\text{ann}}^{d=8} = & \sum_{\chi\chi \rightarrow \chi\chi} \frac{1}{4M^2} f_{\{e_1e_2\}\{e_4e_3\}}^{\chi\chi \rightarrow \chi\chi} (^1P_1) \mathcal{O}_{\{e_4e_3\}\{e_2e_1\}}^{\chi\chi \rightarrow \chi\chi} (^1P_1) \\ & + \sum_{\chi\chi \rightarrow \chi\chi} \sum_{J=0,1,2} \frac{1}{4M^2} f_{\{e_1e_2\}\{e_4e_3\}}^{\chi\chi \rightarrow \chi\chi} (^3P_J) \mathcal{O}_{\{e_4e_3\}\{e_2e_1\}}^{\chi\chi \rightarrow \chi\chi} (^3P_J) \\ & + \sum_{\chi\chi \rightarrow \chi\chi} \sum_{s=0,1} \frac{1}{4M^2} g_{\{e_1e_2\}\{e_4e_3\}}^{\chi\chi \rightarrow \chi\chi} (^{2s+1}S_s) \mathcal{P}_{\{e_4e_3\}\{e_2e_1\}}^{\chi\chi \rightarrow \chi\chi} (^{2s+1}S_s) \\ & + \sum_{\chi\chi \rightarrow \chi\chi} \sum_{s=0,1} \sum_{i=1,2} \frac{1}{4M^2} h_{i\{e_1e_2\}\{e_4e_3\}}^{\chi\chi \rightarrow \chi\chi} (^{2s+1}S_s) \mathcal{Q}_{i\{e_4e_3\}\{e_2e_1\}}^{\chi\chi \rightarrow \chi\chi} (^{2s+1}S_s) . \quad (3) \end{aligned}$$

The label  $\chi\chi \rightarrow \chi\chi$  stands for all (off-)diagonal non-relativistic scattering processes among neutralino and chargino two-particle states. Neutral reactions involve  $\chi^0\chi^0$  and  $\chi^-\chi^+$  states, while singly-charged and doubly-charged processes include  $\chi^0\chi^\pm$  and  $\chi^\pm\chi^\pm$  states, respectively. The  $f_{\{e_1e_2\}\{e_4e_3\}}^{\chi\chi \rightarrow \chi\chi}$ ,  $g_{\{e_1e_2\}\{e_4e_3\}}^{\chi\chi \rightarrow \chi\chi}$  and  $h_{i\{e_1e_2\}\{e_4e_3\}}^{\chi\chi \rightarrow \chi\chi}$  in (3) denote the Wilson coefficients of the corresponding four-fermion operators  $\mathcal{O}_{\{e_4e_3\}\{e_2e_1\}}$ ,  $\mathcal{P}_{\{e_4e_3\}\{e_2e_1\}}$  and  $\mathcal{Q}_{i\{e_4e_3\}\{e_2e_1\}}$ , whose explicit form for the case of  $\chi_{e_1}^0\chi_{e_2}^0 \rightarrow \chi_{e_4}^0\chi_{e_3}^0$  scattering reactions

---

<sup>1</sup>Let us remark that we do not consider next-to-leading order contributions to  $\delta\mathcal{L}_{\text{ann}}$ , corresponding to dimension-7 four-fermion operators, as these encode  $^1S_0 - ^3P_0$ ,  $^3S_1 - ^1P_1$  and  $^3S_1 - ^3P_1$  transitions which will require the addition of  $v_{\text{rel}}$ -suppressed potential interactions in the long-range part of the annihilation (we consider only  $\mathcal{O}(v_{\text{rel}}^2)$  effects from the short-distance annihilation, and not those arising from sub-leading non-Coulomb (non-Yukawa) potentials, in consistency with paper I).

$\mathcal{O}^{\chi\chi\rightarrow\chi\chi}(^1P_1)$	$\xi_{e_4}^\dagger \left(-\frac{i}{2} \overleftrightarrow{\partial}\right) \xi_{e_3}^c \cdot \xi_{e_2}^{c\dagger} \left(-\frac{i}{2} \overleftrightarrow{\partial}\right) \xi_{e_1}$
$\mathcal{O}^{\chi\chi\rightarrow\chi\chi}(^3P_0)$	$\frac{1}{3} \xi_{e_4}^\dagger \left(-\frac{i}{2} \overleftrightarrow{\partial} \cdot \boldsymbol{\sigma}\right) \xi_{e_3}^c \cdot \xi_{e_2}^{c\dagger} \left(-\frac{i}{2} \overleftrightarrow{\partial} \cdot \boldsymbol{\sigma}\right) \xi_{e_1}$
$\mathcal{O}^{\chi\chi\rightarrow\chi\chi}(^3P_1)$	$\frac{1}{2} \xi_{e_4}^\dagger \left(-\frac{i}{2} \overleftrightarrow{\partial} \times \boldsymbol{\sigma}\right) \xi_{e_3}^c \cdot \xi_{e_2}^{c\dagger} \left(-\frac{i}{2} \overleftrightarrow{\partial} \times \boldsymbol{\sigma}\right) \xi_{e_1}$
$\mathcal{O}^{\chi\chi\rightarrow\chi\chi}(^3P_2)$	$\xi_{e_4}^\dagger \left(-\frac{i}{2} \overleftrightarrow{\partial}^{(i}\boldsymbol{\sigma}^{j)}\right) \xi_{e_3}^c \cdot \xi_{e_2}^{c\dagger} \left(-\frac{i}{2} \overleftrightarrow{\partial}^{(i}\boldsymbol{\sigma}^{j)}\right) \xi_{e_1}$
$\mathcal{P}^{\chi\chi\rightarrow\chi\chi}(^1S_0)$	$\frac{1}{2} \left[ \xi_{e_4}^\dagger \xi_{e_3}^c \cdot \xi_{e_2}^{c\dagger} \left(-\frac{i}{2} \overleftrightarrow{\partial}\right)^2 \xi_{e_1} + \xi_{e_4}^\dagger \left(-\frac{i}{2} \overleftrightarrow{\partial}\right)^2 \xi_{e_3}^c \cdot \xi_{e_2}^{c\dagger} \xi_{e_1} \right]$
$\mathcal{P}^{\chi\chi\rightarrow\chi\chi}(^3S_1)$	$\frac{1}{2} \left[ \xi_{e_4}^\dagger \boldsymbol{\sigma} \xi_{e_3}^c \cdot \xi_{e_2}^{c\dagger} \boldsymbol{\sigma} \left(-\frac{i}{2} \overleftrightarrow{\partial}\right)^2 \xi_{e_1} + \xi_{e_4}^\dagger \boldsymbol{\sigma} \left(-\frac{i}{2} \overleftrightarrow{\partial}\right)^2 \xi_{e_3}^c \cdot \xi_{e_2}^{c\dagger} \boldsymbol{\sigma} \xi_{e_1} \right]$
$\mathcal{Q}_1^{\chi\chi\rightarrow\chi\chi}(^1S_0)$	$(\delta m M) \xi_{e_4}^\dagger \xi_{e_3}^c \cdot \xi_{e_2}^{c\dagger} \xi_{e_1}$
$\mathcal{Q}_1^{\chi\chi\rightarrow\chi\chi}(^3S_1)$	$(\delta m M) \xi_{e_4}^\dagger \boldsymbol{\sigma} \xi_{e_3}^c \cdot \xi_{e_2}^{c\dagger} \boldsymbol{\sigma} \xi_{e_1}$
$\mathcal{Q}_2^{\chi\chi\rightarrow\chi\chi}(^1S_0)$	$(\delta \overline{m} M) \xi_{e_4}^\dagger \xi_{e_3}^c \cdot \xi_{e_2}^{c\dagger} \xi_{e_1}$
$\mathcal{Q}_2^{\chi\chi\rightarrow\chi\chi}(^3S_1)$	$(\delta \overline{m} M) \xi_{e_4}^\dagger \boldsymbol{\sigma} \xi_{e_3}^c \cdot \xi_{e_2}^{c\dagger} \boldsymbol{\sigma} \xi_{e_1}$

Table 1: Explicit form of the  $P$ -wave ( $\mathcal{O}$ ) and next-to-next-to-leading order  $S$ -wave ( $\mathcal{P}$ ,  $\mathcal{Q}_i$ ) four-fermion operators contributing to  $\chi_{e_1}^0 \chi_{e_2}^0 \rightarrow \chi_{e_4}^0 \chi_{e_3}^0$  scattering reactions. Each index  $e_i$  can take the values  $e_i = 1, \dots, n_0$ . The  $P$ - and next-to-next-to-leading order  $S$ -wave four-fermion operators for the remaining neutral, charged and double-charged  $\chi_{e_1} \chi_{e_2} \rightarrow \chi_{e_4} \chi_{e_3}$  processes are obtained by replacing the field operators  $\xi_{e_i}$ ,  $i = 1, \dots, 4$  above by those of the respective particle species involved. The quantity  $\overleftrightarrow{\partial}$  is a 3-vector whose components are  $\partial^i \equiv \partial/\partial x_i$ . The action of  $\overleftrightarrow{\partial}$  on the two field operators at its left and right is defined as  $\xi_{e_b}^{c\dagger} \overleftrightarrow{\partial} \xi_{e_a} \equiv \xi_{e_b}^{c\dagger} (\partial \xi_{e_a}^c) - (\partial \xi_{e_b}^c)^\dagger \xi_{e_a}$ . The symmetric traceless components of a tensor  $T^{ij}$  are denoted by  $T^{(ij)} = (T^{ij} + T^{ji})/2 - T^{kk} \delta^{ij}/3$ . Finally, the mass scale  $M$  is defined in (4) and the mass differences  $\delta m, \delta \overline{m}$  are given in (5).

is given in Tab. 1.<sup>2</sup> The labels  $e_i$  in (3) range over  $e_i = 1, \dots, n_0$  ( $e_i = 1, \dots, n_+$ ), if the respective field  $\chi_{e_i}$  in the  $\chi_{e_1} \chi_{e_2} \rightarrow \chi_{e_4} \chi_{e_3}$  reaction refers to neutralino- (chargino-) species. The factor  $1/4$  in front of the operators in (3) is a convenient normalisation of transitions matrix elements in the effective theory. In addition, a normalisation factor of  $1/M^2$  has been factored out in (3), such that the next-to-next-to-leading order Wilson coefficients have the same mass-dimension ( $-2$ ) as the leading-order ones presented in I. The mass scale  $M$  is equal to half the sum of the masses of the  $\chi_{e_i}$  particles involved

<sup>2</sup>In order to ensure the  $U(1)_{\text{em}}$  gauge invariance of the NRMSSM, all derivatives  $\partial$  in dimension-8 four-fermion operators  $\mathcal{O}$  and  $\mathcal{P}$  that act on chargino fields ( $\eta_i, \zeta_i$ ) have to be replaced by the corresponding covariant derivative  $\mathbf{D} = \partial + i e \mathbf{A}$ , where  $\mathbf{A}$  denotes the spatial components of the photon field  $A^\mu$ .

in the reaction  $\chi_{e_1}\chi_{e_2} \rightarrow \chi_{e_4}\chi_{e_3}$ , *i.e.*

$$M = \frac{1}{2} \sum_{i=1}^4 m_{e_i}, \quad (4)$$

such that  $M$  itself constitutes a process specific quantity. The quantum numbers  $^{2s+1}L_J$  of the operators in  $\delta\mathcal{L}_{\text{ann}}^{d=8}$  correspond to the angular-momentum configuration of the annihilating two-particle state. Note that the operators  $\mathcal{Q}_i(^{2s+1}S_s)$  have the same structure as the dimension-6 operators  $\mathcal{O}(^{2s+1}S_s)$  defined in paper I, but are proportional to the mass differences

$$\delta m = \frac{m_{e_4} - m_{e_1}}{2}, \quad \delta \bar{m} = \frac{m_{e_3} - m_{e_2}}{2}, \quad (5)$$

computed from the masses  $m_{e_i}$  in the reaction  $\chi_{e_1}\chi_{e_2} \rightarrow \chi_{e_4}\chi_{e_3}$ . The mass differences (5) have to be considered as  $\mathcal{O}(v_{\text{rel}}^2)$  effects in the expansion of the amplitudes according to the discussion given in Sec. 2.4 in I. Since  $\delta m = \delta \bar{m} = 0$  for diagonal annihilation reactions  $\chi_{e_1}\chi_{e_2} \rightarrow \chi_{e_1}\chi_{e_2}$  (where the absorptive parts of the respective amplitudes are related to the corresponding annihilation cross section), the  $\mathcal{Q}_i(^{2s+1}S_s)$  are only relevant for the computation of the off-diagonal rates.

We note that dimension-8 operators  $\mathcal{P}(^3S_1, ^3D_1)$ , which describe  $^3S_1 \rightarrow ^3D_1$  transitions, have not been included in  $\delta\mathcal{L}_{\text{ann}}^{d=8}$ . In the calculation of the tree-level annihilation cross section in the centre-of-mass frame, contributions from these operators vanish, while for the Sommerfeld enhanced annihilation cross section they will require to consider a  $v_{\text{rel}}^2$ -suppressed potential interaction in the long-range part of the annihilation in order to compensate for the change in orbital angular momentum in the short-distance part, thus yielding a contribution to the cross section of  $\mathcal{O}(v_{\text{rel}}^4)$ .

As already discussed in I, we construct  $\delta\mathcal{L}_{\text{ann}}$  in such a way that it contains all redundant operators, which arise through interchanging the single-particle field-operators at the first and second (third and fourth) position given a specific four-fermion operator, such that several operators describe one specific scattering reaction with a  $\chi_{e_1}$  and  $\chi_{e_2}$  ( $\chi_{e_4}$  and  $\chi_{e_3}$ ) particle in the initial (final) state. The respective Wilson coefficients reflect the redundancy in symmetry relations under the exchange of the respective particle labels. Generalising from the leading-order  $S$ -wave relations given in Eq. (8)<sup>3</sup> in I, the relations read in case of Wilson coefficients associated with operators  $\mathcal{O}$  and  $\mathcal{P}$  in (3)

$$\begin{aligned} k_{\{e_2e_1\}\{e_4e_3\}}^{\chi_{e_2}\chi_{e_1} \rightarrow \chi_{e_4}\chi_{e_3}}(^{2s+1}L_J) &= (-1)^{s+L} k_{\{e_1e_2\}\{e_4e_3\}}^{\chi_{e_1}\chi_{e_2} \rightarrow \chi_{e_4}\chi_{e_3}}(^{2s+1}L_J), \\ k_{\{e_1e_2\}\{e_3e_4\}}^{\chi_{e_1}\chi_{e_2} \rightarrow \chi_{e_3}\chi_{e_4}}(^{2s+1}L_J) &= (-1)^{s+L} k_{\{e_1e_2\}\{e_4e_3\}}^{\chi_{e_1}\chi_{e_2} \rightarrow \chi_{e_4}\chi_{e_3}}(^{2s+1}L_J), \end{aligned} \quad (6)$$

where  $k = f, g$  for  $P$ - and next-to-next-to-leading order  $S$ -wave coefficients, respectively. Finally note, that the hermiticity property of the non-relativistic Lagrangian leads to the relation

$$k_{\{e_1e_2\}\{e_4e_3\}}^{\chi\chi \rightarrow \chi\chi}(^{2s+1}L_J) = \left[ k_{\{e_4e_3\}\{e_1e_2\}}^{\chi\chi \rightarrow \chi\chi}(^{2s+1}L_J) \right]^* \quad (7)$$

---

<sup>3</sup>The equation numbers from paper I, Ref. [16], always refer to the arXiv version.



for Wilson-coefficients  $k = f, g$  associated with the  $P$ - and next-to-next-to-leading order  $S$ -wave operators  $\mathcal{O}$  and  $\mathcal{P}$ , in analogy to the respective relation given in Eq. (13) in I. Similar relations as (6, 7) above apply for the Wilson coefficients  $h_i$ , where however an additional exchange of the particles in the definition of the mass differences  $\delta m, \delta \overline{m}$  in front of the corresponding operators  $\mathcal{Q}_i$  has to be taken into account.

### 3 (Off-)diagonal annihilation rates $\Gamma^{\chi_{e_1}\chi_{e_2} \rightarrow X_A X_B \rightarrow \chi_{e_4}\chi_{e_3}}$

In order to assess the importance of the non-relativistic corrections computed in this work, we shall compare in Sec. 4 the EFT and full results for the tree-level annihilation rates for some selected processes. To extend this analysis to the case of off-diagonal annihilation rates, we generalise the definition of the rates in the following way. We define the centre-of-mass frame tree-level annihilation rate  $\Gamma$  associated with the (off-)diagonal  $\chi_{e_1}\chi_{e_2} \rightarrow X_A X_B \rightarrow \chi_{e_4}\chi_{e_3}$  scattering reaction as the product of the  $\chi_{e_1}\chi_{e_2} \rightarrow X_A X_B$  tree-level annihilation amplitude with the complex conjugate of the tree-level amplitude for the  $\chi_{e_4}\chi_{e_3} \rightarrow X_A X_B$  annihilation reaction, integrated over the final  $X_A X_B$  particles' phase space<sup>4</sup> and averaged over the spin states of the respective incoming particles  $\chi_{e_i}$ ,  $i = 1, \dots, 4$ . In the latter spin-average it is assumed that the  $\chi_{e_1}\chi_{e_2}$  and  $\chi_{e_4}\chi_{e_3}$  pair reside in the same spin state.<sup>5</sup> The external  $\chi_{e_a}\chi_{e_b}$  states are further taken to be non-relativistic normalised in order to match with the definition of the annihilation cross section times relative velocity in case of diagonal reactions  $\chi_{e_1}\chi_{e_2} \rightarrow X_A X_B \rightarrow \chi_{e_1}\chi_{e_2}$ . In terms of the Wilson coefficients of the four-fermion operators in  $\delta\mathcal{L}_{\text{ann}}$ , the expansion of the annihilation rate  $\Gamma$  in the non-relativistic momenta and in the mass differences  $\delta m, \delta \overline{m}$  is then given by

$$\begin{aligned} \Gamma^{\chi_{e_1}\chi_{e_2} \rightarrow X_A X_B \rightarrow \chi_{e_4}\chi_{e_3}} &= \hat{f}(^1S_0) + 3 \hat{f}(^3S_1) \\ &+ \frac{\delta m}{M} \left( \hat{h}_1(^1S_0) + 3 \hat{h}_1(^3S_1) \right) + \frac{\delta \overline{m}}{M} \left( \hat{h}_2(^1S_0) + 3 \hat{h}_2(^3S_1) \right) \\ &+ \frac{\mathbf{p} \cdot \mathbf{p}'}{M^2} \left( \hat{f}(^1P_1) + \frac{1}{3} \hat{f}(^3P_0) + \hat{f}(^3P_1) + \frac{5}{3} \hat{f}(^3P_2) \right) \\ &+ \frac{\mathbf{p}^2 + \mathbf{p}'^2}{2 M^2} \left( \hat{g}(^1S_0) + 3 \hat{g}(^3S_1) \right) \\ &+ \mathcal{O} \left( (\mathbf{p}^2 + \mathbf{p}'^2)^2, (\mathbf{p} \cdot \mathbf{p}')^2, \mathbf{p}^{(i)2} \delta m, \mathbf{p}^{(i)2} \delta \overline{m}, \delta m \delta \overline{m} \right), \end{aligned} \quad (8)$$

---

<sup>4</sup> The product of tree-level annihilation amplitudes has to be multiplied with an additional symmetry factor of 1/2 if the final state particles are identical,  $X_A = X_B$ .

<sup>5</sup> In the calculation of Sommerfeld enhanced  $\chi_i\chi_j \rightarrow X_A X_B$  pair-annihilation rates through the imaginary part of the  $\chi_i\chi_j \rightarrow \dots \rightarrow \chi_{e_1}\chi_{e_2} \rightarrow X_A X_B \rightarrow \chi_{e_4}\chi_{e_3} \rightarrow \dots \rightarrow \chi_i\chi_j$  forward scattering reaction, the assumption that the incoming and outgoing particle pairs in the  $\chi_{e_1}\chi_{e_2} \rightarrow X_A X_B \rightarrow \chi_{e_4}\chi_{e_3}$  short-distance annihilation part have the same spin state implies that just leading-order potential interactions in the  $\chi_i\chi_j \rightarrow \dots \rightarrow \chi_{e_1}\chi_{e_2}$  and  $\chi_i\chi_j \rightarrow \dots \rightarrow \chi_{e_4}\chi_{e_3}$  scattering reactions are considered, since the long-range potentials are spin-diagonal only at leading order and hence pass the spin-configuration of the incoming  $\chi_i\chi_j$  pair to the  $\chi_{e_1}\chi_{e_2}$  and  $\chi_{e_4}\chi_{e_3}$  pairs.



where  $\mathbf{p}$  and  $\mathbf{p}'$  correspond to the momenta of the  $\chi_{e_1}$  and  $\chi_{e_4}$  particle, respectively, in the centre-of-mass frame of the reaction. To shorten the notation we have suppressed in (8) the label “ $\chi_{e_1}\chi_{e_2} \rightarrow X_AX_B \rightarrow \chi_{e_4}\chi_{e_3}$ ” on the Wilson coefficients  $\hat{f}, \hat{g}$  and  $\hat{h}_i$ . As we study annihilation rates of non-relativistic  $\chi_{e_a}\chi_{e_b}$  particle pairs, the mass differences  $\delta m$  and  $\delta \bar{m}$  have to be (at most) of the order of the  $\chi_{e_a}\chi_{e_b}$  non-relativistic kinetic energy, as argued in Sec. 2.4 of paper I. Note that the non-relativistic expansion (8) incorporates this convention and assumes that  $\delta m, \delta \bar{m} \sim \mathcal{O}(\mathbf{p}^2/M)$ . In case of diagonal  $\chi_{e_1}\chi_{e_2} \rightarrow X_AX_B \rightarrow \chi_{e_1}\chi_{e_2}$  scattering reactions, the definition of the corresponding annihilation rate  $\Gamma$  obviously coincides with the definition of the spin-averaged centre-of-mass frame tree-level  $\chi_{e_1}\chi_{e_2} \rightarrow X_AX_B$  annihilation cross section times relative velocity,  $\sigma^{\chi_{e_1}\chi_{e_2} \rightarrow X_AX_B} v_{\text{rel}}$ , and the expansion in (8), with  $\mathbf{p}' = \mathbf{p}$ , reduces to the non-relativistic expansion of  $\sigma^{\chi_{e_1}\chi_{e_2} \rightarrow X_AX_B} v_{\text{rel}}$  as given in Eq. (27) of paper I (see also Eqs. (9–12) below).

## 4 Results

In paper I we have presented several examples for the numeric comparison of the non-relativistic approximation to the tree-level centre-of-mass frame annihilation cross-section  $\sigma^{\chi_{e_1}\chi_{e_2} \rightarrow X_AX_B}$  times relative velocity  $v_{\text{rel}} = |\vec{v}_{e_1} - \vec{v}_{e_2}|$ ,

$$\sigma^{\chi_{e_1}\chi_{e_2} \rightarrow X_AX_B} v_{\text{rel}} = a + b v_{\text{rel}}^2 + \mathcal{O}(v_{\text{rel}}^4), \quad (9)$$

with the corresponding unexpanded result obtained with MADGRAPH [20]. The coefficient  $a$  in the expansion (9) is expressed in terms of the leading order  $S$ -wave Wilson coefficients as

$$a = \hat{f}({}^1S_0) + 3 \hat{f}({}^3S_1), \quad (10)$$

and the coefficient  $b$  can be written as the sum  $b = b_P + b_S$ , where

$$b_P = \frac{\mu_{e_1e_2}^2}{M^2} \left( \hat{f}({}^1P_1) + \frac{1}{3} \hat{f}({}^3P_0) + \hat{f}({}^3P_1) + \frac{5}{3} \hat{f}({}^3P_2) \right), \quad (11)$$

$$b_S = \frac{\mu_{e_1e_2}^2}{M^2} \left( \hat{g}({}^1S_0) + 3 \hat{g}({}^3S_1) \right), \quad (12)$$

and

$$\mu_{e_1e_2} = \frac{m_{e_1}m_{e_2}}{m_{e_1} + m_{e_2}} \quad (13)$$

is the reduced mass of the  $\chi_{e_1}\chi_{e_2}$  two-particle state. We have again suppressed in (10–12) the labels on the Wilson coefficients  $\hat{f}$  and  $\hat{g}$  that indicate the specific  $\chi_{e_1}\chi_{e_2} \rightarrow X_AX_B \rightarrow \chi_{e_1}\chi_{e_2}$  reaction under consideration to simplify the notation. The prefactor  $(\mu_{e_1e_2}/M)^2$  in front of the Wilson coefficients in (11–12) is needed to translate the cross section’s expansion in  $\mathbf{p}^2$ , Eq. (8) with  $\mathbf{p}' = \mathbf{p}$ , to the  $v_{\text{rel}}^2$  expansion used in (9).

From the comparison of the non-relativistic approximation to  $\sigma^{\chi_{e1}\chi_{e2}\rightarrow X_AX_B} v_{\text{rel}}$  with the full result from MADGRAPH, it was shown in paper I that the non-relativistic approximation reproduces the behaviour of the exact tree-level cross section times relative velocity within a percent level deviation up to  $v_{\text{rel}}/c \sim 0.6$ .<sup>6</sup> The numeric extraction of the coefficients  $a$  and  $b$  from MADGRAPH data by means of a parabola fit to  $\sigma^{\chi_{e1}\chi_{e2}\rightarrow X_AX_B} v_{\text{rel}}$  in the non-relativistic regime thus provides a useful numeric check for the sum of leading-order  $S$ -wave Wilson coefficients (10), as well as for the sum of next-to-next-to-leading order  $S$ -wave and  $P$ -wave Wilson coefficients in (11,12). However, a splitting of the numerically extracted coefficients  $a$  and  $b$  into their constituting partial-wave contributions is not straightforward from publicly available numeric codes, as this requires manipulations at the amplitude level. The separate knowledge of the different  $^{2s+1}L_J$  partial wave contributions to the tree-level (co-)annihilation rates is essential for a precise determination of Sommerfeld enhanced neutralino (co-)annihilation cross sections, because the Sommerfeld enhancements depend both on the spin- and orbital angular momentum quantum numbers of the annihilating particle pair. Therefore a consistent treatment of the Sommerfeld enhancement including  $P$ -wave effects requires the separate knowledge of all relevant (off-)diagonal tree-level  $^1S_0$  and  $^3S_1$  partial-wave annihilation rates both at leading and next-to-next-to-leading order, as well as the individual (off-)diagonal tree-level  $^1P_1$  and  $^3P_J$  partial-wave annihilation rates. In the latter case, the knowledge of the (spin-weighted) sum over the three different  $^3P_0$ ,  $^3P_1$  and  $^3P_2$  partial-wave Wilson coefficients,

$$\hat{f}(^3P_{\mathcal{J}}) = \frac{1}{3}\hat{f}(^3P_0) + \hat{f}(^3P_1) + \frac{5}{3}\hat{f}(^3P_2) , \quad (14)$$

is sufficient, as long as only leading-order non-relativistic potential interactions between the neutralino and chargino states are taken into account in the full annihilation amplitudes. This is because the leading-order potential interactions depend on the spin ( $s = 0, 1$ ) of the  $\chi_{e_a}\chi_{e_b}$  particle pairs taking part in the  $\chi_i\chi_j \rightarrow \dots \rightarrow \chi_{e1}\chi_{e2} \rightarrow X_AX_B \rightarrow \chi_{e4}\chi_{e3} \rightarrow \dots \rightarrow \chi_i\chi_j$  scattering process, but do not discriminate among the three spin-1  $P$ -wave states  $^3P_J$  with different total angular momentum  $J = 0, 1, 2$ .

Recently, Sommerfeld corrections including  $P$ -wave effects have been subject of study at 1-loop [10] and with full resummation [17]. In these studies, the next-to-next-to-leading order contributions in the expansion of the relevant (co-)annihilation rates were assumed to be given only by  $P$ -waves. While such reasoning is justified when the leading-order  $S$ -wave contributions to the annihilation rates are strongly suppressed with respect to the next-to-next-to-leading order coefficients in (8, 9), it does not hold for the general case. In particular,  $P$ - and next-to-next-to-leading order  $S$ -wave terms can come with differing signs, such that a partial compensation of different next-to-next-to-leading order contributions to the annihilation rates may occur.

In order to illustrate the different behaviour of the  $P$ - and next-to-next-to-leading order  $S$ -wave contributions to the tree-level annihilation cross sections, we show in

---

<sup>6</sup>In case of processes with vanishing  $S$ -wave contributions the agreement between MADGRAPH and the non-relativistic approximation is a bit worse, but still with an accuracy at the level of  $\sim 6\%$  for  $v_{\text{rel}}/c \sim 0.4$ .

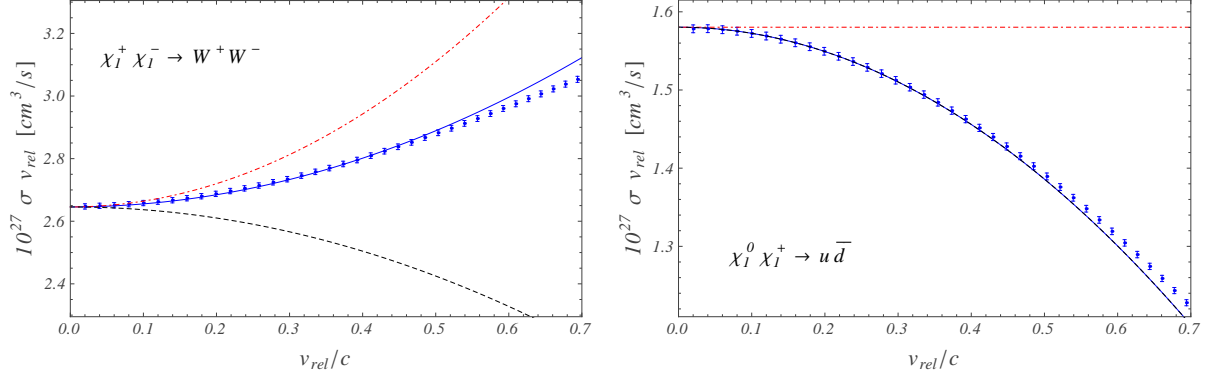


Figure 1: Numeric comparison of the non-relativistic approximation (solid lines) to the tree-level annihilation cross section times relative velocity,  $\sigma v_{\text{rel}}$ , for the  $\chi_1^+ \chi_1^- \rightarrow W^+ W^-$  process (left) and for the  $S$ -wave dominated reaction  $\chi_1^0 \chi_1^+ \rightarrow u \bar{d}$  (right) with the corresponding unexpanded annihilation cross sections produced with MADGRAPH. Numeric errors on the MADGRAPH data are given by  $\sigma v_{\text{rel}}/\sqrt{N}$ , where  $N = 10^5$  gives the number of events used in the MADGRAPH calculation of each cross section value. The dash-dotted red (dashed black) curves represent the constant leading-order term in the non-relativistic expansion of the cross section plus the  $P$ -wave (next-to-next-to-leading order  $S$ -wave) contribution,  $a + b_P v_{\text{rel}}^2$  ( $a + b_S v_{\text{rel}}^2$ ).

Figs. 1 and 2 results for the tree-level annihilation cross section times relative velocity,  $\sigma^{\chi_{e1} \chi_{e2} \rightarrow X_A X_B} v_{\text{rel}}$ , for three different processes. The plots refer to the same SUSY spectrum that was used in paper I, which contains a wino-like neutralino LSP with mass  $m_{\chi_1^0} = 2748.92 \text{ GeV}$ , and an almost mass-degenerate wino-like chargino partner with  $m_{\chi_1^\pm} = 2749.13 \text{ GeV}$ . The next-to-lightest chargino state has a mass  $m_{\chi_2^\pm} = 3073.31 \text{ GeV}$ .

#### 4.1 Example 1: $\chi_1^+ \chi_1^- \rightarrow W^+ W^-$

The plot on the left hand side in Fig. 1 shows the  $\chi_1^+ \chi_1^- \rightarrow W^+ W^-$  tree-level annihilation rate, a relevant co-annihilation rate in the neutralino LSP relic density computation. The solid blue line corresponds to the non-relativistic approximation to the tree-level annihilation cross section,  $\sigma^{\chi_1^+ \chi_1^- \rightarrow W^+ W^-} v_{\text{rel}}$ , and the points correspond to the full tree-level result obtained with MADGRAPH. The deviation between our approximation and the MADGRAPH data is at one percent level for  $v_{\text{rel}}/c \sim 0.6$  and in the permille regime for smaller relative velocities. Further, the composition of the non-relativistic approximation to  $\sigma^{\chi_1^+ \chi_1^- \rightarrow W^+ W^-} v_{\text{rel}}$  out of  $P$ - and next-to-next-to-leading order  $S$ -wave contributions can be read off from Fig. 1: the dash-dotted red line represents the contribution  $a + b_P v_{\text{rel}}^2$  to (9), while the dashed black line is  $a + b_S v_{\text{rel}}^2$ . While both  $b_P$  and  $b_S$  are roughly of the same order of magnitude, the summed  $P$ -wave contributions enter with a positive sign ( $b_P c^2 = 1.86 \cdot 10^{-27} \text{ cm}^3 \text{ s}^{-1}$ ), whereas the summed next-to-next-to-leading order  $S$ -wave contributions come with a negative weight,  $b_S c^2 = -0.88 \cdot 10^{-27} \text{ cm}^3 \text{ s}^{-1}$ . It is worth noting that the sum of next-to-next-to-leading order corrections in the  $\chi_1^+ \chi_1^- \rightarrow W^+ W^-$

tree-level cross section times relative velocity gives a  $\sim 6\%$  correction to the leading-order approximation for  $v_{\text{rel}}/c \sim 0.4$ . For this relative velocity, the corrections to the leading-order approximation from  $P$ -waves only amount to  $\sim 11\%$ , while those from next-to-next-to-leading order  $S$ -wave contributions amount to  $\sim -5\%$ . Hence, in the light of the expected future experimental precision on the measured dark matter density, it is crucial to take these corrections into account. Further, as generically the Sommerfeld enhancements for each of the contributing partial waves are different, it will be needed to investigate the Sommerfeld enhanced annihilation cross section including  $P$ - and next-to-next-to-leading order  $S$ -wave enhancements separately. This study within our formalism is postponed to [21].

The fact that the  $P$ -wave terms in the example of Fig. 1 contribute with positive sign is generic: the sum of all  $^{2s+1}P_J$  partial-wave contributions to any  $\chi_{e_1}\chi_{e_2} \rightarrow X_A X_B$  annihilation cross section has to be positive, as it results from the absolute square of the coefficient of the  $\mathcal{O}(\mathbf{p})$  terms in the expansion of the annihilation amplitude. Moreover, the separate  $^{2s+1}P_J$  partial-wave contributions must also be positive, since different  $^{2s+1}P_J$ -wave amplitudes do not interfere in the absolute square of the annihilation amplitude due to total angular-momentum conservation and the additional conservation of spin in the non-relativistic regime. The next-to-next-to-leading order  $S$ -wave contributions to the  $\chi_{e_1}\chi_{e_2} \rightarrow X_A X_B$  annihilation cross section, however, result from the product of leading-order and next-to-next-to-leading order  $S$ -wave contributions in the expansion of the  $\chi_{e_1}\chi_{e_2} \rightarrow X_A X_B$  amplitude. There is a priori no reason why this product should be positive, and hence negative next-to-next-to-leading order  $S$ -wave contributions to the cross section can occur, as can be explicitly seen in the examples presented in this section.

## 4.2 Example 2: $\chi_1^0 \chi_1^+ \rightarrow u \bar{d}$

The right plot in Fig. 1 shows results for the  $S$ -wave dominated tree-level  $\chi_1^0 \chi_1^+ \rightarrow u \bar{d}$  annihilation process, also of importance in the neutralino relic abundance calculation including co-annihilations. The dashed black line, representing the  $a + b_S v_{\text{rel}}^2$  contribution to the non-relativistic expansion of the annihilation rate with  $b_S c^2 = -0.78 \cdot 10^{-27} \text{ cm}^3 \text{ s}^{-1}$ , basically coincides with the solid blue line, which corresponds to the complete non-relativistic approximation (9). Data produced with MADGRAPH for the  $\chi_1^0 \chi_1^+ \rightarrow u \bar{d}$  tree-level annihilation rate are shown in addition, illustrating once again the nice agreement of the non-relativistic approximation with the unexpanded tree-level cross section results for relative velocities up to  $v_{\text{rel}}/c \sim 0.6$ . It is worthwhile to understand the suppression of  $P$ -waves with respect to the next-to-next-to-leading order  $S$ -wave contributions in the  $\chi_1^0 \chi_1^+ \rightarrow u \bar{d}$  process as well as the composition of the coefficient  $b_S$  out of its  $^1S_0$  and  $^3S_1$  partial-wave contributions: First note, that in the case of vanishing final state masses,  $m_u = m_d = 0$ , the contributions to both  $a$  and  $b_S$  can be attributed solely to  $^3S_1$  partial waves. The absence (or more generally the suppression in  $m_q/M$ ,  $q = u, d$ ) of  $^1S_0$  partial-wave contributions both in the leading-order coefficient  $a$  and in  $b_S$  is a helicity suppression effect. The helicity suppression argument applies

to all  $^{2s+1}L_J$  partial-wave reactions with  $J = 0$ , as the final state of a massless (left-handed) quark and a massless (right-handed) anti-quark in its centre-of-mass system cannot build a total angular-momentum state  $J = 0$ . Hence both  $^1S_0$  as well as  $^3P_0$  partial-wave contributions are helicity suppressed.

The suppression of  $^1P_1$ ,  $^3P_1$  and  $^3P_2$  partial-wave contributions that proceed through single  $s$ -channel gauge-boson or Higgs exchange is related to either factors of  $\Delta_m = (m_{\chi_1^0} - m_{\chi_1^+})/(m_{\chi_1^0} + m_{\chi_1^+})$  or to vertex couplings that vanish in the exact  $SU(2)_L$  symmetric limit. Similarly, contributions from  $t$ -channel exchange amplitudes introduce  $\Delta_m$  factors or coupling factor combinations that lead to vanishing contributions in the  $SU(2)_L$  symmetric theory (case of  $^1P_1$  waves), or are additionally suppressed (as it is the case of  $^3P_1$  and  $^3P_2$  partial-wave configurations) by the masses of  $t$ -channel exchanged sfermions, since the mass scale of the latter is above 5 TeV in the MSSM scenario considered. Consequently, as the initial two particle state in the reaction  $\chi_1^0\chi_1^+ \rightarrow u\bar{d}$  consists of two wino-like particles with  $|\Delta_m| \sim 4 \cdot 10^{-5}$ , the  $^1P_1$ ,  $^3P_1$  and  $^3P_2$  partial waves give suppressed contributions to the tree-level annihilation rate.

### 4.3 Example 3: $\chi_2^+\chi_2^- \rightarrow h^0h^0$

An example of a  $P$ -wave dominated process is provided in the left plot of Fig. 2. It corresponds to the tree-level  $\chi_2^+\chi_2^- \rightarrow h^0h^0$  annihilation, wherein  $S$ -wave contributions vanish, such that the process is purely  $P$ -wave mediated in the non-relativistic regime (the coefficient  $b_P c^2$  is given by  $9.94 \cdot 10^{-29} \text{ cm}^3 \text{ s}^{-1}$ ). The absence of  $S$ -wave contributions can be explained by  $CP$  and total angular-momentum conservation in the  $\chi_2^+\chi_2^- \rightarrow h^0h^0$  reaction.<sup>7</sup> The  $CP$  quantum number of the final two-particle state  $h^0h^0$  is given by  $CP = (-1)^L = (-1)^J$ , as the total angular momentum of a  $h^0h^0$  state coincides with its orbital angular momentum and the parity of such a state is given by  $P = (-1)^L$ , while its charge conjugation is  $C = 1$ . In case of the annihilating  $\chi_a^+\chi_a^-$  two-particle state the  $J^{PC}$  quantum numbers are  $0^{-+}$  for a  $^1S_0$  partial-wave configuration and  $1^{--}$  for a  $^3S_1$  partial-wave state. Hence, for the  $\chi_a^+\chi_a^-$  state,  $CP = -1$  is realised in case of  $S$ -waves for the  $J = 0$  configuration, and  $CP = +1$  for  $J = 1$ , which are opposite to the  $CP$  quantum numbers of a  $h^0h^0$  final state with the same total angular momentum. The same reasoning explains the absence of  $^3P_1$  annihilations in any of the processes  $\chi_a^+\chi_a^- \rightarrow X_AX_B$  with  $X_AX_B = h^0h^0, h^0H^0, H^0H^0$ , as the  $J^{PC}$  quantum numbers of the  $^3P_1$  partial-wave configuration of the incoming  $\chi_a^+\chi_a^-$  states are  $1^{++}$ , hence  $CP = +1$  for  $J = 1$ . This is opposite to the  $CP$  quantum number of the two  $CP$ -even Higgs boson final state with total angular momentum  $J = 1$ .

Let us finally note that there are also no contributions from  $^1P_1$  partial waves in the process shown in the left plot in Fig. 2. This feature is generic to  $\chi_a^+\chi_b^- \rightarrow X_AX_B$  annihilations with identical scalar particles in the final state,  $X_AX_B = h^0h^0, H^0H^0$ .

---

<sup>7</sup>The following reasoning applies to all possible  $\chi_a^+\chi_a^- \rightarrow X_AX_B$  annihilation reactions with two  $CP$ -even MSSM Higgs particles in the final state,  $X_AX_B = h^0h^0, h^0H^0, H^0H^0$ . Note that  $CP$  is conserved in these reactions if the mixing matrices in the chargino sector are real, which is the case for the scenario we consider.

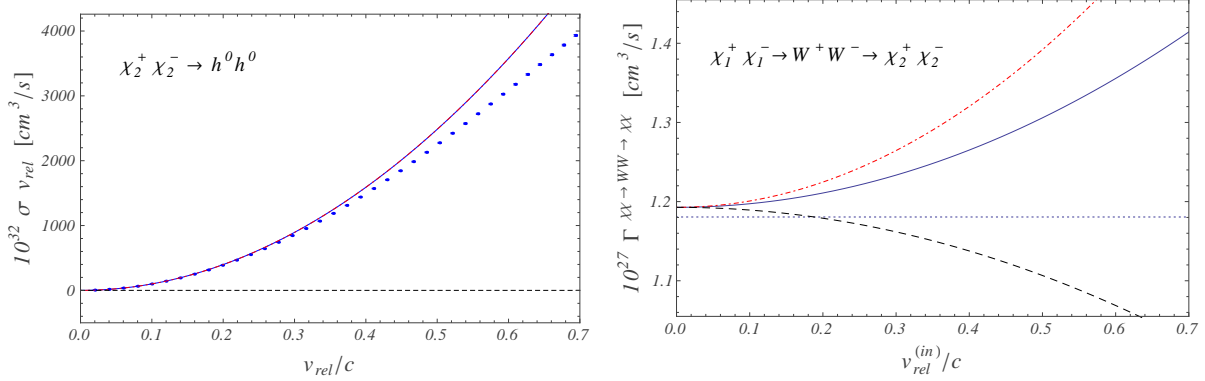


Figure 2: Left plot: Numeric comparison of the non-relativistic approximation (solid blue curve) to the tree-level annihilation cross section times relative velocity,  $\sigma v_{\text{rel}}$ , for the  $P$ -wave dominated  $\chi_2^+ \chi_2^- \rightarrow h^0 h^0$  reaction to data for the corresponding unexpanded annihilation cross section produced with MADGRAPH. Numeric errors on the MADGRAPH data are taken to be  $\sigma v_{\text{rel}}/\sqrt{N}$ , where  $N = 10^5$  gives the number of events used in the MADGRAPH calculation of each cross section value. The dash-dotted red and dashed black lines represent the constant leading-order term plus the  $P$ -wave or the next-to-next-to-leading order  $S$ -wave contribution,  $a + b_P v_{\text{rel}}^2$  or  $a + b_S v_{\text{rel}}^2$ , respectively. Note that the  $a + b_P v_{\text{rel}}^2$  contribution and the non-relativistic approximation coincide, as there are no  $S$ -wave contributions in this particular annihilation reaction. Right plot: Off-diagonal annihilation rate  $\Gamma$  for the reaction  $\chi_1^+ \chi_1^- \rightarrow W^+ W^- \rightarrow \chi_2^+ \chi_2^-$ . The solid line includes all contributions to  $\Gamma$  up to next-to-next-to-leading order in the non-relativistic expansion. It is obtained from (8) assuming that  $\mathbf{p}$  and  $\mathbf{p}'$  are parallel to each other. The constant dotted blue line gives the leading-order approximation to  $\Gamma$ . Summing the  $P$ - or the (momentum-dependent) next-to-next-to-leading order  $S$ -wave contributions to the constant  $S$ -wave terms (given by the leading order plus the terms proportional to  $\delta m$  and  $\delta \bar{m}$ ) yields the dash-dotted red or the dashed black line, respectively. The curves are plotted against the relative velocity  $v_{\text{rel}}^{(\text{in})}$  of the incoming state  $\chi_1^+ \chi_1^-$ .

The argument relies on the statistics of the final state identical bosons, and applies to all  $\chi_a^+ \chi_b^-$  incoming states and not only to particle-anti-particle states  $\chi_a^+ \chi_a^-$ : Bose statistics forbids the two identical final state scalars to be in a  $J = L = 1$  state, as the corresponding two-particle wave-function for odd total angular momentum  $J$  would be anti-symmetric. This argument can also be used to explain the absence of the  $J = 1$   $^3S_1$  and  $^3P_1$  states in a  $\chi_a^+ \chi_b^- \rightarrow h^0 h^0, H^0 H^0$  annihilation reaction.

#### 4.4 Example 4: $\chi_1^+ \chi_1^- \rightarrow W^+ W^- \rightarrow \chi_2^+ \chi_2^-$

Let us finally turn to the case of an off-diagonal annihilation rate. The right plot in Fig. 2 shows the off-diagonal annihilation rate  $\Gamma$  associated with the process  $\chi_1^+ \chi_1^- \rightarrow W^+ W^- \rightarrow \chi_2^+ \chi_2^-$ , which is relevant, for instance, in the calculation of the Sommerfeld enhanced  $\chi_1^0 \chi_1^0 \rightarrow W^+ W^-$  and  $\chi_1^+ \chi_1^- \rightarrow W^+ W^-$  (co-)annihilation cross sections. The



mass splitting between the  $\chi_1^\pm$  and  $\chi_2^\pm$  charginos is given by 324.18 GeV in the MSSM scenario considered, which results in rather large mass differences, namely  $\delta m = \delta \overline{m} = 162.09$  GeV. In this case, the Wilson coefficients  $h_1$  and  $h_2$ , that are proportional to  $\delta m$  and  $\delta \overline{m}$ , lead to a 1% positive correction to the constant leading-order rate. This positive shift corresponds to the difference between the leading-order approximation to the annihilation rate  $\Gamma$  (first line in (8), dotted blue line in the right plot in Fig. 2), and the complete non-relativistic result for  $\Gamma$  including next-to-next-to-leading corrections (solid blue line) at zero momentum. The corrections induced by the terms proportional to  $\delta m$ ,  $\delta \overline{m}$  turn out to be somewhat smaller than the naive expectation  $\delta m/M = \delta \overline{m}/M = 2.78\%$ , but represent nevertheless the dominant next-to-next-to-leading order correction up to  $v_{\text{rel}}/c \sim 0.16$ . For larger relative velocities, the  $P$ - and next-to-next-to-leading order  $S$ -wave terms provide larger contributions to the absorptive part of the  $\chi_1^+ \chi_1^- \rightarrow W^+ W^- \rightarrow \chi_2^+ \chi_2^-$  scattering amplitude. This is indicated by the dash-dotted red and dashed black curves, which result from the addition of the constant  $S$ -wave contributions (first two lines in (8)) and the  $P$ -wave contributions (third line in (8)) or the momentum-dependent  $S$ -wave next-to-next-to-leading terms (fourth line in (8)), respectively. The correction to the leading-order  $\Gamma$  rate due to the  $P$ - and next-to-next-to-leading order  $S$ -wave terms amounts to a 7% for  $v_{\text{rel}}/c = 0.4$ .

Note that no comparison with public numeric codes providing results for (tree-level)  $\chi\chi \rightarrow X_A X_B$  annihilation rates is available for the off-diagonal annihilation rates. We emphasise that the calculation of the partial-wave decomposed off-diagonal annihilation rates therefore constitutes one of the main results presented in paper I and in this work. The relevance of off-diagonal annihilation rates in the calculation of Sommerfeld enhanced (co-)annihilation amplitudes in context of the  $\chi_1^0$  relic abundance calculation was in particular pointed out in Sec. 4.2 of I, and will be further investigated in subsequent work [21].

## 5 Summary

With this work we finish the presentation of results associated to the short-distance annihilation rates, that are prerequisites for a refined study of Sommerfeld enhancements in neutralino dark matter (co-)annihilation processes in the MSSM including  $P$ - and next-to-next-to-leading order  $S$ -wave contributions. Our analysis can be applied to a set of nearly mass-degenerate non-relativistic neutralino and chargino states with masses around the TeV scale and excludes accidental mass-degeneracies with further supersymmetric or Higgs particles.

A factorisation between the short- and long-distance contributions in the pair annihilation of non-relativistic neutralino and chargino pairs is possible given the large separation between the associated scales. Paper I [16] introduced an effective field theory set-up (the NRMSSM), that provides the basis for a systematic study of radiative corrections in (co-)annihilation processes of non-relativistic neutralinos and charginos, applicable to both neutralino DM freeze-out in the Early Universe as well as to neu-



trino pair-annihilations today. In the EFT approach, the tree-level (co-)annihilation rates of neutral, single and double charged neutralino/chargino pairs into SM and Higgs two-particle final states  $X_A X_B$ , related to the absorptive parts of the 1-loop scattering reactions  $\chi_{e_1} \chi_{e_2} \rightarrow X_A X_B \rightarrow \chi_{e_4} \chi_{e_3}$ , are encoded in the absorptive parts of the Wilson coefficients of four-fermion operators. As the first step in the construction of the NRMSSM, paper I provided the basis of dimension-6 four-fermion operators, which describe leading-order  $S$ -wave annihilation processes. The absorptive parts of the corresponding four-fermion operators' Wilson coefficients are provided in analytic form in the appendix of paper I. In the present work, we extend the results from paper I and provide the operator basis for dimension-8 four-fermion operators, contributing at next-to-next-to-leading order in the non-relativistic expansion of  $\chi_{e_1} \chi_{e_2} \rightarrow X_A X_B \rightarrow \chi_{e_4} \chi_{e_3}$  annihilation rates, and present analytic results for the absorptive parts of the corresponding  $^1P_1$ -wave Wilson coefficients as well as the spin-averaged sum of spin-1  $P$ -wave ( $^3P_J$ ) Wilson coefficients in the Appendix A. An electronic supplement [18] to this paper contains analytic results for all kinematic factors that are needed in the construction of the absorptive part of partial-wave separated (next-to-next-to-)leading order  $S$ - and  $P$ -wave Wilson coefficients, relevant for the determination of the  $\mathcal{O}(v_{\text{rel}}^2)$  approximation to any (off-)diagonal tree-level (co-)annihilation rate. Our results apply to neutralino and chargino states with arbitrary composition and include the full mass dependence of the final state SM and Higgs particles. As a straightforward application of our work, we have provided in Appendix C the previously unknown  $\mathcal{O}(v_{\text{rel}}^2)$  corrections to the exclusive (off-)diagonal (co-)annihilation rates for the same pure-wino neutralino dark matter scenario considered in earlier works [11–13].

While there are situations where the main part of the  $\mathcal{O}(v_{\text{rel}}^2)$  corrections to a given annihilation rate can be attributed to a specific partial wave (for instance when  $CP$ -conservation or helicity-suppression forbids or suppresses annihilation reactions from other partial-wave states), we have presented two examples in Sec. 4, where the  $\mathcal{O}(v_{\text{rel}}^2)$   $P$ - and next-to-next-to-leading order  $S$ -wave contributions in the annihilation rates are roughly of the same order of magnitude and enter with differing signs. A proper treatment of Sommerfeld enhanced annihilation rates beyond leading order  $S$ -wave annihilations therefore generally requires the knowledge of each separate partial-wave contribution, which is now available with the analytic results given in the appendices of paper I and II as well as those collected in the electronic supplement. In particular a numeric extraction of the  $\mathcal{O}(v_{\text{rel}}^2)$  contributions in the non-relativistic expansion of the annihilation rates without a separation of the different constituting  $P$ - and next-to-next-to-leading order  $S$ -waves will, in general, not be sufficient in a rigorous analysis of the Sommerfeld effect beyond leading-order  $S$ -wave enhancements.

In addition, it is important to stress that our work allows for a consistent treatment of off-diagonal annihilation rates, required for the accurate description of Sommerfeld enhanced annihilation reactions, as the potential exchange of electroweak gauge-bosons and light Higgses prior to the actual annihilation can change the incoming neutralino or chargino two-particle state to another nearly on-shell two-particle state. This implies that the annihilation process itself is generally described by a non-diagonal

hermitian matrix in the space of neutralino and chargino two-particle states. Apart from the usual expansion in non-relativistic momenta, a consistent treatment of off-diagonal reactions within the NRMSSM requires an additional expansion in the mass differences between initial and final state particles in the off-diagonal annihilation rates  $\chi_{e_1}\chi_{e_2} \rightarrow X_A X_B \rightarrow \chi_{e_4}\chi_{e_3}$ . The respective contributions count as next-to-next-to-leading order in the non-relativistic expansion. Consequently, we account for the corresponding set of four-fermion operators in the basis of the dimension-8 four-fermion operators given in this paper and include the results for their Wilson coefficients in the electronic supplement.

With the above results at hand, the study of the long-range effects in the annihilation of non-relativistic neutralino and chargino pairs as well as their impact on the neutralino relic-abundance calculation in selected examples will be the subject of a forthcoming publication [21].

## Acknowledgements

We would like to thank M. Beneke for very useful discussions and suggestions regarding the preparation of this paper. This work is supported in part by the Gottfried Wilhelm Leibniz programme of the Deutsche Forschungsgemeinschaft (DFG) and the DFG Sonderforschungsbereich/Transregio 9 “Computergestützte Theoretische Teilchenphysik”. C.H. would like to thank the “Deutsche Telekom Stiftung” for its support while the main part of this work was done. The work of P. R. is partially supported by MEC (Spain) under grants FPA2007-60323 and FPA2011-23778 and by the Spanish Consolider-Ingenio 2010 Programme CPAN (CSD2007-00042).

## A Absorptive parts of Wilson coefficients of dimension-8 operators in $\delta\mathcal{L}_{\text{ann}}$

We provide in this appendix analytic expressions for the kinematic factors related to the absorptive part of the  $P$ -wave Wilson coefficients in  $\delta\mathcal{L}_{\text{ann}}^{d=8}$ , Eq. (3). The corresponding expressions for the kinematic factors of the next-to-next-to-leading order  $S$ -wave Wilson coefficients,  $\hat{g}^{(2s+1)S_s}$  and  $\hat{h}_i^{(2s+1)S_s}$  with  $s = 0, 1$  are quite lengthy. Therefore we have collected the latter in an electronic supplement [18] attached to this paper, that also contains the kinematic factors associated with the absorptive part of the  $P$ -wave Wilson coefficients ( $\hat{f}^{(1)P_1}$ ,  $\hat{f}^{(3)P_J}$ ,  $J = 0, 1, 2$ ) and those corresponding to the leading-order  $S$ -wave Wilson coefficients ( $\hat{f}^{(1)S_0}$ ,  $\hat{f}^{(3)S_1}$  in  $\delta\mathcal{L}_{\text{ann}}^{d=6}$ ), which were written in the appendix of paper I. Details on the nomenclature used in the electronic supplement can be found in Appendix B.

We aim at the description of Sommerfeld enhanced annihilation rates, and will in a forthcoming publication [21] consider the potentials which are responsible for the long-range Sommerfeld corrections at leading order. Despite that the leading-order potential interactions cannot change the spin of the incoming two-particle state, they depend

on the spin ( $s = 0, 1$ ) of the latter. Consequently, as far as our study of Sommerfeld enhancements is concerned, the separate knowledge of the different  $\hat{f}({}^3P_J)$  coefficients, which share the same orbital angular-momentum and spin but different total angular momentum ( $J = 0, 1, 2$ ), is not needed. It suffices to consider the combination of spin-1  $P$ -wave Wilson coefficients  $\hat{f}({}^3P_{\mathcal{J}})$  entering the short-distance part, Eqs. (8) and (11),

$$\hat{f}({}^3P_{\mathcal{J}}) = \frac{1}{3} \hat{f}({}^3P_0) + \hat{f}({}^3P_1) + \frac{5}{3} \hat{f}({}^3P_2) \quad (15)$$

that will be multiplied by the  $P$ -wave Sommerfeld correction factor computed with potentials for spin-1 scattering states. Hence we give in this appendix analytic expressions for the kinematic factors corresponding to  $\hat{f}({}^1P_1)$  Wilson coefficients as well as the kinematic factors associated with the combination  $\hat{f}({}^3P_{\mathcal{J}})$ . For completeness, the kinematic factors for the separate  $\hat{f}({}^3P_J)$ ,  $J = 0, 1, 2$ , Wilson coefficients can be found in the electronic attachment [18], together with those of the combination  $\hat{f}({}^3P_{\mathcal{J}})$ .

## A.1 Master formula to build the Wilson coefficients

The results for the Wilson coefficients  $\hat{f}$ ,  $\hat{g}$  and  $\hat{h}_i$  ( $i = 1, 2$ ) at  $\mathcal{O}(\alpha_2^2)$  are obtained through matching of the EFT tree-level matrix element of four-fermion operators in  $\delta\mathcal{L}_{\text{ann}}$  with the absorptive part of the MSSM 1-loop  $\chi_{e1}\chi_{e2} \rightarrow X_AX_B \rightarrow \chi_{e4}\chi_{e3}$  scattering amplitude with states  $\chi_{e1}\chi_{e2}$  and  $\chi_{e4}\chi_{e3}$  in a  ${}^{2s+1}L_J$  partial-wave configuration. In case of  $s = 0$ , the total angular momentum  $J$  of the  ${}^{2s+1}L_J$  state takes the value  $J = L$ , while for  $s = 1$ ,  $J = |L - 1|, \dots, L + 1$ . As tree-level annihilation processes are free from infrared divergences, the individual contributions to the Wilson coefficients from exclusive final states  $X_AX_B$  at  $\mathcal{O}(\alpha_2^2)$  can be given separately. Our results cover separately all possible exclusive SM and light Higgs two-particle final states  $X_AX_B$  in neutral ( $\chi^0\chi^0$ ,  $\chi^-\chi^+$ ), single-charged ( $\chi^0\chi^+$ ,  $\chi^0\chi^-$ ) and double-charged ( $\chi^+\chi^+$ ,  $\chi^-\chi^-$ ) chargino and neutralino pair-annihilation reactions, where the  $X_AX_B$  states are conveniently classified to be of vector-vector ( $VV$ ), vector-scalar ( $VS$ ), scalar-scalar ( $SS$ ), fermion-fermion ( $ff$ ) or ghost-anti-ghost ( $\eta\bar{\eta}$ ) type, see Tab. 3 in paper I.

In paper I we have provided a master formula to obtain the absorptive part  $\hat{f}({}^{2s+1}L_J)$  of a given Wilson coefficient from its constituent parts, the kinematic and coupling factors. For the sake of clarity, we write the formula here as well and briefly comment on its structure. It reads

$$\begin{aligned} & \hat{f}_{\{\chi_{e1}\chi_{e2}\}\{\chi_{e4}\chi_{e3}\}}^{\chi_{e1}\chi_{e2} \rightarrow X_AX_B \rightarrow \chi_{e4}\chi_{e3}}({}^{2s+1}L_J) \\ &= \frac{\pi\alpha_2^2}{M^2} \left( \sum_n \sum_{i_1, i_2} b_{n, i_1 i_2}^{\chi_{e1}\chi_{e2} \rightarrow X_AX_B \rightarrow \chi_{e4}\chi_{e3}} B_{n, i_1 i_2}^{X_AX_B}({}^{2s+1}L_J) \right. \\ & \quad \left. + \sum_{\alpha=1}^4 \sum_n \sum_{i_1, i_2} c_{n, i_1 i_2}^{(\alpha)\chi_{e1}\chi_{e2} \rightarrow X_AX_B \rightarrow \chi_{e4}\chi_{e3}} C_{n, i_1 i_2}^{(\alpha)X_AX_B}({}^{2s+1}L_J) \right) \end{aligned}$$

$$+ \sum_{\alpha=1}^4 \sum_n \sum_{i_1, i_2} d_{n, i_1 i_2}^{(\alpha) \chi_{e_1} \chi_{e_2} \rightarrow X_A X_B \rightarrow \chi_{e_4} \chi_{e_3}} D_{n, i_1 i_2}^{(\alpha) X_A X_B (2s+1) L_J} \Big) . \quad (16)$$

Formula (16) also applies to the next-to-next-to-leading order  $S$ -wave Wilson coefficients denoted with  $g$  and  $h_i$  ( $i = 1, 2$ ) in (3), with  $\hat{f}$  being replaced by  $\hat{g}$  or  $\hat{h}_i$ . However in the discussion that follows, we will generically refer to the absorptive part of any four-fermion operator's Wilson coefficient as  $\hat{f}$ . An exclusive final state contribution is indicated with the label  $\chi_{e_1} \chi_{e_2} \rightarrow X_A X_B \rightarrow \chi_{e_4} \chi_{e_3}$  on  $\hat{f}$  in (16), while the actual absorptive part of the Wilson coefficient  $\hat{f}^{(2s+1) L_J}$  is given by the inclusive annihilation rate, summed over all accessible final states. Note that we have used  $\alpha_2 = g_2^2/4\pi$ , where  $g_2$  denotes the  $SU(2)_L$  gauge coupling.

The first line on the right-hand side of (16) collects all contributions from  $\chi_{e_1} \chi_{e_2} \rightarrow X_A X_B \rightarrow \chi_{e_4} \chi_{e_3}$  MSSM selfenergy amplitudes, while the second and third lines give the triangle and box amplitudes' contributions, respectively. Quantities  $B_{n, i_1 i_2}$ ,  $C_{n, i_1 i_2}^{(\alpha)}$  and  $D_{n, i_1 i_2}^{(\alpha)}$  in (16) denote the kinematic factors, which encode the  $^{2s+1} L_J$  partial-wave specific information on the process.<sup>8</sup> They are obtained from a generic  $\chi_{e_1} \chi_{e_2} \rightarrow X_A X_B \rightarrow \chi_{e_4} \chi_{e_3}$  1-loop scattering reaction with generic external Majorana fermions and generic final state particles  $X_A X_B$  of the type vector-vector ( $VV$ ), vector-scalar ( $VS$ ), scalar-scalar ( $SS$ ), fermion-fermion ( $ff$ ) or ghost-anti-ghost ( $\eta\bar{\eta}$ ), respectively, and can be applied to any  $\chi\chi \rightarrow X_A X_B \rightarrow \chi\chi$  annihilation reaction with external Majorana or Dirac fermions by appropriate construction of the corresponding process-specific coupling factors, denoted with lowercase letters ( $b_{n, i_1 i_2}$ ,  $c_{n, i_1 i_2}^{(\alpha)}$ ,  $d_{n, i_1 i_2}^{(\alpha)}$ ) in (16). The index  $\alpha$  enumerates the expressions related to the four different triangle and box amplitudes, as shown in Fig. 3. Depending on the type of the particles  $X_A$  and  $X_B$  as well as on the topology, there is a fixed number of coupling-factor expressions that result from all possible combinations of (axial-)vector or (pseudo-)scalar vertex factors at the four vertices of a given MSSM  $\chi_{e_1} \chi_{e_2} \rightarrow X_A X_B \rightarrow \chi_{e_4} \chi_{e_3}$  1-loop amplitude. These combinations are labelled with the index  $n$  in (16). Finally, in each of the processes there is a certain set of particle species that can be exchanged in the  $s$ - or the  $t$ -channels of the contributing amplitudes. These are labelled with the indices  $i_1$  and  $i_2$ . The general recipe on how to derive the coupling factors is given in Appendix A.2 of paper I. Note that the coupling factors do not depend on the kinematics and hence are the same for Wilson coefficients with different quantum numbers  $^{2s+1} L_J$ . With the purpose to illustrate how to obtain the annihilation rates from our results, we build in Appendix C the Wilson coefficients needed to describe up to next-to-next-to-leading non-relativistic corrections for the case of pure-wino neutralino dark matter.

---

<sup>8</sup>In order to distinguish the kinematic factors associated with the leading and  $\mathcal{O}(v_{\text{rel}}^2)$   $S$ -wave Wilson coefficients  $\hat{f}$  and  $\hat{g}, \hat{h}_i$ , we write the partial-wave state label  $^{2s+1} L_J$  in the latter as  $^{2s+1} L_J = {}^1 S_0, {}^3 S_1$  for kinematic factors related to  $\hat{f}$ , and  $^{2s+1} L_J = {}^1 S_0^{(p^2)}, {}^3 S_1^{(p^2)}$  as well as  $^{2s+1} L_J = {}^1 S_0^{(\delta m)}, {}^3 S_1^{(\delta m)}, {}^1 S_0^{(\delta \overline{m})}, {}^3 S_1^{(\delta \overline{m})}$  if the kinematic factors are related to  $\hat{g}$  or  $\hat{h}_i$ , respectively.

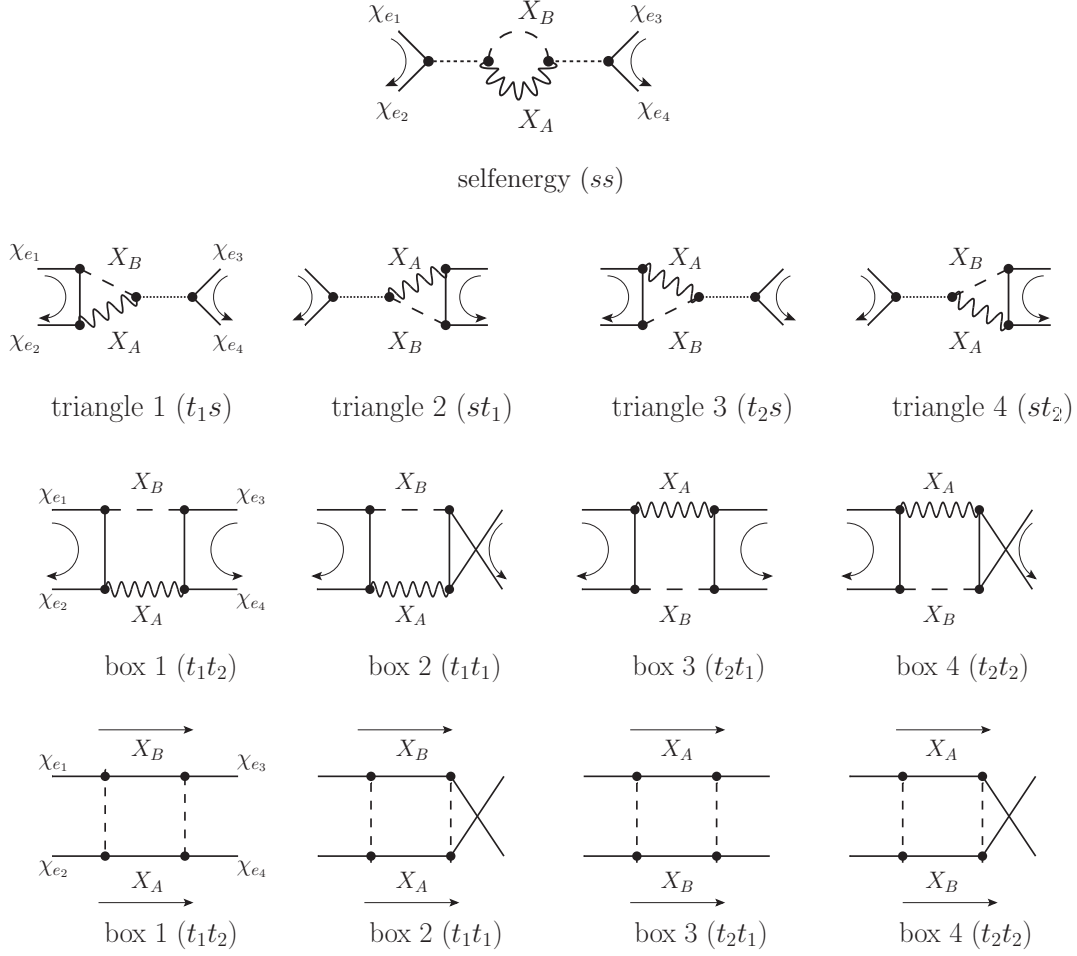


Figure 3: Generic selfenergy-, triangle- and box-diagrams in  $\chi\chi \rightarrow X_A X_B \rightarrow \chi\chi$  reactions, with  $X_A$  and  $X_B$  representing any two-body final state of SM and Higgs particles. The box-amplitudes in the third line refer to  $X_A X_B = VV, VS, SS$  while the box-amplitudes in the last line apply to  $X_A X_B = ff$ . The shorthand  $a\tilde{a}$  notation, with  $a, \tilde{a} = s, t_1, t_2$ , indicates the tree-level diagrams  $a$  and  $\tilde{a}$  in the  $\chi_{e1}\chi_{e2} \rightarrow X_A X_B$  and  $\chi_{e4}\chi_{e3} \rightarrow X_A X_B$  processes, respectively, to which the coupling factors in a specific reaction are related (see Figs. 9, 10 in paper I for details on the latter).

## A.2 Kinematic factors

Let us first collect from paper I the relevant notation that enters the formulae for the kinematic factors. The kinematic factors for a given  $\chi_{e1}\chi_{e2} \rightarrow X_A X_B \rightarrow \chi_{e4}\chi_{e3}$  scattering reaction depend on the external particles' masses, which are rewritten in terms of two (in principle) different reference mass scales  $m, \overline{m}$  and two mass differences  $\delta m, \delta \overline{m}$

as

$$\begin{aligned} m_{e_1} &= m - \delta m, & m_{e_2} &= \bar{m} - \delta \bar{m}, \\ m_{e_4} &= m + \delta m, & m_{e_3} &= \bar{m} + \delta \bar{m}, \end{aligned} \quad (17)$$

such that

$$\begin{aligned} m &= \frac{m_{e_1} + m_{e_4}}{2}, & \bar{m} &= \frac{m_{e_2} + m_{e_3}}{2}, \\ \delta m &= \frac{m_{e_4} - m_{e_1}}{2}, & \delta \bar{m} &= \frac{m_{e_3} - m_{e_2}}{2}. \end{aligned} \quad (18)$$

The mass differences  $\delta m, \delta \bar{m}$  vanish for the diagonal reactions,  $\chi_{e_1} \chi_{e_2} \rightarrow \chi_{e_1} \chi_{e_2}$ , while they have to be considered as  $\mathcal{O}(v_{\text{rel}}^2)$  corrections in the non-relativistic expansion for the off-diagonal amplitudes. The convention established by (17) implies that particles 1 and 4 have masses closer to the reference mass scale  $m$ , while particles 2 and 3 share the reference scale  $\bar{m}$ . Introducing two distinct mass scales for the particle species allows our results for the absorptive part of the Wilson coefficients to cover both the cases of a set of particles nearly mass-degenerate with the neutralino LSP ( $m \sim \bar{m}$ ) and that of a set of non-relativistic hydrogen-like neutralino and chargino systems ( $m \gg \bar{m}$  or  $m \ll \bar{m}$ ). If in a process  $\chi_i \chi_j \rightarrow \chi_l \chi_k$ , the mass  $m_k(m_l)$  is actually closer to the mass  $m_i(m_j)$  and the mass scales  $m$  and  $\bar{m}$  differ beyond  $\mathcal{O}(v_{\text{rel}}^2)$ , the results for the kinematic factors presented below and collected in the electronic attachment cannot directly be used to determine the corresponding  $\hat{f}$  expressions, as the mass differences  $\delta m, \delta \bar{m}$  related to this reaction are not necessarily small. However the absorptive part of the Wilson coefficients for the reaction with particles 3 and 4 exchanged,  $\chi_i \chi_j \rightarrow \chi_k \chi_l$ , can be obtained from the kinematic factors presented in this work if for that case the particle masses obey (17) with mass differences  $\delta m, \delta \bar{m}$  of  $\mathcal{O}(v_{\text{rel}}^2)$ . The symmetry relations given in (6) then allow to relate the obtained result for the  $\hat{f}$  in  $\chi_i \chi_j \rightarrow \chi_k \chi_l$  rates to the  $\hat{f}$  for the  $\chi_i \chi_j \rightarrow \chi_l \chi_k$  reactions.

We use the hat notation  $\hat{m}_a$  to denote the mass  $m_a$  rescaled by the mass scale  $M = m + \bar{m}$ , *i.e.*

$$\hat{m}_a = \frac{m_a}{M}, \quad (19)$$

and define the dimensionless quantities

$$\begin{aligned} \Delta_m &= \hat{m} - \hat{\bar{m}}, \\ \Delta_{AB} &= \hat{m}_A^2 - \hat{m}_B^2, \\ \beta &= \sqrt{1 - 2(\hat{m}_A^2 + \hat{m}_B^2) + \Delta_{AB}^2}, \end{aligned} \quad (20)$$

where  $m_A$  and  $m_B$  are the masses of the particles  $X_A$  and  $X_B$ , and for  $X_A = X_B$   $\beta$  corresponds to the relative velocity of the  $X_A$  and  $X_B$  particle at leading order in the

expansion in the non-relativistic 3-momenta and the mass differences of the  $\chi_{e_i}$ .<sup>9</sup> Performing the same expansion for the single  $s$ -channel (gauge or Higgs boson  $X_i$ ) exchange propagators, we obtain the following denominator-structure at leading order:

$$P_i^s = 1 - \widehat{m}_i^2 . \quad (21)$$

The corresponding leading-order expansion of  $t$ - and  $u$ -channel chargino, neutralino and sfermion propagators gives

$$\begin{aligned} P_{iAB} &= \widehat{m} \widehat{\overline{m}} + \widehat{m}_i^2 - \widehat{m} \widehat{m}_A^2 - \widehat{\overline{m}} \widehat{m}_B^2 , \\ P_{iBA} &= P_{iAB} \big|_{A \leftrightarrow B} . \end{aligned} \quad (22)$$

The index  $i$  in (22) refers to the  $t$ -channel exchanged particle species and the labels  $A$  and  $B$  are related to the final state particles  $X_A$  and  $X_B$  in the actual  $\chi\chi \rightarrow X_A X_B$  annihilation reaction.

It is convenient to write the kinematic factors for the Wilson coefficients of dimension-8 operators by pulling out factors of the leading-order propagator and  $(\widehat{m} \widehat{\overline{m}})$ , as well as the factor  $\beta$  arising from the phase-space integration. For instance, for the kinematic factors related to dimension-8 four-fermion operators, that derive from the selfenergy topology we define

$$B_{n,i_1 i_2}^{X_A X_B (2s+1) L_J} = \frac{\beta}{(\widehat{m} \widehat{\overline{m}})^2 P_{i_1}^s P_{i_2}^s} \tilde{B}_{n,i_1 i_2}^{X_A X_B (2s+1) L_J} , \quad (23)$$

where the labels  $i_1$  and  $i_2$  refer to the particle species that are exchanged in the left and right  $s$ -channel propagator of the selfenergy diagram. As generically either gauge-boson ( $V$ ) or Higgs ( $S$ )  $s$ -channel exchange occurs in the processes under consideration, the combination  $i_1 i_2$  is given by  $i_1 i_2 = VV, VS, SV, SS$ . Note that with respect to the definitions in the first paper, there are additional normalisation factors in the prefactor's denominator of (23). Likewise, kinematic factors of dimension-8 Wilson coefficients arising from the triangle-topologies are rewritten as

$$\begin{aligned} C_{n,i_1 X}^{(\alpha) X_A X_B (2s+1) L_J} &= \frac{\beta}{\widehat{m} \widehat{\overline{m}} P_{i_1 AB} P_X^s} \tilde{C}_{n,i_1 X}^{(\alpha) X_A X_B (2s+1) L_J} \quad \alpha = 1, 2 , \\ C_{n,i_1 X}^{(\alpha) X_A X_B (2s+1) L_J} &= \frac{\beta}{\widehat{m} \widehat{\overline{m}} P_{i_1 BA} P_X^s} \tilde{C}_{n,i_1 X}^{(\alpha) X_A X_B (2s+1) L_J} \quad \alpha = 3, 4 , \end{aligned} \quad (24)$$

where the index  $i_1$  is now related to the  $t$ - or  $u$ -channel exchanged particle species, and the subscript-index  $X$  indicates the type of exchanged particle ( $X = V, S$ ) in the  $s$ -channel. Finally, the kinematic factors associated with the box topologies are written in

---

<sup>9</sup>For a set of nearly mass-degenerate particles  $\chi_{e_i}$ ,  $\Delta_m$  will be of the order of the mass differences  $\delta m$  and  $\delta \overline{m}$ , and thus yield terms beyond  $\mathcal{O}(v_{\text{rel}}^2)$ . The exact dependence on  $\Delta_m$  is however kept in our results, which in particular allows us to cover the case of annihilation reactions in hydrogen-like  $\chi\chi$  systems as well.



the same form as the correspondent expressions related to leading dimension-6 operators:

$$\begin{aligned}
D_{n, i_1 i_2}^{(1) X_A X_B} ({}^{2s+1} L_J) &= \frac{\beta}{P_{i_1 AB} P_{i_2 BA}} \tilde{D}_{n, i_1 i_2}^{(1) X_A X_B} ({}^{2s+1} L_J) , \\
D_{n, i_1 i_2}^{(2) X_A X_B} ({}^{2s+1} L_J) &= \frac{\beta}{P_{i_1 AB} P_{i_2 AB}} \tilde{D}_{n, i_1 i_2}^{(2) X_A X_B} ({}^{2s+1} L_J) , \\
D_{n, i_1 i_2}^{(3) X_A X_B} ({}^{2s+1} L_J) &= \frac{\beta}{P_{i_1 BA} P_{i_2 AB}} \tilde{D}_{n, i_1 i_2}^{(3) X_A X_B} ({}^{2s+1} L_J) , \\
D_{n, i_1 i_2}^{(4) X_A X_B} ({}^{2s+1} L_J) &= \frac{\beta}{P_{i_1 BA} P_{i_2 BA}} \tilde{D}_{n, i_1 i_2}^{(4) X_A X_B} ({}^{2s+1} L_J) . \tag{25}
\end{aligned}$$

In (25) the indices  $i_1$  and  $i_2$  refer to the exchanged particle species in the left and right  $t$ - and  $u$ -channels of the 1-loop box amplitudes, respectively.

Finally, let us recall the conventions for the label  $n$  established in paper I. Each entry for the index  $n$  in (23–25) is given by a character string with a length equal to the number of vertices that involve fermions in the underlying 1-loop amplitude. In case of  $X_A X_B = VV, VS, SS$  or  $\eta\bar{\eta}$ , the string  $n$  hence has 2, 3 and 4 characters for the selfenergy, triangle and box amplitudes, respectively. If  $X_A X_B = ff$ , the string  $n$  has always 4 characters. The  $i$ th element in a string  $n$  indicates if the coupling factor at the  $i$ th vertex of the respective 1-loop amplitude is of vector/scalar ( $r$ ) or axialvector/pseudoscalar ( $q$ ) type. We enumerate the vertices of box amplitudes according to the respective attached external particles  $\chi_{e_i}, i = 1, \dots, 4$  in ascending order. In case of selfenergy and triangle diagrams with inner vertices without an attached external  $\chi_{e_i}$  our convention to enumerate the vertices is from top to bottom and from left to right. Only those kinematic factors with a given label  $n$  that are non-vanishing are quoted in the following.

### A.2.1 $P$ -wave kinematic factors for $X_A X_B = VV$

The only non-vanishing kinematic factor  $\tilde{B}_{n, i_1 i_2}^{VV}$  in case of  ${}^1P_1$  partial-wave reactions is given by

$$\tilde{B}_{qq, VV}^{VV} ({}^1P_1) = \frac{\Delta_m^2}{24} (8 \beta^2 - 3 \Delta_{AB}^2 - 27) , \tag{26}$$

while for the combined  ${}^3P_J$  waves the non-vanishing kinematic factors read

$$\tilde{B}_{rr, VV}^{VV} ({}^3P_J) = - \frac{\Delta_m^2}{8} (\beta^2 - 6 \Delta_{AB}^2) , \tag{27}$$

$$\tilde{B}_{qq, VV}^{VV} ({}^3P_J) = \frac{1}{12} (8 \beta^2 - 3 \Delta_{AB}^2 - 27) , \tag{28}$$

$$\tilde{B}_{rr, VS}^{VV} ({}^3P_J) = \tilde{B}_{rr, SV}^{VV} ({}^3P_J) = -\frac{3}{4} \hat{m}_W \Delta_m \Delta_{AB} , \tag{29}$$

$$\tilde{B}_{rr, SS}^{VV} ({}^3P_J) = \hat{m}_W^2 . \tag{30}$$

In the case  $X_A X_B = VV$ , there are relations among the  $\alpha = 1(2)$  and  $\alpha = 3(4)$  kinematic factors for the triangle and box topologies which are fulfilled for any  $^{2s+1}L_J$  configuration (in particular also for the kinematic factors associated with the absorptive part of the next-to-next-to-leading order  $S$ -wave Wilson coefficients,  $\hat{g}^{(2s+1)}S_s$  and  $\hat{h}_i^{(2s+1)}S_s$ ). These can be found in paper I, but are repeated here for completeness:

$$\begin{aligned}
\tilde{C}_{n,i_1 V}^{(3)VV}(^{2s+1}L_J) &= -\tilde{C}_{n,i_1 V}^{(1)VV}(^{2s+1}L_J) |_{A \leftrightarrow B} , \\
\tilde{C}_{n,i_1 V}^{(4)VV}(^{2s+1}L_J) &= -\tilde{C}_{n,i_1 V}^{(2)VV}(^{2s+1}L_J) |_{A \leftrightarrow B} , \\
\tilde{C}_{n,i_1 S}^{(3)VV}(^{2s+1}L_J) &= \tilde{C}_{n,i_1 S}^{(1)VV}(^{2s+1}L_J) |_{A \leftrightarrow B} , \\
\tilde{C}_{n,i_1 S}^{(4)VV}(^{2s+1}L_J) &= \tilde{C}_{n,i_1 S}^{(2)VV}(^{2s+1}L_J) |_{A \leftrightarrow B} , \\
\tilde{D}_{n,i_1 i_2}^{(3)VV}(^{2s+1}L_J) &= \tilde{D}_{n,i_1 i_2}^{(1)VV}(^{2s+1}L_J) |_{A \leftrightarrow B} , \\
\tilde{D}_{n,i_1 i_2}^{(4)VV}(^{2s+1}L_J) &= \tilde{D}_{n,i_1 i_2}^{(2)VV}(^{2s+1}L_J) |_{A \leftrightarrow B} .
\end{aligned} \tag{31}$$

The minus sign in the relation for the triangle coefficients  $\tilde{C}_{n,i_1 V}^{(\alpha)VV}$  is a consequence of interchanging the two gauge bosons  $X_A$  and  $X_B$  at the internal three-gauge boson vertex. By virtue of the relations (31), we only need to give the kinematic factors for diagram-topologies  $\alpha = 1, 2$  for both the cases of triangle and box diagram kinematic factors. Starting with the expressions  $\tilde{C}_{n,i_1 V}^{(\alpha)VV}$  for  $^1P_1$  partial waves we have

$$\begin{aligned}
\tilde{C}_{rqq,i_1 V}^{(1)VV}(^1P_1) &= \frac{3}{4} \frac{\hat{m}_{i_1}}{\hat{m} \hat{\bar{m}}} \Delta_m + \frac{\beta^2}{12} \frac{\Delta_m}{P_{i_1 AB}} (\Delta_m - 6 \hat{m}_{i_1} + 2 \Delta_{AB}) \\
&\quad + \frac{\Delta_m}{24} \frac{\Delta_m}{\hat{m} \hat{\bar{m}}} (6 \Delta_m^2 \Delta_{AB} - \Delta_m (5 \beta^2 - 3 \Delta_{AB}^2) - 3 \Delta_{AB}) ,
\end{aligned} \tag{32}$$

$$\tilde{C}_{qqr,i_1 V}^{(2)VV}(^1P_1) = \tilde{C}_{rqq,i_1 V}^{(1)VV}(^1P_1) , \tag{33}$$

whereas for the combined  $^3P_J$  quantum numbers we find

$$\begin{aligned}
\tilde{C}_{rrr,i_1 V}^{(1)VV}(^3P_J) &= \frac{3}{4} \frac{\hat{m}_{i_1}}{\hat{m} \hat{\bar{m}}} \Delta_m \Delta_{AB} + \frac{\beta^2}{12} \frac{\Delta_m}{P_{i_1 AB}} (\Delta_m + 2 \Delta_{AB}) \\
&\quad - \frac{\Delta_m}{8} \frac{\Delta_m}{\hat{m} \hat{\bar{m}}} (2 \Delta_m^2 \Delta_{AB} - \Delta_m (\beta^2 - 3 \Delta_{AB}^2) + \Delta_{AB}) ,
\end{aligned} \tag{34}$$

$$\tilde{C}_{rrr,i_1 V}^{(2)VV}(^3P_J) = \tilde{C}_{rrr,i_1 V}^{(1)VV}(^3P_J) , \tag{35}$$

$$\begin{aligned}
\tilde{C}_{rqq,i_1 V}^{(1)VV}(^3P_J) &= \frac{3}{2} \frac{\hat{m}_{i_1}}{\hat{m} \hat{\bar{m}}} \Delta_m - \frac{\beta^2}{2} \frac{\Delta_m}{P_{i_1 AB}} \\
&\quad - \frac{1}{12} \frac{\Delta_m}{\hat{m} \hat{\bar{m}}} (5 \beta^2 - 9 + 9 \Delta_m^2 - 3 \Delta_{AB} (\Delta_m + \Delta_{AB})) ,
\end{aligned} \tag{36}$$

$$\tilde{C}_{qqr,i_1 V}^{(2)VV}(^3P_J) = \tilde{C}_{rqq,i_1 V}^{(1)VV}(^3P_J) . \tag{37}$$

The coefficients  $\tilde{C}_{n,i_1 S}^{(\alpha)VV}({}^1P_1)$ , corresponding to triangles with a Higgs particle exchanged in the  $s$ -channel, vanish for all  $n$ . The corresponding expressions related to  ${}^3P_J$  reactions read for diagram topologies  $\alpha = 1, 2$

$$\tilde{C}_{rrr,i_1 S}^{(\alpha)VV}({}^3P_J) = -\frac{\hat{m}_W \hat{m}_{i_1}}{\hat{m} \hat{\bar{m}}} - \frac{\beta^2 \hat{m}_W}{6 P_{i_1 AB}} + \frac{\hat{m}_W}{4 \hat{m} \hat{\bar{m}}} (\Delta_m \Delta_{AB} + 1) . \quad (38)$$

All the remaining non-vanishing kinematic factors  $\tilde{C}_{n,i_1 X}^{(\alpha)VV}$  associated with  ${}^1P_1$  and  ${}^3P_J$  scattering reactions with both  $X = V, S$  are related to the above expressions by

$$\begin{aligned} \tilde{C}_{qqr,i_1 X}^{(1)VV}({}^{2s+1}P_J) &= \tilde{C}_{rqq,i_1 X}^{(2)VV}({}^{2s+1}P_J) = \tilde{C}_{rrr,i_1 X}^{(1)VV}({}^{2s+1}P_J)|_{m_{i_1} \rightarrow -m_{i_1}} , \\ \tilde{C}_{qrq,i_1 X}^{(1)VV}({}^{2s+1}P_J) &= \tilde{C}_{qrq,i_1 X}^{(2)VV}({}^{2s+1}P_J) = \tilde{C}_{rqq,i_1 X}^{(1)VV}({}^{2s+1}P_J)|_{m_{i_1} \rightarrow -m_{i_1}} , \end{aligned} \quad (39)$$

where these relations hold in particular in case of separate  ${}^3P_J$ ,  $J = 0, 1, 2$ , partial-wave configurations and hence trivially for the combined  ${}^3P_J$  waves. Finally, the terms related to box diagrams give rise to the following non-vanishing coefficients

$$\begin{aligned} &\tilde{D}_{rrrr,i_1 i_2}^{(1)VV}({}^1P_1) \\ &= -\frac{\hat{m}_{i_1} \hat{m}_{i_2}}{4 (\hat{m} \hat{\bar{m}})^2} - \frac{\hat{m}_{i_1}}{4 (\hat{m} \hat{\bar{m}})^2} (\Delta_m \Delta_{AB} - 1) \\ &\quad - \frac{1}{48 (\hat{m} \hat{\bar{m}})^2} (\Delta_m^2 (2 \beta^2 - 3 \Delta_{AB}^2) + 3) - \frac{\beta^4}{12 P_{i_1 AB} P_{i_2 BA}} \\ &\quad - \frac{\beta^2}{12 \hat{m} \hat{\bar{m}} P_{i_1 AB}} (\Delta_m \Delta_{AB} + 2 \hat{m}_{i_2} - 1) + \left\{ A \leftrightarrow B, i_1 \leftrightarrow i_2 \right\} , \end{aligned} \quad (40)$$

$$\begin{aligned} &\tilde{D}_{rrrr,i_1 i_2}^{(2)VV}({}^1P_1) \\ &= \frac{\hat{m}_{i_1} \hat{m}_{i_2}}{4 (\hat{m} \hat{\bar{m}})^2} - \frac{\hat{m}_{i_1}}{4 (\hat{m} \hat{\bar{m}})^2} (\Delta_m \Delta_{AB} + 1) \\ &\quad - \frac{1}{48 (\hat{m} \hat{\bar{m}})^2} (\Delta_m^2 (2 \beta^2 - 3 \Delta_{AB}^2) - 6 \Delta_m \Delta_{AB} - 3) + \frac{\beta^4}{12 P_{i_1 AB} P_{i_2 AB}} \\ &\quad - \frac{\beta^2}{12 \hat{m} \hat{\bar{m}} P_{i_1 AB}} (\Delta_m \Delta_{AB} - 2 \hat{m}_{i_2} + 1) + \left\{ i_1 \leftrightarrow i_2 \right\} , \end{aligned} \quad (41)$$

$$\begin{aligned} &\tilde{D}_{rqqr,i_1 i_2}^{(1)VV}({}^1P_1) \\ &= \frac{\hat{m}_{i_1} \hat{m}_{i_2}}{4 (\hat{m} \hat{\bar{m}})^2} - \frac{1}{48 (\hat{m} \hat{\bar{m}})^2} (12 \Delta_m^4 - \Delta_m^2 (12 - 4 \beta^2 + 3 \Delta_{AB}^2) + 3) \\ &\quad - \frac{\beta^2}{12 \hat{m} \hat{\bar{m}} P_{i_1 AB}} (2 \Delta_m^2 + \Delta_m (2 \hat{m}_{i_1} - \Delta_{AB}) - 1) \end{aligned}$$

$$\begin{aligned}
& - \frac{\beta^2}{12 P_{i_1 AB} P_{i_2 BA}} \left( 2 \Delta_m^2 - 2 \Delta_m (\hat{m}_{i_1} + \hat{m}_{i_2}) + \beta^2 + 8 \hat{m}_{i_1} \hat{m}_{i_2} \right. \\
& \quad \left. + 2 (\hat{m}_{i_1} - \hat{m}_{i_2}) \Delta_{AB} - 2 \Delta_{AB}^2 \right) + \left\{ A \leftrightarrow B, i_1 \leftrightarrow i_2 \right\}, \quad (42)
\end{aligned}$$

$$\begin{aligned}
& \tilde{D}_{rqr, i_1 i_2}^{(2)VV}({}^1P_1) \\
& = - \frac{\hat{m}_{i_1} \hat{m}_{i_2}}{4 (\hat{m} \hat{\bar{m}})^2} - \frac{\beta^2}{12 \hat{m} \hat{\bar{m}} P_{i_1 AB}} \left( 2 \Delta_m^2 - \Delta_m (2 \hat{m}_{i_1} - \Delta_{AB}) - 1 \right) \\
& \quad - \frac{1}{48 (\hat{m} \hat{\bar{m}})^2} \left( 12 \Delta_m^3 (\Delta_m + \Delta_{AB}) - \Delta_m^2 (12 + 4 \beta^2 - 3 \Delta_{AB}^2) \right. \\
& \quad \left. - 6 \Delta_m \Delta_{AB} + 3 \right) \\
& \quad + \frac{\beta^2}{12 P_{i_1 AB} P_{i_2 AB}} \left( 2 \Delta_m^2 - 2 \Delta_m (\hat{m}_{i_1} + \hat{m}_{i_2} - 2 \Delta_{AB}) \right. \\
& \quad \left. - 2 \Delta_{AB} (\hat{m}_{i_1} + \hat{m}_{i_2} - \Delta_{AB}) - \beta^2 + 8 \hat{m}_{i_1} \hat{m}_{i_2} \right) \\
& \quad + \left\{ i_1 \leftrightarrow i_2 \right\}. \quad (43)
\end{aligned}$$

In case of combined  ${}^3P_{\mathcal{J}}$  waves we have

$$\begin{aligned}
& \tilde{D}_{rrrr, i_1 i_2}^{(1)VV}({}^3P_{\mathcal{J}}) \\
& = \frac{\hat{m}_{i_1} \hat{m}_{i_2}}{2 (\hat{m} \hat{\bar{m}})^2} (1 - \Delta_m^2) + \frac{\hat{m}_{i_1}}{4 (\hat{m} \hat{\bar{m}})^2} (2 \Delta_m^2 - \Delta_m \Delta_{AB} - 1) \\
& \quad + \frac{1}{48 (\hat{m} \hat{\bar{m}})^2} (18 \Delta_m^4 + 3 \Delta_m^2 (\beta^2 - 2 \Delta_{AB}^2 - 10) - 4 \beta^2 + 6 \Delta_{AB}^2 + 12) \\
& \quad + \frac{\beta^2}{12 \hat{m} \hat{\bar{m}} P_{i_1 AB}} (5 \Delta_m^2 + \Delta_m \Delta_{AB} + 2 (2 \hat{m}_{i_1} + \hat{m}_{i_2} - 2)) \\
& \quad + \frac{\beta^2}{12 P_{i_1 AB} P_{i_2 BA}} (3 \Delta_m^2 + 4 (\beta^2 - 3 \hat{m}_{i_1} \hat{m}_{i_2}) - 3 \Delta_{AB}^2) \\
& \quad + \left\{ A \leftrightarrow B, i_1 \leftrightarrow i_2 \right\}, \quad (44)
\end{aligned}$$

$$\tilde{D}_{rrrr, i_1 i_2}^{(2)VV}({}^3P_{\mathcal{J}})$$

$$\begin{aligned}
&= \frac{\widehat{m}_{i_1} \widehat{m}_{i_2}}{2 (\widehat{m} \widehat{\widehat{m}})^2} (1 + \Delta_m^2) - \frac{\widehat{m}_{i_1}}{4 (\widehat{m} \widehat{\widehat{m}})^2} (2 \Delta_m^2 + 3 \Delta_m \Delta_{AB} + 1) \\
&\quad + \frac{1}{48 (\widehat{m} \widehat{\widehat{m}})^2} (18 \Delta_m^4 + 12 \Delta_m^3 \Delta_{AB} - 3 \Delta_m^2 (\beta^2 - 2 \Delta_{AB}^2 + 6) + 12 \Delta_m \Delta_{AB} \\
&\quad \quad - 4 \beta^2 + 6 \Delta_{AB}^2 + 12) \\
&\quad + \frac{\beta^2}{12 \widehat{m} \widehat{\widehat{m}} P_{i_1 AB}} (3 \Delta_m^2 - \Delta_m \Delta_{AB} + 2 (2 \widehat{m}_{i_1} + \widehat{m}_{i_2} - 2)) \\
&\quad - \frac{\beta^2}{36 P_{i_1 AB} P_{i_2 AB}} (9 \Delta_m^2 + 18 \Delta_m \Delta_{AB} - 12 (\beta^2 - 3 \widehat{m}_{i_1} \widehat{m}_{i_2}) + 9 \Delta_{AB}^2) \\
&\quad + \left\{ i_1 \leftrightarrow i_2 \right\}, \tag{45}
\end{aligned}$$

$$\begin{aligned}
&\tilde{D}_{rqqr, i_1 i_2}^{(1)VV}({}^3P_{\mathcal{J}}) \\
&= \frac{\widehat{m}_{i_1} \widehat{m}_{i_2}}{2 (\widehat{m} \widehat{\widehat{m}})^2} \Delta_m^2 + \frac{2 \widehat{m}_{i_1}}{\widehat{m} \widehat{\widehat{m}}} \Delta_m \\
&\quad + \frac{1}{48 (\widehat{m} \widehat{\widehat{m}})^2} (6 \Delta_m^4 + 3 \Delta_m^2 (\beta^2 - 6) - 8 \beta^2 + 6 \Delta_{AB}^2 + 6) \\
&\quad + \frac{\beta^2}{12 \widehat{m} \widehat{\widehat{m}} P_{i_1 AB}} (\Delta_m^2 + \Delta_m (2 \widehat{m}_{i_1} - 4 \widehat{m}_{i_2} - \Delta_{AB}) - 2) \\
&\quad + \frac{\beta^2}{12 P_{i_1 AB} P_{i_2 BA}} (3 \Delta_m^2 - 6 \Delta_m (\widehat{m}_{i_1} + \widehat{m}_{i_2}) + 2 (\beta^2 + 6 \widehat{m}_{i_1} \widehat{m}_{i_2}) \\
&\quad \quad + 6 (\widehat{m}_{i_1} - \widehat{m}_{i_2}) \Delta_{AB} - 3 \Delta_{AB}^2) + \left\{ A \leftrightarrow B, i_1 \leftrightarrow i_2 \right\}, \tag{46}
\end{aligned}$$

$$\begin{aligned}
&\tilde{D}_{rqqr, i_1 i_2}^{(2)VV}({}^3P_{\mathcal{J}}) \\
&= - \frac{\widehat{m}_{i_1} \widehat{m}_{i_2}}{2 (\widehat{m} \widehat{\widehat{m}})^2} \Delta_m^2 - \frac{2 \widehat{m}_{i_1}}{\widehat{m} \widehat{\widehat{m}}} \Delta_m \\
&\quad - \frac{1}{48 (\widehat{m} \widehat{\widehat{m}})^2} (6 \Delta_m^4 - 3 \Delta_m^2 (\beta^2 + 2) + 12 \Delta_m \Delta_{AB} - 8 \beta^2 + 6 \Delta_{AB}^2 + 6) \\
&\quad - \frac{\beta^2}{12 \widehat{m} \widehat{\widehat{m}} P_{i_1 AB}} (3 \Delta_m^2 - \Delta_m (2 \widehat{m}_{i_1} + 4 \widehat{m}_{i_2} - \Delta_{AB}) - 2)
\end{aligned}$$

$$\begin{aligned}
& + \frac{\beta^2}{12 P_{i_1 AB} P_{i_2 AB}} \left( 3 \Delta_m^2 - 6 \Delta_m (\widehat{m}_{i_1} + \widehat{m}_{i_2} - \Delta_{AB}) - 2 (\beta^2 - 6 \widehat{m}_{i_1} \widehat{m}_{i_2}) \right. \\
& \quad \left. - 6 (\widehat{m}_{i_1} + \widehat{m}_{i_2}) \Delta_{AB} + 3 \Delta_{AB}^2 \right) + \left\{ i_1 \leftrightarrow i_2 \right\} . \tag{47}
\end{aligned}$$

The remaining non-vanishing kinematic factors  $\tilde{D}_{n,i_1 i_2}^{(\alpha)VV}$  for diagram topologies  $\alpha = 1, 2$  are related to the expressions given above by

$$\begin{aligned}
\tilde{D}_{qqqq,i_1 i_2}^{(\alpha)VV}(^{2s+1}L_J) &= \tilde{D}_{rrrr,i_1 i_2}^{(\alpha)VV}(^{2s+1}L_J)|_{m_{i_1,2} \rightarrow -m_{i_1,2}} , \\
\tilde{D}_{rrqq,i_1 i_2}^{(\alpha)VV}(^{2s+1}L_J) &= \tilde{D}_{rrrr,i_1 i_2}^{(\alpha)VV}(^{2s+1}L_J)|_{m_{i_2} \rightarrow -m_{i_2}} , \\
\tilde{D}_{qrrr,i_1 i_2}^{(\alpha)VV}(^{2s+1}L_J) &= \tilde{D}_{rrrr,i_1 i_2}^{(\alpha)VV}(^{2s+1}L_J)|_{m_{i_1} \rightarrow -m_{i_1}} , \\
\tilde{D}_{qrrq,i_1 i_2}^{(\alpha)VV}(^{2s+1}L_J) &= \tilde{D}_{rqqr,i_1 i_2}^{(\alpha)VV}(^{2s+1}L_J)|_{m_{i_1,2} \rightarrow -m_{i_1,2}} , \\
\tilde{D}_{rqrr,i_1 i_2}^{(\alpha)VV}(^{2s+1}L_J) &= \tilde{D}_{rqqr,i_1 i_2}^{(\alpha)VV}(^{2s+1}L_J)|_{m_{i_2} \rightarrow -m_{i_2}} , \\
\tilde{D}_{qrqr,i_1 i_2}^{(\alpha)VV}(^{2s+1}L_J) &= \tilde{D}_{rqqr,i_1 i_2}^{(\alpha)VV}(^{2s+1}L_J)|_{m_{i_1} \rightarrow -m_{i_1}} , \tag{48}
\end{aligned}$$

where these relations hold for the kinematic factors related to any  $^{2s+1}L_J$  partial-wave reaction.

### A.2.2 $P$ -wave kinematic factors for $X_A X_B = VS$

The only non-vanishing kinematic factor expression associated with  $^1P_1$  partial-wave reactions and related to selfenergy diagrams reads

$$\tilde{B}_{qq,VV}^{VS}(^1P_1) = \frac{\widehat{m}_W^2}{4} \Delta_m^2 .$$

In case of combined  $^3P_J$  waves we have

$$\tilde{B}_{rr,VV}^{VS}(^3P_J) = -\frac{\widehat{m}_W^2}{4} \Delta_m^2 , \tag{49}$$

$$\tilde{B}_{qq,VV}^{VS}(^3P_J) = \frac{\widehat{m}_W^2}{2} , \tag{50}$$

$$\tilde{B}_{rr,VS}^{VS}(^3P_J) = \tilde{B}_{rr,SV}^{VS}(^3P_J) = \frac{\widehat{m}_W}{8} \Delta_m (3 - \Delta_{AB}) , \tag{51}$$

$$\tilde{B}_{rr,SS}^{VS}(^3P_J) = \frac{1}{16} (\beta^2 - 9 + 6 \Delta_{AB} - \Delta_{AB}^2) . \tag{52}$$

The non-vanishing kinematic factors  $\tilde{C}_{n,i_1 V}^{(\alpha)VS}$  related to the four generic triangle topologies with gauge-boson exchange  $V$  in the single  $s$ -channel read

$$\tilde{C}_{rqq,i_1 V}^{(1)VS}(^1P_1) = \frac{\widehat{m}_W \widehat{m}_{i_1}}{4 \widehat{m} \widehat{m}} \Delta_m^2 + \frac{\widehat{m}_W \Delta_m}{8 \widehat{m} \widehat{m}} (\Delta_m^2 + \Delta_m - 1 + \Delta_{AB}) + \frac{\beta^2 \widehat{m}_W \Delta_m}{12 P_{i_1 AB}} , \tag{53}$$

$$\tilde{C}_{qq, i_1 V}^{(2) VS}(^1 P_1) = \tilde{C}_{rq, i_1 V}^{(1) VS}(^1 P_1) , \quad (54)$$

$$\tilde{C}_{rr, i_1 V}^{(3) VS}(^1 P_1) = -\frac{\hat{m}_W \hat{m}_{i_1}}{4 \hat{m} \hat{\bar{m}}} \Delta_m^2 - \frac{\hat{m}_W \Delta_m}{8 \hat{m} \hat{\bar{m}}} (\Delta_m^2 - \Delta_m - 1 + \Delta_{AB}) - \frac{\beta^2 \hat{m}_W \Delta_m}{12 P_{i_1 BA}} , \quad (55)$$

$$\tilde{C}_{qr, i_1 V}^{(4) VS}(^1 P_1) = \tilde{C}_{rq, i_1 V}^{(3) VS}(^1 P_1) . \quad (56)$$

In case of combined  $^3 P_J$  wave reactions the kinematic factors  $\tilde{C}_{n, i_1 V}^{(\alpha) VS}$  read

$$\tilde{C}_{rrr, i_1 V}^{(1) VS}(^3 P_J) = \tilde{C}_{rrr, i_1 V}^{(2) VS}(^3 P_J) = -\tilde{C}_{rq, i_1 V}^{(1) VS}(^1 P_1) , \quad (57)$$

$$\tilde{C}_{rrr, i_1 V}^{(3) VS}(^3 P_J) = \tilde{C}_{rrr, i_1 V}^{(4) VS}(^3 P_J) = -\tilde{C}_{rq, i_1 V}^{(3) VS}(^1 P_1)|_{\hat{m}_{i_1} \rightarrow -\hat{m}_{i_1}} , \quad (58)$$

$$\tilde{C}_{rq, i_1 V}^{(1) VS}(^3 P_J) = \tilde{C}_{qr, i_1 V}^{(2) VS}(^3 P_J) = \frac{\hat{m}_W \hat{m}_{i_1}}{2 \hat{m} \hat{\bar{m}}} + \frac{\hat{m}_W}{4 \hat{m} \hat{\bar{m}}} (\Delta_m \Delta_{AB} + 1) - \frac{\beta^2 \hat{m}_W}{6 P_{i_1 AB}} , \quad (59)$$

$$\begin{aligned} \tilde{C}_{rq, i_1 V}^{(3) VS}(^3 P_J) &= \tilde{C}_{qr, i_1 V}^{(4) VS}(^3 P_J) \\ &= -\frac{\hat{m}_W \hat{m}_{i_1}}{2 \hat{m} \hat{\bar{m}}} - \frac{\hat{m}_W}{4 \hat{m} \hat{\bar{m}}} (\Delta_m \Delta_{AB} - 1) - \frac{\beta^2 \hat{m}_W}{6 P_{i_1 BA}} . \end{aligned} \quad (60)$$

Turning to  $\tilde{C}_{n, i_1 S}^{(\alpha) VS}$  factors we find that all kinematic factors corresponding to the  $^1 P_1$  configuration vanish. Kinematic factors  $\tilde{C}_{n, i_1 S}^{(\alpha) VS}$  in combined  $^3 P_J$  partial-wave reactions read

$$\begin{aligned} \tilde{C}_{rrr, i_1 S}^{(1) VS}(^3 P_J) &= \frac{\hat{m}_{i_1} \Delta_m}{8 \hat{m} \hat{\bar{m}}} (3 - \Delta_{AB}) + \frac{\beta^2}{24 P_{i_1 AB}} (\Delta_m + 3 + 2 \hat{m}_{i_1}) \\ &\quad + \frac{1}{16 \hat{m} \hat{\bar{m}}} (\beta^2 - 3 + (4 - \Delta_{AB}) \Delta_{AB} + (\Delta_m^2 + \Delta_m)(3 - \Delta_{AB})) , \end{aligned} \quad (61)$$

$$\tilde{C}_{rrr, i_1 S}^{(2) VS}(^3 P_J) = \tilde{C}_{rrr, i_1 S}^{(1) VS}(^3 P_J) , \quad (62)$$

$$\begin{aligned} \tilde{C}_{rrr, i_1 S}^{(3) VS}(^3 P_J) &= \frac{\hat{m}_{i_1} \Delta_m}{8 \hat{m} \hat{\bar{m}}} (3 - \Delta_{AB}) + \frac{\beta^2}{24 P_{i_1 BA}} (\Delta_m - 3 - 2 \hat{m}_{i_1}) \\ &\quad - \frac{1}{16 \hat{m} \hat{\bar{m}}} (\beta^2 - 3 + (4 - \Delta_{AB}) \Delta_{AB} + (\Delta_m^2 - \Delta_m)(3 - \Delta_{AB})) , \end{aligned} \quad (63)$$

$$\tilde{C}_{rrr, i_1 S}^{(4) VS}(^3 P_J) = \tilde{C}_{rrr, i_1 S}^{(3) VS}(^3 P_J) . \quad (64)$$

The additional non-vanishing kinematic factor expressions  $\tilde{C}_{n, i_1 X}^{(\alpha) VS}$  with  $X = V, S$  are related to the above given expressions via

$$\begin{aligned} \tilde{C}_{qr, i_1 X}^{(1) VS}(^{2s+1} P_J) &= \tilde{C}_{rq, i_1 X}^{(2) VS}(^{2s+1} P_J) = -\tilde{C}_{rrr, i_1 X}^{(1) VS}(^{2s+1} P_J)|_{\hat{m}_{i_1} \rightarrow -\hat{m}_{i_1}} , \\ \tilde{C}_{qqr, i_1 X}^{(3) VS}(^{2s+1} P_J) &= \tilde{C}_{rrq, i_1 X}^{(4) VS}(^{2s+1} P_J) = \tilde{C}_{rrr, i_1 X}^{(3) VS}(^{2s+1} P_J)|_{\hat{m}_{i_1} \rightarrow -\hat{m}_{i_1}} , \\ \tilde{C}_{qrq, i_1 X}^{(1) VS}(^{2s+1} P_J) &= \tilde{C}_{qrr, i_1 X}^{(2) VS}(^{2s+1} P_J) = -\tilde{C}_{rrq, i_1 X}^{(1) VS}(^{2s+1} P_J)|_{\hat{m}_{i_1} \rightarrow -\hat{m}_{i_1}} , \end{aligned}$$



$$\tilde{C}_{qrq, i_1 X}^{(3) VS} ({}^{2s+1}P_J) = \tilde{C}_{qrq, i_1 X}^{(4) VS} ({}^{2s+1}P_J) = \tilde{C}_{rrq, i_1 X}^{(3) VS} ({}^{2s+1}P_J)|_{\hat{m}_{i_1} \rightarrow -\hat{m}_{i_1}} . \quad (65)$$

The above relations hold for kinematic factors  $\tilde{C}_{n, i_1 X}^{(\alpha) VS} ({}^{2s+1}L_J)$  associated with the absorptive part of Wilson coefficients  $f({}^{2s+1}L_J)$  and  $g({}^{2s+1}S_s)$  in  $\delta\mathcal{L}_{\text{ann}}^{d=6}$  and  $\delta\mathcal{L}_{\text{ann}}^{d=8}$ .

Finally, kinematic factors  $\tilde{D}_{n, i_1 i_2}^{(\alpha)}$  for  ${}^1P_1$  partial wave reactions are given by

$$\begin{aligned} \tilde{D}_{rrrr, i_1 i_2}^{(\alpha) VS} ({}^1P_1) &= \frac{\beta^2}{24 (\hat{m} \hat{\bar{m}})^2} , \\ \tilde{D}_{rqqr, i_1 i_2}^{(1) VS} ({}^1P_1) &= -\frac{\Delta_m}{8 (\hat{m} \hat{\bar{m}})^2} ((\Delta_m^2 - 1 + \Delta_{AB}) (\hat{m}_{i_1} + \hat{m}_{i_2}) - \Delta_m (\hat{m}_{i_1} - \hat{m}_{i_2})) \\ &\quad - \frac{\hat{m}_{i_1} \hat{m}_{i_2}}{4 (\hat{m} \hat{\bar{m}})^2} \Delta_m^2 - \frac{1}{48 (\hat{m} \hat{\bar{m}})^2} (\Delta_m^2 (3 \Delta_m^2 - 9 + 6 \Delta_{AB}) \\ &\quad - \beta^2 + 3 - 3 (2 - \Delta_{AB}) \Delta_{AB}) \\ &\quad - \frac{\beta^2}{24 \hat{m} \hat{\bar{m}} P_{i_1 AB}} (\Delta_m (\Delta_m + 2 \hat{m}_{i_2} - 2) - 1 - 2 \hat{m}_{i_1}) \\ &\quad - \frac{\beta^2}{24 \hat{m} \hat{\bar{m}} P_{i_2 BA}} (\Delta_m (\Delta_m + 2 \hat{m}_{i_1} + 2) - 1 + 2 \hat{m}_{i_2}) \\ &\quad - \frac{\beta^2}{12 P_{i_1 AB} P_{i_2 BA}} (\Delta_m (\Delta_m + 2 \hat{m}_{i_1} + 2 \hat{m}_{i_2}) + \beta^2 + 4 \hat{m}_{i_1} \hat{m}_{i_2} \\ &\quad - (2 \hat{m}_{i_1} - 2 \hat{m}_{i_2} + \Delta_{AB}) \Delta_{AB}) , \end{aligned} \quad (66)$$

$$\begin{aligned} \tilde{D}_{rqqr, i_1 i_2}^{(2) VS} ({}^1P_1) &= \frac{\hat{m}_{i_1} \Delta_m}{8 (\hat{m} \hat{\bar{m}})^2} (\Delta_m^2 + \Delta_m - 1 + \Delta_{AB}) + \frac{\hat{m}_{i_1} \hat{m}_{i_2}}{8 (\hat{m} \hat{\bar{m}})^2} \Delta_m^2 \\ &\quad + \frac{1}{96 (\hat{m} \hat{\bar{m}})^2} (3 (\Delta_m^2 + \Delta_m - 1) (\Delta_m^2 + \Delta_m - 1 + 2 \Delta_{AB}) - \beta^2 + 3 \Delta_{AB}^2) \\ &\quad + \frac{\beta^2}{24 \hat{m} \hat{\bar{m}} P_{i_1 AB}} (\Delta_m (\Delta_m + 2 \hat{m}_{i_2}) - 2 \hat{m}_{i_1} - 1) \\ &\quad - \frac{\beta^2}{24 P_{i_1 AB} P_{i_2 AB}} ((\Delta_m + 2 (\hat{m}_{i_1} + \hat{m}_{i_2} + \Delta_{AB})) \Delta_m - \beta^2 + 4 \hat{m}_{i_1} \hat{m}_{i_2}) \end{aligned}$$

$$+ (2 (\widehat{m}_{i_1} + \widehat{m}_{i_2}) + \Delta_{AB}) \Delta_{AB} \Big) + \{i_1 \leftrightarrow i_2\} , \quad (67)$$

$$\tilde{D}_{rqq, i_1 i_2}^{(3)VS}(^1P_1) = \tilde{D}_{rqq, i_1 i_2}^{(1)VS}(^1P_1)|_{\widehat{m}_{i_1} \leftrightarrow \widehat{m}_{i_2}} , \quad (68)$$

$$\tilde{D}_{rqq, i_1 i_2}^{(4)VS}(^1P_1) = \tilde{D}_{rqq, i_1 i_2}^{(2)VS}(^1P_1)|_{\widehat{m} \leftrightarrow \widehat{m}, \widehat{m}_{i_1,2} \rightarrow -\widehat{m}_{i_1,2}} . \quad (69)$$

The kinematic factor expressions  $\tilde{D}_{n, i_1 i_2}^{(\alpha)}$  related to  $^3P_{\mathcal{J}}$  partial-wave reactions read

$$\begin{aligned} & \tilde{D}_{rrrr, i_1 i_2}^{(1)VS}(^3P_{\mathcal{J}}) \\ &= \frac{\Delta_m}{8 (\widehat{m} \widehat{\widehat{m}})^2} ((\widehat{m}_{i_1} - \widehat{m}_{i_2}) (\Delta_m^2 + \Delta_{AB} - 1) - (\widehat{m}_{i_1} + \widehat{m}_{i_2}) \Delta_m) - \frac{\widehat{m}_{i_1} \widehat{m}_{i_2}}{4 (\widehat{m} \widehat{\widehat{m}})^2} \Delta_m^2 \\ &+ \frac{1}{48 (\widehat{m} \widehat{\widehat{m}})^2} ((3 \Delta_m^2 + 4 \beta^2 - 9 + 6 \Delta_{AB}) \Delta_m^2 - 3 (\beta^2 - (1 - \Delta_{AB})^2)) \\ &- \frac{\beta^2}{24 \widehat{m} \widehat{\widehat{m}} P_{i_1 AB}} ((\Delta_m + 2 (2 \widehat{m}_{i_1} + \widehat{m}_{i_2} + \Delta_{AB} + 1)) \Delta_m + 2 \widehat{m}_{i_1} + 1) \\ &- \frac{\beta^2}{24 \widehat{m} \widehat{\widehat{m}} P_{i_2 BA}} ((\Delta_m - 2 (2 \widehat{m}_{i_2} + \widehat{m}_{i_1} + \Delta_{AB} + 1)) \Delta_m + 2 \widehat{m}_{i_2} + 1) \\ &+ \frac{\beta^2}{12 P_{i_1 AB} P_{i_2 BA}} (3 \Delta_m (\Delta_m + 2 (\widehat{m}_{i_1} - \widehat{m}_{i_2})) - 12 \widehat{m}_{i_1} \widehat{m}_{i_2} + \beta^2 \\ &- 3 \Delta_{AB} (2 (\widehat{m}_{i_1} + \widehat{m}_{i_2}) + \Delta_{AB})) , \end{aligned} \quad (70)$$

$$\begin{aligned} & \tilde{D}_{rrrr, i_1 i_2}^{(2)VS}(^3P_{\mathcal{J}}) \\ &= - \frac{\widehat{m}_{i_1} \Delta_m}{8 (\widehat{m} \widehat{\widehat{m}})^2} (\Delta_m (\Delta_m + 1) + \Delta_{AB} - 1) - \frac{\widehat{m}_{i_1} \widehat{m}_{i_2}}{8 (\widehat{m} \widehat{\widehat{m}})^2} \Delta_m^2 \\ &- \frac{1}{96 (\widehat{m} \widehat{\widehat{m}})^2} \left( (3 \Delta_m^2 + 6 \Delta_m - 4 \beta^2 - 3 + 6 \Delta_{AB}) \Delta_m^2 \right. \\ &\quad \left. + 6 \Delta_m (\Delta_{AB} - 1) - 3 (\beta^2 - (1 - \Delta_{AB})^2) \right) \\ &- \frac{\beta^2}{24 \widehat{m} \widehat{\widehat{m}} P_{i_1 AB}} (\Delta_m (3 \Delta_m + 2 (2 \widehat{m}_{i_1} + \widehat{m}_{i_2} + \Delta_{AB})) - 2 \widehat{m}_{i_1} - 1) \\ &+ \frac{\beta^2}{24 P_{i_1 AB} P_{i_2 AB}} \left( 3 \Delta_m (\Delta_m + 2 (\widehat{m}_{i_1} + \widehat{m}_{i_2} + \Delta_{AB})) + 12 \widehat{m}_{i_1} \widehat{m}_{i_2} - \beta^2 \right) \end{aligned}$$

$$+ 3 \Delta_{AB} (2 (\widehat{m}_{i_1} + \widehat{m}_{i_2}) + \Delta_{AB}) \Big) + \left\{ i_1 \leftrightarrow i_2 \right\} , \quad (71)$$

$$\tilde{D}_{rrrr, i_1 i_2}^{(3)VS}({}^3P_J) = \tilde{D}_{rrrr, i_1 i_2}^{(1)VS}({}^3P_J)|_{\widehat{m}_{i_1} \leftrightarrow \widehat{m}_{i_2}} , \quad (72)$$

$$\tilde{D}_{rrrr, i_1 i_2}^{(4)VS}({}^3P_J) = \tilde{D}_{rrrr, i_1 i_2}^{(2)VS}({}^3P_J)|_{\widehat{m} \leftrightarrow \widehat{\bar{m}}} , \quad (73)$$

$$\begin{aligned} & \tilde{D}_{rqqr, i_1 i_2}^{(1)VS}({}^3P_J) \\ = & -\frac{1}{4 (\widehat{m} \widehat{\bar{m}})^2} ((\widehat{m}_{i_1} + \widehat{m}_{i_2}) \Delta_m \Delta_{AB} - \widehat{m}_{i_1} + \widehat{m}_{i_2}) - \frac{\widehat{m}_{i_1} \widehat{m}_{i_2}}{2 (\widehat{m} \widehat{\bar{m}})^2} \\ & + \frac{1}{24 (\widehat{m} \widehat{\bar{m}})^2} (\Delta_m^2 (\beta^2 - 3 \Delta_{AB}^2) + 3) + \frac{\beta^2}{12 \widehat{m} \widehat{\bar{m}} P_{i_1 AB}} (\Delta_m \Delta_{AB} + 2 \widehat{m}_{i_2} - 1) \\ & - \frac{\beta^2}{12 \widehat{m} \widehat{\bar{m}} P_{i_2 BA}} (\Delta_m \Delta_{AB} + 2 \widehat{m}_{i_1} + 1) + \frac{\beta^4}{6 P_{i_1 AB} P_{i_2 BA}} , \end{aligned} \quad (74)$$

$$\begin{aligned} & \tilde{D}_{rqqr, i_1 i_2}^{(2)VS}({}^3P_J) \\ = & \frac{\widehat{m}_{i_1}}{4 (\widehat{m} \widehat{\bar{m}})^2} (\Delta_m \Delta_{AB} + 1) + \frac{\widehat{m}_{i_1} \widehat{m}_{i_2}}{4 (\widehat{m} \widehat{\bar{m}})^2} \\ & - \frac{1}{48 (\widehat{m} \widehat{\bar{m}})^2} (\Delta_m^2 (\beta^2 - 3 \Delta_{AB}^2) - 6 \Delta_m \Delta_{AB} - 3) + \frac{\beta^4}{12 P_{i_1 AB} P_{i_2 AB}} \\ & - \frac{\beta^2}{12 \widehat{m} \widehat{\bar{m}} P_{i_1 AB}} (\Delta_m \Delta_{AB} + 2 \widehat{m}_{i_2} + 1) + \left\{ i_1 \leftrightarrow i_2 \right\} , \end{aligned} \quad (75)$$

$$\tilde{D}_{rqqr, i_1 i_2}^{(3)VS}({}^3P_J) = \tilde{D}_{rqqr, i_1 i_2}^{(1)VS}({}^3P_J)|_{\widehat{m}_{i_1} \leftrightarrow \widehat{m}_{i_2}} , \quad (76)$$

$$\tilde{D}_{rqqr, i_1 i_2}^{(4)VS}({}^3P_J) = \tilde{D}_{rqqr, i_1 i_2}^{(2)VS}({}^3P_J)|_{\widehat{m} \leftrightarrow \widehat{\bar{m}}, \widehat{m}_{i_1,2} \rightarrow -\widehat{m}_{i_1,2}} . \quad (77)$$

Note that relation (72) implies that the denominator structures  $P_{i_1 AB}$  and  $P_{i_2 BA}$  in the kinematic factor corresponding to diagram topology  $\alpha = 1$  have to be replaced by  $P_{i_2 AB}$  and  $P_{i_1 BA}$  respectively, in order to arrive at the kinematic factor related to diagram topology  $\alpha = 3$ . Likewise, in (73) the replacement rule for the kinematic factor for diagram-topology  $\alpha = 2$  implies the replacement of  $P_{i_1 AB}$  and  $P_{i_2 AB}$  by  $P_{i_1 BA}$  and  $P_{i_2 BA}$ , respectively. Similar replacements are needed to obtain the  $\alpha = 3, 4$  kinematic factors from the  $\alpha = 1, 2$  expressions with  $n = rqqr$  using (76) and (77). The relations among kinematic factors in (72–73) and (76–77) also hold for the individual kinematic factors related to  ${}^3P_J$  partial-wave reactions with  $J = 0, 1, 2$ .

The remaining non-vanishing kinematic factors  $\tilde{D}_{n, i_1 i_2}^{(\alpha)}$  for diagram topologies  $\alpha = 1, 2$

derive from the above given expressions in the following way:

$$\begin{aligned}
\tilde{D}_{qqqq, i_1 i_2}^{(\alpha) VS} (2s+1 L_J) &= (-1)^\alpha \tilde{D}_{rrrr, i_1 i_2}^{(\alpha) VS} (2s+1 L_J) | \hat{m}_{i_{1,2}} \rightarrow -\hat{m}_{i_{1,2}} , \\
\tilde{D}_{rrqq, i_1 i_2}^{(\alpha) VS} (2s+1 L_J) &= (-1)^{\alpha+1} \tilde{D}_{rrrr, i_1 i_2}^{(\alpha) VS} (2s+1 L_J) | \hat{m}_{i_2} \rightarrow -\hat{m}_{i_2} , \\
\tilde{D}_{qrrr, i_1 i_2}^{(\alpha) VS} (2s+1 L_J) &= -\tilde{D}_{rrrr, i_1 i_2}^{(\alpha) VS} (2s+1 L_J) | \hat{m}_{i_1} \rightarrow -\hat{m}_{i_1} , \\
\tilde{D}_{qrrq, i_1 i_2}^{(\alpha) VS} (2s+1 L_J) &= (-1)^\alpha \tilde{D}_{rqqr, i_1 i_2}^{(\alpha) VS} (2s+1 L_J) | \hat{m}_{i_{1,2}} \rightarrow -\hat{m}_{i_{1,2}} , \\
\tilde{D}_{rqrq, i_1 i_2}^{(\alpha) VS} (2s+1 L_J) &= (-1)^{\alpha+1} \tilde{D}_{rqqr, i_1 i_2}^{(\alpha) VS} (2s+1 L_J) | \hat{m}_{i_2} \rightarrow -\hat{m}_{i_2} , \\
\tilde{D}_{qrqr, i_1 i_2}^{(\alpha) VS} (2s+1 L_J) &= -\tilde{D}_{rqqr, i_1 i_2}^{(\alpha) VS} (2s+1 L_J) | \hat{m}_{i_1} \rightarrow -\hat{m}_{i_1} .
\end{aligned} \tag{78}$$

Similarly, in case of diagram topologies  $\alpha = 3, 4$  we find

$$\begin{aligned}
\tilde{D}_{qqqq, i_1 i_2}^{(\alpha) VS} (2s+1 L_J) &= (-1)^\alpha \tilde{D}_{rrrr, i_1 i_2}^{(\alpha) VS} (2s+1 L_J) | \hat{m}_{i_{1,2}} \rightarrow -\hat{m}_{i_{1,2}} , \\
\tilde{D}_{rrqq, i_1 i_2}^{(\alpha) VS} (2s+1 L_J) &= (-1)^\alpha \tilde{D}_{rrrr, i_1 i_2}^{(\alpha) VS} (2s+1 L_J) | \hat{m}_{i_2} \rightarrow -\hat{m}_{i_2} , \\
\tilde{D}_{qrrr, i_1 i_2}^{(\alpha) VS} (2s+1 L_J) &= \tilde{D}_{rrrr, i_1 i_2}^{(\alpha) VS} (2s+1 L_J) | \hat{m}_{i_1} \rightarrow -\hat{m}_{i_1} , \\
\tilde{D}_{qrrq, i_1 i_2}^{(\alpha) VS} (2s+1 L_J) &= (-1)^\alpha \tilde{D}_{rqqr, i_1 i_2}^{(\alpha) VS} (2s+1 L_J) | \hat{m}_{i_{1,2}} \rightarrow -\hat{m}_{i_{1,2}} , \\
\tilde{D}_{rqrq, i_1 i_2}^{(\alpha) VS} (2s+1 L_J) &= (-1)^\alpha \tilde{D}_{rqqr, i_1 i_2}^{(\alpha) VS} (2s+1 L_J) | \hat{m}_{i_2} \rightarrow -\hat{m}_{i_2} , \\
\tilde{D}_{qrqr, i_1 i_2}^{(\alpha) VS} (2s+1 L_J) &= \tilde{D}_{rqqr, i_1 i_2}^{(\alpha) VS} (2s+1 L_J) | \hat{m}_{i_1} \rightarrow -\hat{m}_{i_1} .
\end{aligned} \tag{79}$$

The relations in (78)–(79) are valid for  $\tilde{D}_{n, i_1 i_2}^{(\alpha) VS} (2s+1 L_J)$  expressions related to any  $^{2s+1} L_J$  partial-wave reaction.

### A.2.3 $P$ -wave kinematic factors for $X_A X_B = SS$

In case of  $X_A X_B = SS$  the only non-vanishing kinematic factor  $\tilde{B}_{n, i_1 i_2}^{SS}$  in  $^1 P_1$  partial-wave scattering reactions reads

$$\tilde{B}_{qq, VV}^{SS} (^1 P_1) = \frac{\beta^2}{12} \Delta_m^2 , \tag{80}$$

while the corresponding kinematic factors for combined  $^3 P_J$  reactions read

$$\tilde{B}_{rr, VV}^{SS} (^3 P_J) = \frac{1}{4} \Delta_m^2 \Delta_{AB}^2 , \tag{81}$$

$$\tilde{B}_{qq, VV}^{SS} (^3 P_J) = \frac{\beta^2}{6} , \tag{82}$$

$$\tilde{B}_{rr, VS}^{SS} (^3 P_J) = \tilde{B}_{rr, SV}^{SS} (^3 P_J) = \frac{\hat{m}_W}{4} \Delta_m \Delta_{AB} , \tag{83}$$

$$\tilde{B}_{rr,SS}^{SS}(^3P_J) = \frac{\hat{m}_W^2}{4} . \quad (84)$$

The kinematic factors for diagram topologies  $\alpha = 3(4)$  and  $\alpha = 1(2)$  obey in both the cases of triangle and box diagrams certain relations,

$$\begin{aligned} \tilde{C}_{n,i_1V}^{(3)SS}(^{2s+1}L_J) &= - \tilde{C}_{n,i_1V}^{(1)SS}(^{2s+1}L_J) |_{A \leftrightarrow B} , \\ \tilde{C}_{n,i_1V}^{(4)SS}(^{2s+1}L_J) &= - \tilde{C}_{n,i_1V}^{(2)SS}(^{2s+1}L_J) |_{A \leftrightarrow B} , \\ \tilde{C}_{n,i_1S}^{(3)SS}(^{2s+1}L_J) &= \tilde{C}_{n,i_1S}^{(1)SS}(^{2s+1}L_J) |_{A \leftrightarrow B} , \\ \tilde{C}_{n,i_1S}^{(4)SS}(^{2s+1}L_J) &= \tilde{C}_{n,i_1S}^{(2)SS}(^{2s+1}L_J) |_{A \leftrightarrow B} , \\ \tilde{D}_{n,i_1i_2}^{(3)SS}(^{2s+1}L_J) &= \tilde{D}_{n,i_1i_2}^{(1)SS}(^{2s+1}L_J) |_{A \leftrightarrow B} , \\ \tilde{D}_{n,i_1i_2}^{(4)SS}(^{2s+1}L_J) &= \tilde{D}_{n,i_1i_2}^{(2)SS}(^{2s+1}L_J) |_{A \leftrightarrow B} , \end{aligned} \quad (85)$$

that generically apply for the respective kinematic factors related to a given  $^{2s+1}L_J$  partial-wave configuration, including kinematic factors related to coefficients  $\hat{g}(^{2s+1}S_s)$  and  $\hat{h}_i(^{2s+1}S_s)$  (see also Eq. (111) in paper I).

In case of  $^1P_1$  waves we find the following expressions for kinematic factors  $\tilde{C}_{n,i_1V}^{(\alpha)SS}$  and diagram topologies  $\alpha = 1, 2$ :

$$\tilde{C}_{rrq, i_1V}^{(1)SS}(^1P_1) = \tilde{C}_{qqr, i_1V}^{(2)SS}(^1P_1) = \frac{\beta^2}{24 \hat{m} \hat{\bar{m}}} \Delta_m^2 - \frac{\beta^2 \Delta_m}{12 P_{i_1AB}} (\Delta_m + 2 \hat{m}_{i_1} + \Delta_{AB}) . \quad (86)$$

In case of combined  $^3P_J$  reactions the corresponding expressions read

$$\begin{aligned} \tilde{C}_{rrr, i_1V}^{(1)SS}(^3P_J) &= \tilde{C}_{rrr, i_1V}^{(2)SS}(^3P_J) \\ &= - \frac{\hat{m}_{i_1}}{4 \hat{m} \hat{\bar{m}}} \Delta_m \Delta_{AB} - \frac{\Delta_m \Delta_{AB}}{8 \hat{m} \hat{\bar{m}}} (\Delta_m \Delta_{AB} + 1) + \frac{\beta^2 \Delta_m \Delta_{AB}}{12 P_{i_1AB}} , \end{aligned} \quad (87)$$

$$\tilde{C}_{rrq, i_1V}^{(1)SS}(^3P_J) = \tilde{C}_{qqr, i_1V}^{(2)SS}(^3P_J) = \frac{\beta^2}{12 \hat{m} \hat{\bar{m}}} . \quad (88)$$

Turning to kinematic factors  $\tilde{C}_{n, i_1S}^{(\alpha)SS}$  with  $\alpha = 1, 2$  we find

$$\begin{aligned} \tilde{C}_{rrr, i_1S}^{(1)SS}(^3P_J) &= \tilde{C}_{rrr, i_1S}^{(2)SS}(^3P_J) \\ &= - \frac{\hat{m}_W}{8 \hat{m} \hat{\bar{m}}} (\Delta_m \Delta_{AB} + 1) - \frac{\hat{m}_W}{4 \hat{m} \hat{\bar{m}}} \hat{m}_{i_1} + \frac{\beta^2}{12 P_{i_1AB}} \hat{m}_W , \end{aligned} \quad (89)$$

and, as in the case of leading-order  $^1S_0$  and  $^3S_1$  kinematic factors (see Eq.(115) in paper I), the remaining non-vanishing expressions for  $\tilde{C}_{n, i_1X}^{(\alpha)SS}$  with both  $X = V, S$  and  $\alpha = 1, 2$

that are associated with  $^1P_1$  and  $^3P_J$  (as well as the separate  $^3P_J, J = 0, 1, 2$ ) partial-wave configurations, derive from the above given expressions in the following way:

$$\begin{aligned}\tilde{C}_{qqr, i_1 X}^{(1) SS}(^{2s+1}P_J) &= \tilde{C}_{rqq, i_1 X}^{(2) SS}(^{2s+1}P_J) = -\tilde{C}_{rrr, i_1 X}^{(1) SS}(^{2s+1}P_J)|_{\hat{m}_{i_1} \rightarrow -\hat{m}_{i_1}}, \\ \tilde{C}_{qrq, i_1 X}^{(1) SS}(^{2s+1}P_J) &= \tilde{C}_{qrq, i_1 X}^{(2) SS}(^{2s+1}P_J) = -\tilde{C}_{rrq, i_1 X}^{(1) SS}(^{2s+1}P_J)|_{\hat{m}_{i_1} \rightarrow -\hat{m}_{i_1}}.\end{aligned}\quad (90)$$

Finally, the box-diagram related kinematic factors  $\tilde{D}_{n, i_1 i_2}^{(\alpha) SS}$  for diagram topologies  $\alpha = 1, 2$  are given by

$$\begin{aligned}\tilde{D}_{rqq, i_1 i_2}^{(1) SS}(^1P_1) &= -\frac{\beta^2 \Delta_m^2}{96 (\hat{m} \hat{\bar{m}})^2} + \frac{\beta^2 \Delta_m}{24 \hat{m} \hat{\bar{m}} P_{i_1 AB}} (\Delta_m + 2 \hat{m}_{i_1} + \Delta_{AB}) \\ &\quad - \frac{\beta^2}{24 P_{i_1 AB} P_{i_2 BA}} (\Delta_m^2 + 2 \Delta_m (\hat{m}_{i_1} + \hat{m}_{i_2}) \\ &\quad + (2 \hat{m}_{i_1} + \Delta_{AB}) (2 \hat{m}_{i_2} - \Delta_{AB})) \\ &\quad + \left\{ A \leftrightarrow B, i_1 \leftrightarrow i_2 \right\},\end{aligned}\quad (91)$$

$$\begin{aligned}\tilde{D}_{rqq, i_1 i_2}^{(2) SS}(^1P_1) &= \frac{\beta^2 \Delta_m^2}{96 (\hat{m} \hat{\bar{m}})^2} - \frac{\beta^2 \Delta_m}{24 \hat{m} \hat{\bar{m}} P_{i_1 AB}} (\Delta_m + 2 \hat{m}_{i_1} + \Delta_{AB}) \\ &\quad + \frac{\beta^2}{24 P_{i_1 AB} P_{i_2 AB}} (\Delta_m^2 + 2 \Delta_m (\hat{m}_{i_1} + \hat{m}_{i_2} + \Delta_{AB}) \\ &\quad + (2 \hat{m}_{i_1} + \Delta_{AB}) (2 \hat{m}_{i_2} + \Delta_{AB})) \\ &\quad + \left\{ i_1 \leftrightarrow i_2 \right\}.\end{aligned}\quad (92)$$

For the combined  $^3P_J$  reactions we have

$$\begin{aligned}\tilde{D}_{rrr, i_1 i_2}^{(1) SS}(^3P_J) &= \frac{\hat{m}_{i_1} \hat{m}_{i_2}}{8 (\hat{m} \hat{\bar{m}})^2} - \frac{\hat{m}_{i_1}}{8 (\hat{m} \hat{\bar{m}})^2} (\Delta_m \Delta_{AB} - 1) \\ &\quad + \frac{\beta^2}{24 \hat{m} \hat{\bar{m}} P_{i_1 AB}} (\Delta_m \Delta_{AB} - 2 \hat{m}_{i_2} - 1) + \frac{\beta^4}{24 P_{i_1 AB} P_{i_2 BA}} \\ &\quad - \frac{1}{32 (\hat{m} \hat{\bar{m}})^2} (\Delta_m^2 \Delta_{AB}^2 - 1) + \left\{ A \leftrightarrow B, i_1 \leftrightarrow i_2 \right\},\end{aligned}\quad (93)$$

$$\begin{aligned}\tilde{D}_{rrr, i_1 i_2}^{(2) SS}(^3P_J) &= \frac{\hat{m}_{i_1} \hat{m}_{i_2}}{8 (\hat{m} \hat{\bar{m}})^2} + \frac{\hat{m}_{i_1}}{8 (\hat{m} \hat{\bar{m}})^2} (\Delta_m \Delta_{AB} + 1) \\ &\quad - \frac{\beta^2}{24 \hat{m} \hat{\bar{m}} P_{i_1 AB}} (\Delta_m \Delta_{AB} + 2 \hat{m}_{i_2} + 1) + \frac{\beta^4}{24 P_{i_1 AB} P_{i_2 AB}}\end{aligned}$$

$$+ \frac{1}{32 (\widehat{m} \widehat{\overline{m}})^2} (\Delta_m \Delta_{AB} + 1)^2 + \left\{ i_1 \leftrightarrow i_2 \right\} , \quad (94)$$

$$\tilde{D}_{rqq, i_1 i_2}^{(\alpha) SS}({}^3P_J) = (-1)^\alpha \frac{\beta^2}{24 (\widehat{m} \widehat{\overline{m}})^2} . \quad (95)$$

The remaining non-vanishing kinematic factors can be related to the above given expressions by making use of the following relations among  $\tilde{D}_{n, i_1 i_2}^{(\alpha) SS}$  kinematic factors with different labels  $n$ :

$$\begin{aligned} \tilde{D}_{qqqq, i_1 i_2}^{(\alpha) SS}({}^{2s+1}L_J) &= \tilde{D}_{rrrr, i_1 i_2}^{(\alpha) SS}({}^{2s+1}L_J) | \hat{m}_{i_1,2} \rightarrow -\hat{m}_{i_1,2} , \\ \tilde{D}_{rrqq, i_1 i_2}^{(\alpha) SS}({}^{2s+1}L_J) &= -\tilde{D}_{rrrr, i_1 i_2}^{(\alpha) SS}({}^{2s+1}L_J) | \hat{m}_{i_2} \rightarrow -\hat{m}_{i_2} , \\ \tilde{D}_{qqrr, i_1 i_2}^{(\alpha) SS}({}^{2s+1}L_J) &= -\tilde{D}_{rrrr, i_1 i_2}^{(\alpha) SS}({}^{2s+1}L_J) | \hat{m}_{i_1} \rightarrow -\hat{m}_{i_1} , \\ \tilde{D}_{qrrq, i_1 i_2}^{(\alpha) SS}({}^{2s+1}L_J) &= \tilde{D}_{rqq, i_1 i_2}^{(\alpha) SS}({}^{2s+1}L_J) | \hat{m}_{i_1,2} \rightarrow -\hat{m}_{i_1,2} , \\ \tilde{D}_{rqq, i_1 i_2}^{(\alpha) SS}({}^{2s+1}L_J) &= -\tilde{D}_{rqq, i_1 i_2}^{(\alpha) SS}({}^{2s+1}L_J) | \hat{m}_{i_2} \rightarrow -\hat{m}_{i_2} , \\ \tilde{D}_{qrqr, i_1 i_2}^{(\alpha) SS}({}^{2s+1}L_J) &= -\tilde{D}_{rqq, i_1 i_2}^{(\alpha) SS}({}^{2s+1}L_J) | \hat{m}_{i_1} \rightarrow -\hat{m}_{i_1} . \end{aligned} \quad (96)$$

Note that these relations hold among the kinematic factors associated with any of the Wilson coefficients  $\hat{f}({}^{2s+1}L_J)$ ,  $\hat{g}({}^{2s+1}S_s)$  and  $\hat{h}_i({}^{2s+1}S_s)$ .

#### A.2.4 $P$ -wave kinematic factors for $X_A X_B = ff$

The relevant kinematic factors  $\tilde{B}_{n, i_1 i_2}^{ff}$ , related to the selfenergy diagram topology with a fermion-fermion final state, read

$$\tilde{B}_{qqqq, VV}^{ff}({}^1P_1) = \frac{\Delta_m^2}{12} (\beta^2 + 3 - 12 \hat{m}_A \hat{m}_B - 3 \Delta_{AB}^2) , \quad (97)$$

for the  ${}^1P_1$  partial-wave configuration, and

$$\tilde{B}_{rrrr, VV}^{ff}({}^3P_J) = -\frac{\Delta_m^2}{4} (\beta^2 - 1 + 4 \hat{m}_A \hat{m}_B + \Delta_{AB}^2) , \quad (98)$$

$$\tilde{B}_{rrrr, VS}^{ff}({}^3P_J) = \tilde{B}_{rrrr, SV}^{ff}({}^3P_J) = -\frac{\Delta_m}{2} (\hat{m}_A - \hat{m}_B - (\hat{m}_A + \hat{m}_B) \Delta_{AB}) , \quad (99)$$

$$\tilde{B}_{rrrr, SS}^{ff}({}^3P_J) = \frac{1}{4} (\beta^2 + 1 - 4 \hat{m}_A \hat{m}_B - \Delta_{AB}^2) , \quad (100)$$

$$\tilde{B}_{qqq, VV}^{ff}({}^3P_J) = \frac{1}{6} (\beta^2 + 3 - 12 \hat{m}_A \hat{m}_B - 3 \Delta_{AB}^2) , \quad (101)$$

for the  ${}^3P_J$  case. In the case that the  $s$ -channel exchanged particles are of the same type ( $i_1 i_2 = VV, SS$ ), the additional non-vanishing kinematic factors are related to the expressions (97)–(101) as

$$\tilde{B}_{rqq, i_1 i_2}^{ff}({}^{2s+1}P_J) = \tilde{B}_{rrrr, i_1 i_2}^{ff}({}^{2s+1}P_J) | \hat{m}_A \hat{m}_B \rightarrow -\hat{m}_A \hat{m}_B , \quad (102)$$



$$\tilde{B}_{qrrq, i_1 i_2}^{ff}(^{2s+1}P_J) = \tilde{B}_{qqqq, i_1 i_2}^{ff}(^{2s+1}P_J)|_{\hat{m}_A \hat{m}_B \rightarrow -\hat{m}_A \hat{m}_B}, \quad (103)$$

where the notation for the replacement rule applies to the term  $\hat{m}_A \hat{m}_B$ , but all other occurrences of  $\hat{m}_A$  or  $\hat{m}_B$  shall be left untouched. Similarly, in case of  $s$ -channel particles of different type ( $i_1 i_2 = VS, SV$ ), the additional non-vanishing  $\tilde{B}_{n, i_1 i_2}^{ff}$  terms are given by

$$\tilde{B}_{rqqr, i_1 i_2}^{ff}(^{2s+1}P_J) = -\tilde{B}_{rrrr, i_1 i_2}^{ff}(^{2s+1}P_J)|_{\hat{m}_A \rightarrow -\hat{m}_A}, \quad (104)$$

$$\tilde{B}_{qrrq, i_1 i_2}^{ff}(^{2s+1}P_J) = -\tilde{B}_{qqqq, i_1 i_2}^{ff}(^{2s+1}P_J)|_{\hat{m}_A \rightarrow -\hat{m}_A}. \quad (105)$$

There are relations among kinematic factors for diagram topologies  $\alpha = 3(4)$  and diagram topologies  $\alpha = 1(2)$  for both the cases of box and triangle diagrams, that are given by ( $X = V, S$ )

$$\begin{aligned} C_{n, i_1 X}^{(3)ff}(^{2s+1}L_J) &= C_{n, i_1 X}^{(1)ff}(^{2s+1}L_J) |_{A \leftrightarrow B}, \\ C_{n, i_1 X}^{(4)ff}(^{2s+1}L_J) &= C_{n, i_1 X}^{(2)ff}(^{2s+1}L_J) |_{A \leftrightarrow B}, \\ D_{n, i_1 i_2}^{(3)ff}(^{2s+1}L_J) &= D_{n, i_1 i_2}^{(1)ff}(^{2s+1}L_J) |_{A \leftrightarrow B}, \\ D_{n, i_1 i_2}^{(4)ff}(^{2s+1}L_J) &= D_{n, i_1 i_2}^{(2)ff}(^{2s+1}L_J) |_{A \leftrightarrow B}. \end{aligned} \quad (106)$$

Note that these relations are valid among kinematic factors associated with any  $^{2s+1}L_J$  partial wave (in particular also for  $\hat{g}^{(2s+1)}S_s$  and  $\hat{h}_i^{(2s+1)}S_s$  associated kinematic factors).

The structures  $C_{n, i_1 V}^{(\alpha)ff}(^{2s+1}P_J)$  that we obtain for diagram topologies  $\alpha = 1, 2$  read

$$\begin{aligned} C_{qqqq, i_1 X}^{(\alpha)ff}(^1P_1) &= \frac{\Delta_m}{48 \hat{m} \hat{\bar{m}}} \left( 6 (\hat{m}_A + \hat{m}_B) \Delta_{AB} - 6 (\hat{m}_A - \hat{m}_B) \right. \\ &\quad \left. - \Delta_m (\beta^2 + 3 - 12 \hat{m}_A \hat{m}_B - 3 \Delta_{AB}^2) \right) \\ &\quad + \frac{\beta^2 \Delta_m}{12 P_{i_1 AB}} (\hat{m}_A - \hat{m}_B - \Delta_{AB}), \end{aligned} \quad (107)$$

and, for the combined  $^3P_J$  partial-wave reactions,

$$\begin{aligned} C_{rrrr, i_1 X}^{(\alpha)ff}(^3P_J) &= \frac{\Delta_m}{16 \hat{m} \hat{\bar{m}}} \left( -2 (\hat{m}_A + \hat{m}_B) \Delta_{AB} + 2 (\hat{m}_A - \hat{m}_B) \right. \\ &\quad \left. + \Delta_m (\beta^2 - 1 + 4 \hat{m}_A \hat{m}_B + \Delta_{AB}^2) \right) \\ &\quad - \frac{\beta^2 \Delta_m}{12 P_{i_1 AB}} (\hat{m}_A - \hat{m}_B + \Delta_{AB}), \end{aligned} \quad (108)$$

$$C_{rqqr, i_1 X}^{(1)ff}(^3P_J) = \frac{1}{24 \hat{m} \hat{\bar{m}}} \left( 6 (\hat{m}_A + \hat{m}_B - (\hat{m}_A - \hat{m}_B) \Delta_{AB}) \Delta_m \right.$$

$$\begin{aligned}
& + \beta^2 + 3 + 12 \hat{m}_A \hat{m}_B - 3 \Delta_{AB}^2 \Big) \\
& - \frac{\beta^2}{6 P_{i_1 AB}} (1 - \hat{m}_A + \hat{m}_B) , \tag{109}
\end{aligned}$$

$$C_{qrqr, i_1 X}^{(2) ff}({}^3P_{\mathcal{J}}) = C_{qrqr, i_1 X}^{(1) ff}({}^3P_{\mathcal{J}}) . \tag{110}$$

The following relations for the additional non-vanishing  $C_{n, i_1 V}^{(\alpha) ff}$  hold:

$$\begin{aligned}
\tilde{C}_{qrqr, i_1 V}^{(1) ff}({}^1P_1) &= \tilde{C}_{qrqr, i_1 V}^{(2) ff}({}^1P_1) = - \tilde{C}_{qqqq, i_1 V}^{(\alpha) ff}({}^1P_1)|_{m_B \rightarrow -m_B} , \\
\tilde{C}_{qrrq, i_1 V}^{(\alpha) ff}({}^1P_1) &= \tilde{C}_{qqqq, i_1 V}^{(\alpha) ff}({}^1P_1)|_{m_A \rightarrow -m_A} , \\
\tilde{C}_{rrqq, i_1 V}^{(1) ff}({}^1P_1) &= \tilde{C}_{qrrr, i_1 V}^{(2) ff}({}^1P_1) = - \tilde{C}_{qqqq, i_1 V}^{(\alpha) ff}({}^1P_1)|_{m_{A,B} \rightarrow -m_{A,B}} , \\
\tilde{C}_{qrrr, i_1 V}^{(1) ff}({}^3P_{\mathcal{J}}) &= \tilde{C}_{rrqq, i_1 V}^{(2) ff}({}^3P_{\mathcal{J}}) = - \tilde{C}_{rrrr, i_1 V}^{(1) ff}({}^3P_{\mathcal{J}})|_{m_{A,B} \rightarrow -m_{A,B}} , \\
\tilde{C}_{qrrq, i_1 V}^{(\alpha) ff}({}^3P_{\mathcal{J}}) &= - \tilde{C}_{qrqr, i_1 V}^{(1) ff}({}^3P_{\mathcal{J}})|_{m_{A,B} \rightarrow -m_{A,B}} . \tag{111}
\end{aligned}$$

Turning to the expressions  $C_{n, i_1 S}^{(\alpha) ff}$ , we find that all kinematic factors in case of  ${}^1P_1$  reactions vanish, as it has to be due to total angular-momentum conservation. The non-vanishing kinematic factors in combined  ${}^3P_{\mathcal{J}}$  reactions read ( $\alpha = 1, 2$ )

$$\begin{aligned}
\tilde{C}_{rrrr, i_1 S}^{(\alpha) ff}({}^3P_{\mathcal{J}}) &= \frac{1}{16 \hat{m} \hat{\bar{m}}} \Big( 2(-\hat{m}_A + \hat{m}_B + (\hat{m}_A + \hat{m}_B) \Delta_{AB}) \Delta_m \\
& + \beta^2 + 1 - 4 \hat{m}_A \hat{m}_B - \Delta_{AB}^2 \Big) \\
& - \frac{\beta^2}{12 P_{i_1 AB}} (1 + \hat{m}_A + \hat{m}_B) , \tag{112}
\end{aligned}$$

$$\tilde{C}_{qrrr, i_1 S}^{(1) ff}({}^3P_{\mathcal{J}}) = \tilde{C}_{rrqq, i_1 S}^{(2) ff}({}^3P_{\mathcal{J}}) = \tilde{C}_{rrrr, i_1 S}^{(1) ff}({}^3P_{\mathcal{J}})|_{m_{A,B} \rightarrow -m_{A,B}} . \tag{113}$$

In case of  ${}^1P_1$  partial-wave reactions the kinematic factors  $\tilde{D}_{n, i_1 i_2}^{(\alpha) ff}$  for  $\alpha = 1, 2$  read

$$\begin{aligned}
& \tilde{D}_{rrrr, i_1 i_2}^{(1) ff}({}^1P_1) \\
&= \frac{1}{384 (\hat{m} \hat{\bar{m}})^2} \Big( \beta^2 (1 + \Delta_m^2) - (3 - 12 \hat{m}_A \hat{m}_B - 3 \Delta_{AB}^2) (1 - \Delta_m^2) \Big) \\
& + \frac{\beta^2}{48 \hat{m} \hat{\bar{m}} P_{i_1 AB}} \Big( 1 + \hat{m}_A + \hat{m}_B + \Delta_m (\hat{m}_A - \hat{m}_B + \Delta_{AB}) \Big) \\
& - \frac{\beta^2}{48 P_{i_1 AB} P_{i_2 BA}} (1 + 2 \hat{m}_A + \Delta_{AB}) (1 + 2 \hat{m}_B - \Delta_{AB}) \\
& + \left\{ A \leftrightarrow B, i_1 \leftrightarrow i_2 \right\} , \tag{114}
\end{aligned}$$

$$\begin{aligned}
& \tilde{D}_{rrrr, i_1 i_2}^{(2)ff} (^1P_1) \\
&= \frac{1}{384 (\widehat{m} \widehat{\bar{m}})^2} \left( \beta^2 (\Delta_m^2 - 1) + (3 - 12 \widehat{m}_A \widehat{m}_B - 3 \Delta_{AB}^2) (\Delta_m^2 + 1) \right. \\
&\quad \left. - 12 \Delta_m (\widehat{m}_A - \widehat{m}_B - (\widehat{m}_A + \widehat{m}_B) \Delta_{AB}) \right) \\
&\quad - \frac{\beta^2}{48 \widehat{m} \widehat{\bar{m}} P_{i_1 AB}} \left( 1 + \widehat{m}_A + \widehat{m}_B - \Delta_m (\widehat{m}_A - \widehat{m}_B + \Delta_{AB}) \right) \\
&\quad + \frac{\beta^2}{48 P_{i_1 AB} P_{i_2 AB}} (1 + 2 \widehat{m}_A + \Delta_{AB}) (1 + 2 \widehat{m}_B - \Delta_{AB}) + \left\{ i_1 \leftrightarrow i_2 \right\} , \quad (115)
\end{aligned}$$

$$\begin{aligned}
& \tilde{D}_{rrqq, i_1 i_2}^{(1)ff} (^1P_1) \\
&= \frac{1}{192 (\widehat{m} \widehat{\bar{m}})^2} \left( \beta^2 - 3 + 3 \Delta_{AB}^2 + 12 \Delta_m (\widehat{m}_A - \widehat{m}_B - (\widehat{m}_A + \widehat{m}_B) \Delta_{AB}) \right. \\
&\quad \left. - \Delta_m^2 (\beta^2 + 3 + 24 \widehat{m}_A \widehat{m}_B - 3 \Delta_{AB}^2) \right) \\
&\quad + \frac{\beta^2}{48 \widehat{m} \widehat{\bar{m}} P_{i_1 AB}} \left( 1 + \widehat{m}_A + \widehat{m}_B - \Delta_m (\widehat{m}_A - \widehat{m}_B + \Delta_{AB}) \right) \\
&\quad + \frac{\beta^2}{48 \widehat{m} \widehat{\bar{m}} P_{i_2 BA}} \left( 1 - \widehat{m}_A - \widehat{m}_B - \Delta_m (\widehat{m}_A - \widehat{m}_B - \Delta_{AB}) \right) \\
&\quad - \frac{\beta^2}{24 P_{i_1 AB} P_{i_2 BA}} (\beta^2 - 4 \widehat{m}_A \widehat{m}_B) , \quad (116)
\end{aligned}$$

$$\begin{aligned}
& \tilde{D}_{rrqq, i_1 i_2}^{(2)ff} (^1P_1) \\
&= - \frac{1}{192 (\widehat{m} \widehat{\bar{m}})^2} \left( \beta^2 - 3 + 3 \Delta_{AB}^2 + \Delta_m^2 (\beta^2 + 3 + 24 \widehat{m}_A \widehat{m}_B - 3 \Delta_{AB}^2) \right) \\
&\quad - \frac{\beta^2}{48 \widehat{m} \widehat{\bar{m}} P_{i_1 AB}} \left( 1 + \widehat{m}_A + \widehat{m}_B + \Delta_m (\widehat{m}_A - \widehat{m}_B + \Delta_{AB}) \right) \\
&\quad - \frac{\beta^2}{48 \widehat{m} \widehat{\bar{m}} P_{i_2 AB}} \left( 1 - \widehat{m}_A - \widehat{m}_B - \Delta_m (\widehat{m}_A - \widehat{m}_B - \Delta_{AB}) \right) \\
&\quad + \frac{\beta^2}{24 P_{i_1 AB} P_{i_2 AB}} (\beta^2 - 4 \widehat{m}_A \widehat{m}_B) . \quad (117)
\end{aligned}$$

The corresponding expressions for combined  ${}^3P_{\mathcal{J}}$  partial-wave reactions are

$$\tilde{D}_{rrrr, i_1 i_2}^{(1)ff}({}^3P_{\mathcal{J}}) = -3 \tilde{D}_{rrrr, i_1 i_2}^{(1)ff}({}^1P_1) + \frac{\beta^2}{24 (\widehat{m} \widehat{m})^2} (1 + \Delta_m^2) , \quad (118)$$

$$\tilde{D}_{rrrr, i_1 i_2}^{(2)ff}({}^3P_{\mathcal{J}}) = 3 \tilde{D}_{rrrr, i_1 i_2}^{(2)ff}({}^1P_1) + \frac{\beta^2}{24 (\widehat{m} \widehat{m})^2} (1 - \Delta_m^2) , \quad (119)$$

$$\tilde{D}_{rrqq, i_1 i_2}^{(1)ff}({}^3P_{\mathcal{J}}) = \tilde{D}_{rrqq, i_1 i_2}^{(1)ff}({}^1P_1) - \frac{\widehat{m}_A \widehat{m}_B}{2 (\widehat{m} \widehat{m})^2} - \frac{\beta^2}{3 P_{i_1 AB} P_{i_2 BA}} 2 \widehat{m}_A \widehat{m}_B , \quad (120)$$

$$\tilde{D}_{rrqq, i_1 i_2}^{(2)ff}({}^3P_{\mathcal{J}}) = -\tilde{D}_{rrqq, i_1 i_2}^{(2)ff}({}^1P_1) - \frac{\widehat{m}_A \widehat{m}_B}{2 (\widehat{m} \widehat{m})^2} - \frac{\beta^2}{3 P_{i_1 AB} P_{i_2 AB}} 2 \widehat{m}_A \widehat{m}_B . \quad (121)$$

The following relations can be used to obtain the remaining non-vanishing  $\tilde{D}_{n, i_1 i_2}^{(\alpha)ff}$  expressions in case of diagram topology  $\alpha = 1$ . Note that they hold for any  ${}^{2s+1}L_J$  partial-wave configuration.

$$\begin{aligned} \tilde{D}_{qqqq, i_1 i_2}^{(1)ff}({}^{2s+1}L_J) &= \tilde{D}_{rrrr, i_1 i_2}^{(1)ff}({}^{2s+1}L_J)|_{m_{A,B} \rightarrow -m_{A,B}} , \\ \tilde{D}_{qqrr, i_1 i_2}^{(1)ff}({}^{2s+1}L_J) &= \tilde{D}_{rrqq, i_1 i_2}^{(1)ff}({}^{2s+1}L_J)|_{m_{A,B} \rightarrow -m_{A,B}} , \\ \tilde{D}_{rqq, i_1 i_2}^{(1)ff}({}^{2s+1}L_J) &= \tilde{D}_{rrqq, i_1 i_2}^{(1)ff}({}^{2s+1}L_J)|_{m_A \rightarrow -m_A} , \\ \tilde{D}_{qrrq, i_1 i_2}^{(1)ff}({}^{2s+1}L_J) &= \tilde{D}_{rrqq, i_1 i_2}^{(1)ff}({}^{2s+1}L_J)|_{m_B \rightarrow -m_B} , \\ \tilde{D}_{rqrq, i_1 i_2}^{(1)ff}({}^{2s+1}L_J) &= \tilde{D}_{rrrr, i_1 i_2}^{(1)ff}({}^{2s+1}L_J)|_{m_A \rightarrow -m_A} , \\ \tilde{D}_{qrqr, i_1 i_2}^{(1)ff}({}^{2s+1}L_J) &= \tilde{D}_{rrrr, i_1 i_2}^{(1)ff}({}^{2s+1}L_J)|_{m_B \rightarrow -m_B} . \end{aligned} \quad (122)$$

In case of diagram topology  $\alpha = 2$  analogous relations exist:

$$\begin{aligned} \tilde{D}_{qqqq, i_1 i_2}^{(2)ff}({}^{2s+1}L_J) &= \tilde{D}_{rrrr, i_1 i_2}^{(2)ff}({}^{2s+1}L_J)|_{m_{A,B} \rightarrow -m_{A,B}} , \\ \tilde{D}_{qqrr, i_1 i_2}^{(2)ff}({}^{2s+1}L_J) &= \tilde{D}_{rrqq, i_1 i_2}^{(2)ff}({}^{2s+1}L_J)|_{m_{A,B} \rightarrow -m_{A,B}} , \\ \tilde{D}_{rqrq, i_1 i_2}^{(2)ff}({}^{2s+1}L_J) &= \tilde{D}_{rrqq, i_1 i_2}^{(2)ff}({}^{2s+1}L_J)|_{m_A \rightarrow -m_A} , \\ \tilde{D}_{qrqr, i_1 i_2}^{(2)ff}({}^{2s+1}L_J) &= \tilde{D}_{rrqq, i_1 i_2}^{(2)ff}({}^{2s+1}L_J)|_{m_B \rightarrow -m_B} , \\ \tilde{D}_{rqq, i_1 i_2}^{(2)ff}({}^{2s+1}L_J) &= \tilde{D}_{rrrr, i_1 i_2}^{(2)ff}({}^{2s+1}L_J)|_{m_A \rightarrow -m_A} , \\ \tilde{D}_{qrrq, i_1 i_2}^{(2)ff}({}^{2s+1}L_J) &= \tilde{D}_{rrrr, i_1 i_2}^{(2)ff}({}^{2s+1}L_J)|_{m_B \rightarrow -m_B} . \end{aligned} \quad (123)$$

### A.2.5 $P$ -wave kinematic factors for $X_A X_B = \eta \bar{\eta}$

The use of Feynman gauge for our computation of the absorptive parts of the Wilson coefficients requires to consider unphysical particles in the final states, such as pseudo-

Goldstone Higgs bosons and ghosts. While the results for final states with pseudo-Goldstone Higgses can be obtained from the  $VS$  and  $SS$  kinematic factors and corresponding coupling structures, the ghosts constitute a different class ( $\eta\bar{\eta}$ ). In order to properly construct the coupling factors that go along the kinematic factors  $\tilde{B}_{n,i_1i_2}^{\eta\bar{\eta}}$  presented below, we refer the reader to the rules set up in section A.3.5 of paper I.

For  $^1P_1$  partial-wave processes, there is only one non-vanishing kinematic factor with ghosts in the final state:

$$\tilde{B}_{qq,VV}^{\eta\bar{\eta}}(^1P_1) = -\frac{\beta^2}{48} \Delta_m^2 . \quad (124)$$

The corresponding kinematic factors in combined  $^3P_J$  partial-wave processes read

$$\tilde{B}_{rr,VV}^{\eta\bar{\eta}}(^3P_J) = \frac{\Delta_m^2}{16} (1 - \Delta_{AB}^2) , \quad (125)$$

$$\tilde{B}_{qq,VV}^{\eta\bar{\eta}}(^3P_J) = -\frac{\beta^2}{24} , \quad (126)$$

$$\tilde{B}_{rr,VS}^{\eta\bar{\eta}}(^3P_J) = \frac{\hat{m}_W}{8} \Delta_m (1 + \Delta_{AB}) , \quad (127)$$

$$\tilde{B}_{rr,SV}^{\eta\bar{\eta}}(^3P_J) = -\frac{\hat{m}_W}{8} \Delta_m (1 - \Delta_{AB}) , \quad (128)$$

$$\tilde{B}_{rr,SS}^{\eta\bar{\eta}}(^3P_J) = -\frac{\hat{m}_W^2}{4} . \quad (129)$$

## B Notation for the kinematic factors in the electronic supplement

The analytic expressions for the kinematic factors needed to construct the absorptive part of the Wilson coefficients up to next-to-next-to-leading order have been stored in the `Mathematica` package attached to this paper. They can be loaded into a `Mathematica` session using the command

```
<< kinfactors`
```

The introductory text in the file explains in detail the notation used for the kinematic factors, which we summarise in Tab. 2.

The argument `XAXB` inside the kinematic factors in Tab. 2 can be given the values

$$\text{XAXB} = \text{VV}, \text{VS}, \text{SS}, \text{ff}, \text{GG}$$

depending on the type of particles in the final state. The partial-wave configuration

Kinematic factor	Name in electronic supplement	Coupling string n
$\tilde{B}_{n,i_1 i_2}^{X_A X_B (2s+1) L_J}$	$\text{Btilde}["(i_1 i_2) X A X B", n, \{2s+1\}^{\sim} L_J]$  $i_1, i_2 = V, S$	$"rr", "qq" (X_A X_B = VV, VS, SS, GG)$  $\left. \begin{array}{l} "rrrr", "rqqr", \\ "qrrq", "qqqq" \end{array} \right\} (X_A X_B = ff)$
$\tilde{C}_{n,i_1 X}^{(\alpha) X_A X_B (2s+1) L_J}$	$\text{Ctilde}[\text{alpha}, "(X) X A X B", n, \{2s+1\}^{\sim} L_J]$  $X = V, S$	$\left. \begin{array}{l} "rrr", "qqr", \\ "rqq", "qrq" \end{array} \right\} (X_A X_B = VV, VS, SS)$  $\left. \begin{array}{l} "rrrr", "qqqq", "rrrq", \\ "qqrr", "rqqr", "qrrq", \\ "rqrq", "qrqr" \end{array} \right\} (X_A X_B = ff)$
$\tilde{D}_{n,i_1 i_2}^{(\alpha) X_A X_B (2s+1) L_J}$	$\text{Dtilde}[\text{alpha}, "X A X B", n, \{2s+1\}^{\sim} L_J]$	$"rrrr", "qqqq", "rrrq", "qqrr",$ $"rqqr", "qrrq", "rqrq", "qrqr"$

Table 2: Notation for the kinematic factors used in the **Mathematica** package

$\{2s+1\}^{\sim} L_J$  is specified by one of the following strings:

$$\{2s+1\}^{\sim} L_J = \begin{cases} "1S0", "3S1", & \text{for the leading-order } S\text{-wave coefficients} \\ "1P1", "3P0", "3P1", "3P2", "3PJ", & \text{for the } P\text{-wave coefficients} \\ "1S0, p2", "3S1, p2", & \text{for the } g^{(2s+1) S_s} \text{ coefficients} \\ "1S0, dm", "1S0, dmbar", "3S1, dm", "3S1, dmbar", & \text{for } h_i^{(2s+1) S_s} \text{ coefficients.} \end{cases}$$

Note that for  $S$ -wave partial-wave configurations, the label  $\{2s+1\}^{\sim} L_J$  also contains the information about the type of Wilson coefficient ( $f$ ,  $g$  or  $h_i$ , with  $g$  and  $h_i$  describing NNLO  $S$ -wave coefficients, see Eq. (3)). The argument **alpha** inside the kinematic factors **Ctilde** and **Dtilde** in Tab. 2 can get as input

$$\text{alpha} = 1, 2, 3, 4$$

referring to our enumeration scheme for the respective four triangle and box topologies. Finally, the equivalence between the mass variables and propagator structures introduced in Appendix A that enter the expressions for the kinematic factors and the corresponding names in the **Mathematica** package are collected in Tab. 3.

## C Annihilation rates in the pure-wino NRMSSM at $\mathcal{O}(v_{\text{rel}}^2)$

In this appendix we illustrate the usage of the kinematic and coupling factor results given in paper I and in this work by presenting a detailed end-to-end calculation of the

Quantity	Name in electronic supplement
$\hat{m}_{i_1}, \hat{m}_{i_2}$	mi1, mi2
$\hat{m}_A, \hat{m}_B$	mA, mB
$\hat{m}_W$	mWr
$\Delta_m$	Dm
$\Delta_{AB}$	DAB
$P_{i_1}^s, P_{i_2}^s$	Psi1, Psi2
$P_X^s$	PsX
$P_{i_1 AB}, P_{i_2 AB}$	Pti1[A,B], Pti2[A,B]

Table 3: Equivalence between the variables in the kinematic factors introduced in Appendix A and the corresponding names in the **Mathematica** package.

non-relativistic annihilation cross section for the  $\chi_1^+ \chi_1^- \rightarrow W^+ W^-$  reaction including up to  $\mathcal{O}(v_{\text{rel}}^2)$  effects. The calculation is performed in the idealised case of the pure-wino NRMSSM, which allows to present compact analytic results. For completeness, we also provide in Sec. C.3 the results for the Wilson coefficients needed to determine all exclusive (off-)diagonal (co-)annihilation rates  $\chi_{e_1} \chi_{e_2} \rightarrow X_A X_B \rightarrow \chi_{e_4} \chi_{e_3}$  in the decoupling limit of the pure-wino scenario. To the best of our knowledge the analytic results for the  $P$ - and  $\mathcal{O}(v_{\text{rel}}^2)$   $S$ -wave (off-)diagonal annihilation rates in the pure-wino NRMSSM have not been given before in the literature and could be of interest in the study of next-to-next-to-leading order effects in Sommerfeld-enhanced pure-wino dark matter annihilations in the Early Universe.

The pure-wino (toy-)NRMSSM scenario is characterised by the mass-degenerate  $SU(2)_L$  fermion triplet states  $\chi_1^0, \chi_1^\pm$  (winos) with mass scale  $M_2 > 0$ , where the latter denotes the soft SUSY-breaking wino mass. All other SUSY mass-parameters including the Bino soft mass  $M_1$  and the Higgsino mass parameter  $\mu$  as well as all sfermion mass parameters are assumed to be much larger than  $M_2$ , namely  $M_1, |\mu| \gg M_2$ . Consequently all heavier states  $\chi_i^0, i = 2, 3, 4$  and  $\chi_2^\pm$  as well as all sfermion states are treated as completely decoupled. According to the  $SU(2)_L$  symmetric limit the  $SU(2)_L$  gauge bosons as well as all Standard Model fermions are treated as massless, in agreement with the complete mass-degeneracy between the non-relativistic states  $\chi_1^0$  and  $\chi_1^\pm$ . The neutralino and chargino mixing matrix entries relevant to the calculation in the pure-wino NRMSSM read

$$\tilde{Z}_{N i 1} = \delta_{i 2}, \quad \tilde{Z}_{\pm i 1} = \delta_{i 1}, \quad (130)$$

where the  $\tilde{Z}_N, \tilde{Z}_\pm$  derive from the conventionally defined neutralino and chargino mixing matrices  $Z_N, Z_\pm$  by accounting for a potentially necessary rotation to positive mass-parameters in the NRMSSM, as defined through Eqs. (38–41) in paper I. Such a rotation does however not affect the above mixing-matrix entries relevant in the pure-wino NRMSSM with  $M_2 > 0$ . Finally, let us introduce the notation  $m_\chi = M_2$  for the only mass parameter present in the pure-wino NRMSSM scenario.

Our goal is the determination of the Wilson coefficients  $\hat{f}^{(2s+1)} L_J$  that enter the coefficients  $a$  and  $b$  in the non-relativistic expansion of the  $\chi_1^+ \chi_1^- \rightarrow W^+ W^-$  annihilation cross section, see (9). The  $\hat{f}^{(2s+1)} L_J$  are determined from coupling and kinematic factors using the master formula (16). We discuss the construction of the relevant coupling factors in Sec. C.1. The corresponding kinematic factors, the resulting absorptive part of the Wilson coefficients as well as the final result for the  $\chi_1^+ \chi_1^- \rightarrow W^+ W^-$  annihilation cross section in the non-relativistic regime are given in Sec. C.2. The co-annihilation rates into all other exclusive final states in this scenario including  $P$ - and next-to-next-to-leading order  $S$ -wave corrections are obtained from the contributions to the Wilson coefficients from these exclusive final states that we present in Sec. C.3.

## C.1 Coupling factors

Let us recall from paper I that each of the coupling factors  $b_n, c_n^{(\alpha)}, d_n^{(\alpha)}$  in (16) related to a specific  $\chi_{e_1} \chi_{e_2} \rightarrow X_A X_B \rightarrow \chi_{e_4} \chi_{e_3}$  reaction is given by a product of two coupling factors associated with the two vertices occurring in the tree-level annihilation amplitude  $\mathcal{A}_{\chi_{e_1} \chi_{e_2} \rightarrow X_A X_B}^{(0)}$  and the complex conjugate of another such two-coupling factor product related to the tree-level amplitude  $\mathcal{A}_{\chi_{e_4} \chi_{e_3} \rightarrow X_A X_B}^{(0)}$ . Hence, the building blocks of the  $b_n, c_n^{(\alpha)}, d_n^{(\alpha)}$  relevant in  $\chi_1^+ \chi_1^- \rightarrow X_A X_B$  annihilation rates are given by the (axial-) vector or (pseudo-) scalar vertex factors in the  $\chi_1^+ \chi_1^- \rightarrow X_A X_B$  tree-level annihilation amplitudes. Since our results for the kinematic factors refer to Feynman gauge, in order to determine the annihilation rates into a physical  $W^+ W^-$  final state we have to consider  $\chi_1^+ \chi_1^-$  annihilations into the exclusive final states  $X_A X_B = W^+ W^-, W^+ G^-, W^- G^+, G^+ G^-, \eta^+ \eta^+, \eta^- \eta^-$ , with  $G^\pm$  the charged pseudo-Goldstone Higgs and  $\eta^\pm$  the charged ghost particles. In the pure-wino NRMSSM, the only non-vanishing amplitudes are given by the diagrams depicted in Fig. 4, which we should compare with the generic  $\chi\chi \rightarrow X_A X_B$  diagrams drawn in Fig. 9 of paper I in order to extract the coupling factors in accordance to the conventions established therein. Note the fermion flow in these diagrams, which coincides with the convention used in the generic  $\chi_{e_1} \chi_{e_2} \rightarrow X_A X_B$  diagrams in Fig. 9 of paper I. In the case of diagram  $t_2$  in Fig. 4, which contributes both to the box and triangle coupling factors,  $d_{n, i_1 i_2}^{(\alpha)}$  and  $c_{n, i_1 i_2}^{(\alpha)}$ , the vertex factors  $V_{ei}^{\rho(t_2)}$  read

$$V_{e_1 i_1}^{\mu(t_2)} = \gamma^\mu (v_{e_1 i_1}^{W*} + a_{e_1 i_1}^{W*} \gamma_5) , \quad V_{e_2 i_1}^{\nu(t_2)} = \gamma^\nu (v_{e_2 i_1}^W + a_{e_2 i_1}^W \gamma_5) , \quad (131)$$

where  $e_1, e_2 = 1$  as these indices refer to the external states  $\chi_{e_1} = \chi_1^+$  and  $\chi_{e_2} = \chi_1^-$ . In the pure-wino NRMSSM, the only possible  $t$ -channel exchanged particle in diagram  $t_2$  is the  $\chi_1^0$ , therefore  $i_1 = 1$ . Comparing to the generic form of the vertex factor



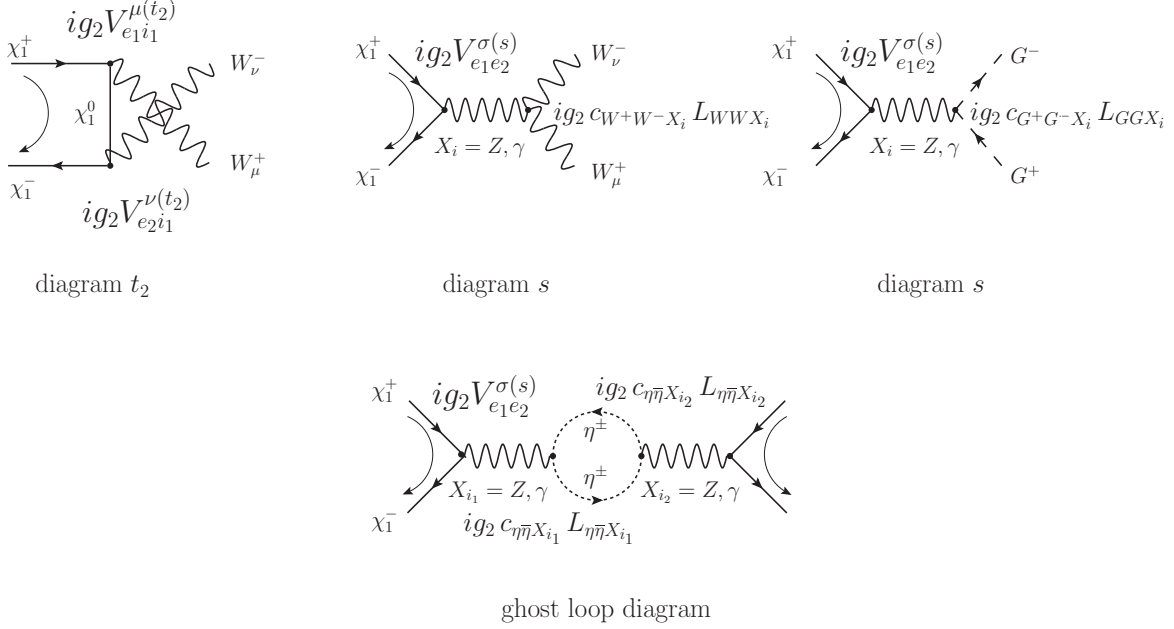


Figure 4: Amplitudes contributing to the physical  $\chi_1^+ \chi_1^- \rightarrow W^+ W^-$  annihilation reaction in Feynman gauge. Note the fermion flow, that has been fixed to match with the conventions established in paper I.

$V_{ei}^{\rho(d)} = \gamma^\rho (r_{ei}^{(d)} + q_{ei}^{(d)} \gamma_5)$ , we identify the expressions that substitute the respective placeholder couplings  $r_{ei}^{(d)}$  and  $q_{ei}^{(d)}$ :

$$\left( \{r_{e_1 i_1}^{(t_2)}, q_{e_1 i_1}^{(t_2)}\}, \{r_{e_2 i_1}^{(t_2)}, q_{e_2 i_1}^{(t_2)}\} \right) \rightarrow \left( \{v_{11}^{W*}, a_{11}^{W*}\}, \{v_{11}^W, a_{11}^W\} \right). \quad (132)$$

Let us obtain first the coupling factors  $d_{n, i_1 i_2}^{(\alpha)}$  related to the four box amplitudes shown in Fig. 3. As there is no  $t$ -channel exchange diagram  $t_1$ , the only non-vanishing coupling factors  $d_{n, i_1 i_2}^{(\alpha)}$  are those with label  $\alpha = 4$ :  $d_{n, i_1 i_2}^{(4)}$  expressions arise from the product of coupling factors in  $\chi_{e_1} \chi_{e_2} \rightarrow X_A X_B$  annihilation diagrams of type  $t_2$  with the complex conjugate of the coupling factors associated with  $\chi_{e_4} \chi_{e_3} \rightarrow X_A X_B$  annihilation via diagram type  $t_2$ .<sup>10</sup> The constituent coupling factors for the  $d_{n, i_1 i_2}^{(4)}$  in  $\chi_1^+ \chi_1^- \rightarrow W^+ W^- \rightarrow \chi_1^+ \chi_1^-$  scattering are collected in the following table:

$$\begin{aligned} \alpha = 4 : \quad & \left( \{r_{e_1 i_1}^{(t_2)}, q_{e_1 i_1}^{(t_2)}\}, \{r_{e_2 i_1}^{(t_2)}, q_{e_2 i_1}^{(t_2)}\}, \{r_{e_3 i_2}^{(t_2)*}, q_{e_3 i_2}^{(t_2)*}\}, \{r_{e_4 i_2}^{(t_2)*}, q_{e_4 i_2}^{(t_2)*}\} \right) \\ & \rightarrow \left( \{v_{11}^{W*}, a_{11}^{W*}\}, \{v_{11}^W, a_{11}^W\}, \{v_{11}^{W*}, a_{11}^{W*}\}, \{v_{11}^W, a_{11}^W\} \right). \end{aligned} \quad (133)$$

Selecting one element from each of the four subsets and multiplying these selected elements with each other gives rise to the  $d_{n, i_1 i_2}^{(4)}$ . The label  $n$  denotes a string of four

<sup>10</sup>For further conventions on the enumeration label  $\alpha$  see Fig. 3.

characters, that indicates which coupling (type  $r$  or  $q$ ) was selected from the  $i$ th subset in (133). For instance

$$d_{rrrr,11}^{(4)\chi_1^+\chi_1^-\rightarrow W^+W^-\rightarrow\chi_1^+\chi_1^-} = v_{11}^{W*}v_{11}^Wv_{11}^{W*}v_{11}^W. \quad (134)$$

Turning to the coupling factors in triangle and selfenergy amplitudes,  $c_{n,i_1i_2}^{(\alpha)}$  and  $b_{n,i_1i_2}$ , they receive contributions from the  $s$ -channel diagrams in Fig. 4. We proceed in a similar way as done for the diagram  $t_2$  and identify the following coupling factors for the case of single  $s$ -channel  $Z$ -exchange (first line) and single  $s$ -channel  $\gamma$ -exchange (second line):

$$\begin{aligned} V_{11}^{\sigma(s)} &= \gamma^\sigma (v_{11}^Z + a_{11}^Z \gamma_5), & c_{W+W-Z} &= c_W, \\ V_{11}^{\sigma(s)} &= \gamma^\sigma (v_{11}^\gamma + a_{11}^\gamma \gamma_5), & c_{W+W-\gamma} &= s_W. \end{aligned} \quad (135)$$

The building blocks for the  $b_{n,i_1i_2}$ ,  $c_{n,i_1i_2}^{(\alpha)}$  and finally these expressions themselves can now be obtained in a similar manner as described for the  $d_{n,i_1i_2}^{(\alpha)}$  expressions. However, before proceeding with their explicit construction, significant simplifications can be performed by noting that the pure-wino NRMSSM exhibits a particularly simple coupling structure: the (axial-)vector couplings of the  $\chi_1^0$  and  $\chi_1^\pm$  to the Standard Model gauge bosons are given by

$$\begin{aligned} v_{11}^W &= 1, \quad a_{11}^W = 0, & v_{11}^\gamma &= -s_W, \quad a_{11}^\gamma = 0, \\ v_{11}^Z &= -c_W, \quad a_{11}^Z = 0. \end{aligned} \quad (136)$$

With the vanishing of all axial-vector couplings the only non-vanishing coupling factor  $d_{n,i_1i_2}^{(\alpha)}$  for  $\chi_1^+\chi_1^-\rightarrow W^+W^-\rightarrow\chi_1^+\chi_1^-$  in the pure-wino NRMSSM hence reads

$$d_{rrrr,11}^{(4)\chi_1^+\chi_1^-\rightarrow W^+W^-\rightarrow\chi_1^+\chi_1^-} = 1. \quad (137)$$

The absence of a  $t$ -channel exchange diagram  $t_1$  implies, that only  $c_{n,i_1i_2}^{(\alpha)}$  factors with  $\alpha = 3, 4$  can be non-vanishing, as these are built from vertex coupling factors associated with diagram type  $t_2$  and diagram type  $s$ , see Fig. 3. In the pure-wino NRMSSM, we find the following expressions

$$c_{rrr,1Z}^{(\alpha=3,4)\chi_1^+\chi_1^-\rightarrow W^+W^-\rightarrow\chi_1^+\chi_1^-} = -c_W^2, \quad c_{rrr,1\gamma}^{(\alpha=3,4)\chi_1^+\chi_1^-\rightarrow W^+W^-\rightarrow\chi_1^+\chi_1^-} = -s_W^2, \quad (138)$$

and all other  $c_{n,i_1i_2}^{(\alpha)}$  vanish. Finally, the non-zero factors  $b_{n,i_1i_2}$  read

$$b_{rr,ZZ} = c_W^4, \quad b_{rr,Z\gamma} = b_{rr,\gamma Z} = c_W^2 s_W^2, \quad b_{rr,\gamma\gamma} = s_W^4, \quad (139)$$

where we have suppressed the superscript  $\chi_1^+\chi_1^-\rightarrow W^+W^-\rightarrow\chi_1^+\chi_1^-$  to shorten the notation. A similar procedure leads to the coupling factors in  $\chi_1^+\chi_1^-\rightarrow X_A X_B$  rates

with the (unphysical) final states  $X_A X_B = G^+ G^-$ ,  $\eta^+ \bar{\eta}^+$  and  $\eta^- \bar{\eta}^-$ . We quote the non-vanishing results for the coupling factors related to  $\chi_1^+ \chi_1^- \rightarrow G^+ G^- \rightarrow \chi_1^+ \chi_1^-$  reactions:

$$\begin{aligned} b_{rr,ZZ} &= \frac{1}{4} (c_W^2 - s_W^2)^2, & b_{rr,Z\gamma} &= b_{rr,\gamma Z} = \frac{s_W^2}{2} (c_W^2 - s_W^2), \\ b_{rr,\gamma\gamma} &= s_W^4. \end{aligned} \quad (140)$$

In case of  $\chi_1^+ \chi_1^- \rightarrow \eta^+ \bar{\eta}^+ \rightarrow \chi_1^+ \chi_1^-$  and  $\chi_1^+ \chi_1^- \rightarrow \eta^- \bar{\eta}^- \rightarrow \chi_1^+ \chi_1^-$  reactions we find in both cases the same result (again suppressing the process-specifying superscripts):

$$b_{rr,ZZ} = c_W^4, \quad b_{rr,Z\gamma} = b_{rr,\gamma Z} = c_W^2 s_W^2, \quad b_{rr,\gamma\gamma} = s_W^4. \quad (141)$$

## C.2 Kinematic factors

As for the coupling factors, the kinematic factors  $B_{n,i_1 i_2}$ ,  $C_{n,i_1 X}^{(\alpha)}$ ,  $D_{n,i_1 i_2}^{(\alpha)}$  reduce to very simple expressions in the pure-wino NRMSSM. As the pure-wino NRMSSM refers to the limit of vanishing  $SU(2)_L$  gauge boson masses, the relevant (mass-)parameters in any of the  $\chi_{e_1} \chi_{e_2} \rightarrow X_A X_B \rightarrow \chi_{e_4} \chi_{e_3}$  scattering reactions with  $\chi_{e_a} = \chi_1^0$ ,  $\chi_1^\pm$  read

$$\begin{aligned} m &= \bar{m} = m_\chi, & M &= 2 m_\chi, & \Delta_{AB} &= 0, \\ \beta &= 1, & P_{Z,\gamma}^s &= 1, & P_{1AB} &= \frac{1}{2}. \end{aligned} \quad (142)$$

Further, the rescaled quantity  $\hat{m}_{i_1,2}$  in the pure-wino limit reads  $\hat{m}_1 = 1/2$  if it refers to the  $\chi_1^0$  or  $\chi_1^\pm$  species and it vanishes if related to  $Z$  and  $\gamma$ ,  $\hat{m}_{Z,\gamma} = 0$ . Taking the relations (142) into account, we obtain concise analytic results for the kinematic factors relevant in  $\chi_1^+ \chi_1^- \rightarrow X_A X_B \rightarrow \chi_1^+ \chi_1^-$  scattering. These are collected in Tab. 4. Note that we have given only those kinematic factors that are associated with non-vanishing coupling factors in the physical  $\chi_1^+ \chi_1^- \rightarrow W^+ W^- \rightarrow \chi_1^+ \chi_1^-$  reaction. Assembling and inserting the above results into the master formula (16) we find the results for the absorptive part of the Wilson coefficients that provide the  $\chi_1^+ \chi_1^- \rightarrow W^+ W^-$  annihilation cross-section (9). For  $^3S_1$  annihilation we have

$$\begin{aligned} &\hat{f}_{\{11\}\{11\}}^{\chi_1^+ \chi_1^- \rightarrow W^+ W^- \rightarrow \chi_1^+ \chi_1^-} (^3S_1) \\ &= \frac{\pi \alpha_2^2}{4 m_\chi^2} \left( \sum_{n=rr} \sum_{i_1, i_2=Z, \gamma} b_{n, i_1 i_2}^{\chi_1^+ \chi_1^- \rightarrow W^+ W^- \rightarrow \chi_1^+ \chi_1^-} B_{n, i_1 i_2}^{VV} (^3S_1) \right. \\ &\quad + \sum_{\alpha=3,4} \sum_{n=rrr} \sum_{i_1=1, i_2=Z, \gamma} c_{n, i_1 i_2}^{(\alpha) \chi_1^+ \chi_1^- \rightarrow W^+ W^- \rightarrow \chi_1^+ \chi_1^-} C_{n, i_1 i_2}^{(\alpha) VV} (^3S_1) \\ &\quad \left. + \sum_{\alpha=4} \sum_{n=rrrr} \sum_{i_1, i_2=1} d_{n, i_1 i_2}^{(\alpha) \chi_1^+ \chi_1^- \rightarrow W^+ W^- \rightarrow \chi_1^+ \chi_1^-} D_{n, i_1 i_2}^{(\alpha) VV} (^3S_1) \right) \end{aligned}$$

	$^1S_0$	$^3S_1$	$^1P_1$	$^3P_J$	$^1S_0^{(p^2)}$	$^3S_1^{(p^2)}$
$B_{rr,VV}^{VV}(^{2s+1}L_J)$	0	$-\frac{19}{6}$	0	0	0	$\frac{152}{9}$
$C_{rrr,1V}^{(\alpha=3,4)VV}(^{2s+1}L_J)$	0	$-\frac{4}{3}$	0	0	0	$\frac{64}{9}$
$D_{rrrr,11}^{(4)VV}(^{2s+1}L_J)$	2	$\frac{2}{3}$	$\frac{8}{3}$	$\frac{56}{3}$	$-\frac{32}{3}$	$-\frac{32}{9}$
$B_{rr,VV}^{SS}(^{2s+1}L_J)$	0	$\frac{1}{3}$	0	0	0	$-\frac{16}{9}$
$B_{rr,VV}^{\eta\bar{\eta}}(^{2s+1}L_J)$	0	$-\frac{1}{12}$	0	0	0	$\frac{4}{9}$

Table 4: Kinematic factors for partial wave reactions up to  $\mathcal{O}(v_{\text{rel}}^2)$  in the pure-wino NRMSSM, relevant for the determination of the  $\chi_1^+ \chi_1^- \rightarrow W^+ W^-$  annihilation rate. The subscript label  $V$  on the kinematic factors  $B$  and  $C$  above refers to both the cases of  $Z$  and  $\gamma$  single  $s$ -channel exchange in the (tree-level) annihilation amplitudes. The results for the kinematic factor  $B$  in the last line apply to  $\eta\bar{\eta} = \eta^+ \bar{\eta}^+, \eta^- \bar{\eta}^-$ .

$$\begin{aligned}
& + \sum_{n=rr} \sum_{i_1, i_2=Z, \gamma} b_{n, i_1 i_2}^{\chi_1^+ \chi_1^- \rightarrow G^+ G^- \rightarrow \chi_1^+ \chi_1^-} B_{n, i_1 i_2}^{SS}(^3S_1) \\
& + \sum_{\eta=\eta^\pm} \sum_{n=rr} \sum_{i_1, i_2=Z, \gamma} b_{n, i_1 i_2}^{\chi_1^+ \chi_1^- \rightarrow \eta\bar{\eta} \rightarrow \chi_1^+ \chi_1^-} B_{n, i_1 i_2}^{\eta\bar{\eta}}(^3S_1) \Big) \\
& = \frac{\pi\alpha_2^2}{4m_\chi^2} \left( (c_W^4 + c_W^2 s_W^2 + s_W^4) \times \left(-\frac{19}{6}\right) + 2(-c_W^2 - s_W^2) \times \left(-\frac{4}{3}\right) \right. \\
& \quad \left. + 1 \times \frac{2}{3} + \frac{1}{4} \times \frac{1}{3} - 2 \times \frac{1}{12} \right) \\
& = \frac{1}{48} \frac{\pi\alpha_2^2}{m_\chi^2}, \tag{143}
\end{aligned}$$

where we have summed over all (unphysical) final states in Feynman gauge,  $X_A X_B = W^+ W^-, G^+ G^-, \eta^+ \bar{\eta}^+, \eta^- \bar{\eta}^-$ , that contribute to the physical  $\chi_1^+ \chi_1^- \rightarrow W^+ W^-$  rate in the pure-wino NRMSSM scenario. In case of the  $^1S_0$  annihilation reaction only the pieces related to the  $\alpha = 4$  box-amplitude contribute, and the only non-vanishing coupling factor  $d_{n, i_1 i_2}^{(4)}$  is  $d_{rrrr, 11}^{(4)}$  given in (137), therefore

$$\begin{aligned}
\hat{f}_{\{11\}\{11\}}^{\chi_1^+ \chi_1^- \rightarrow W^+ W^- \rightarrow \chi_1^+ \chi_1^-}(^1S_0) & = \frac{\pi\alpha_2^2}{4m_\chi^2} d_{rrrr, 11}^{(4) \chi_1^+ \chi_1^- \rightarrow W^+ W^- \rightarrow \chi_1^+ \chi_1^-} D_{rrrr, 11}^{(4)VV}(^1S_0) \\
& = \frac{\pi\alpha_2^2}{2m_\chi^2}. \tag{144}
\end{aligned}$$

Finally, the absorptive parts of the  $\mathcal{O}(v_{\text{rel}}^2)$  partial-wave Wilson coefficients read

$$\begin{aligned}\hat{f}_{\{11\}\{11\}}^{\chi_1^+\chi_1^-\rightarrow W^+W^-\rightarrow\chi_1^+\chi_1^-}(^1P_1) &= \frac{2\pi\alpha_2^2}{3m_\chi^2}, & \hat{f}_{\{11\}\{11\}}^{\chi_1^+\chi_1^-\rightarrow W^+W^-\rightarrow\chi_1^+\chi_1^-}(^3P_J) &= \frac{14\pi\alpha_2^2}{3m_\chi^2}, \\ \hat{g}_{\{11\}\{11\}}^{\chi_1^+\chi_1^-\rightarrow W^+W^-\rightarrow\chi_1^+\chi_1^-}(^1S_0) &= -\frac{8\pi\alpha_2^2}{3m_\chi^2}, & \hat{g}_{\{11\}\{11\}}^{\chi_1^+\chi_1^-\rightarrow W^+W^-\rightarrow\chi_1^+\chi_1^-}(^3S_1) &= -\frac{\pi\alpha_2^2}{9m_\chi^2}.\end{aligned}\quad (145)$$

Hence, following (9), the non-relativistic expansion of the  $\chi_1^+\chi_1^-\rightarrow W^+W^-$  annihilation cross section in the pure-wino NRMSSM is given by

$$\begin{aligned}\sigma_{\chi_1^+\chi_1^-\rightarrow W^+W^-}v_{\text{rel}} &= a + (b_P + b_S)v_{\text{rel}}^2 + \mathcal{O}(v_{\text{rel}}^4) \\ &= \frac{9}{16} \frac{\pi\alpha_2^2}{m_\chi^2} + \left(\frac{1}{3} - \frac{3}{16}\right) \frac{\pi\alpha_2^2}{m_\chi^2} v_{\text{rel}}^2 + \mathcal{O}(v_{\text{rel}}^4), \\ &= \frac{9}{16} \frac{\pi\alpha_2^2}{m_\chi^2} + \frac{7}{48} \frac{\pi\alpha_2^2}{m_\chi^2} v_{\text{rel}}^2 + \mathcal{O}(v_{\text{rel}}^4).\end{aligned}\quad (146)$$

The values for the parameters  $a, b_P$  and  $b_S$ , that one obtains for a pure-wino NRMSSM mass scale  $m_\chi = 2748.92 \text{ GeV}$  read  $a = 3.06 \cdot 10^{-27} \text{ cm}^3 \text{ s}^{-1}$ ,  $b_P c^2 = 1.81 \cdot 10^{-27} \text{ cm}^3 \text{ s}^{-1}$  and  $b_S c^2 = -1.02 \cdot 10^{-27} \text{ cm}^3 \text{ s}^{-1}$ . The mass scale  $m_\chi$  agrees with the neutralino LSP mass of the MSSM scenario introduced in Sec. 4. The latter MSSM scenario features a small but non-vanishing Higgsino admixture to the wino-like  $\chi_1^0$  and  $\chi_1^\pm$ : the Higgsino-like neutralino and chargino states are not at all decoupled but reside at the scale of  $\sim 2.9 - 3 \text{ TeV}$ . Thus we should not expect the results for the wino-like scenario of Sec. 4 to be approximated by the pure-wino NRMSSM. This is in fact what the comparison of the parameters  $a, b_P$  and  $b_S$  for the  $\chi_1^+\chi_1^-\rightarrow W^+W^-$  annihilation cross section shows: the corresponding parameters in the MSSM scenario investigated in Sec. 4 were given by  $a = 2.65 \cdot 10^{-27} \text{ cm}^3 \text{ s}^{-1}$ ,  $b_P c^2 = 1.86 \cdot 10^{-27} \text{ cm}^3 \text{ s}^{-1}$ ,  $b_S c^2 = -0.88 \cdot 10^{-27} \text{ cm}^3 \text{ s}^{-1}$ . The results for the  $S$ -wave parameters  $a$  and  $b_S$  in the pure-wino  $\chi_1^+\chi_1^-\rightarrow W^+W^-$  reaction are a bit larger, which is a consequence of the larger couplings of the pure-wino neutralino and chargino states to the  $SU(2)_L$  gauge bosons and the absence of  $t$ -channel annihilation into the (unphysical) final state  $G^+G^-$ . Due to the non-decoupled higgsino-like neutralino states in the scenario of Sec. 4 the latter contribution is present and interferes destructively with the corresponding  $s$ -channel exchange contribution also present in the pure-wino NRMSSM limit. This leads to a suppression of the  $a$  and  $b_S$  cross section parameters in the wino-like scenario of Sec. 4 with respect to the pure-wino NRMSSM. On the contrary the parameter  $b_P$  turns out to be somewhat larger in the Sec. 4 scenario which traces back to the non-vanishing  $P$ -wave  $t$ -channel annihilations into  $G^+G^-$  final states that are absent in the pure-wino NRMSSM. Note that the  $\chi^+\chi^-\rightarrow W^+W^-$  annihilation cross section for the Sec. 4 scenario in addition exhibits non-vanishing contributions from the (unphysical)  $VS = W^\pm G^\mp$  final states not present in the pure-wino NRMSSM. These are however suppressed with respect to the  $X_A X_B = W^+W^-, G^+G^-$  contributions.

$\chi_1^+ \chi_1^- \rightarrow \chi_1^+ \chi_1^-$ reactions						
physical final state $X_A X_B$	$c(^1S_0)$	$c(^3S_1)$	$c(^1P_1)$	$c(^3P_J)$	$c(^1S_0^{(p^2)})$	$c(^3S_1^{(p^2)})$
$W^+ W^-$	$\frac{1}{2}$	$\frac{1}{48}$	$\frac{2}{3}$	$\frac{14}{3}$	$-\frac{8}{3}$	$-\frac{1}{9}$
$ZZ$	$c_W^4$	0	0	$\frac{28}{3} c_W^4$	$-\frac{16}{3} c_W^4$	0
$Z\gamma$	$2 c_W^2 s_W^2$	0	0	$\frac{56}{3} c_W^2 s_W^2$	$-\frac{32}{3} c_W^2 s_W^2$	0
$\gamma\gamma$	$s_W^4$	0	0	$\frac{28}{3} s_W^4$	$-\frac{16}{3} s_W^4$	0
$Zh^0$	0	$\frac{1}{48}$	0	0	0	$-\frac{1}{9}$
$q\bar{q}$	0	$\frac{1}{8}$	0	0	0	$-\frac{2}{3}$
$l^+ l^-, \nu\bar{\nu}$	0	$\frac{1}{24}$	0	0	0	$-\frac{2}{9}$
$\sum X_A X_B$	$\frac{3}{2}$	$\frac{25}{24}$	$\frac{2}{3}$	14	-8	$-\frac{50}{9}$

$\chi_1^0 \chi_1^0 \rightarrow \chi_1^0 \chi_1^0$ reactions						
$W^+ W^-$	2	0	0	$\frac{56}{3}$	$-\frac{32}{3}$	0

$\chi_1^0 \chi_1^0 \rightarrow \chi_1^+ \chi_1^-$ and $\chi_1^+ \chi_1^- \rightarrow \chi_1^0 \chi_1^0$ reactions						
$W^+ W^-$	1	0	0	$\frac{28}{3}$	$-\frac{16}{3}$	0

Table 5:  $c(^{2s+1}L_J)$  factors that enter the contributions to the pure-wino NRMSSM Wilson coefficients in neutral  $\chi_{e_1} \chi_{e_2} \rightarrow X_A X_B \rightarrow \chi_{e_4} \chi_{e_3}$  processes with exclusive (physical) final states  $X_A X_B$ . In case of  $\chi_1^+ \chi_1^- \rightarrow X_A X_B \rightarrow \chi_1^+ \chi_1^-$  rates where several two-particle final states  $X_A X_B$  are accessible the inclusive result is also given.

### C.3 Exclusive (co-)annihilation rates in the pure-wino NRMSSM

This section collects the results for the exclusive (physical)  $X_A X_B$  final state contributions to the Wilson coefficients  $\hat{f}, \hat{g}$  that determine the (off-)diagonal (co-)annihilation rates  $\chi_{e_1} \chi_{e_2} \rightarrow X_A X_B \rightarrow \chi_{e_4} \chi_{e_3}$  in the pure-wino NRMSSM. The non-relativistic expansion of the respective exclusive rates can then be obtained from (8). For convenience we write the pure-wino NRMSSM Wilson coefficients as

$$\hat{f}_{\chi_{e_1} \chi_{e_2} \rightarrow X_A X_B \rightarrow \chi_{e_4} \chi_{e_3}} (^{2s+1}L_J) = \frac{\pi \alpha_2^2}{m_\chi^2} c^{\chi_{e_1} \chi_{e_2} \rightarrow X_A X_B \rightarrow \chi_{e_4} \chi_{e_3}} (^{2s+1}L_J) . \quad (147)$$

In case of the next-to-next-to-leading order  $S$ -wave coefficients we establish a similar notation with  $\hat{f}$  replaced by  $\hat{g}$  on the l.h.s. of (147) and the  $^{2s+1}L_J = ^1S_0, ^3S_1$  label of the factor  $c$  on the r.h.s. substituted by  $^1S_0^{(p^2)}, ^3S_1^{(p^2)}$ . Note that the Wilson coefficients

$\chi_1^0 \chi_1^+ \rightarrow \chi_1^0 \chi_1^+$ reactions						
physical final state $X_A X_B$	$c(^1S_0)$	$c(^3S_1)$	$c(^1P_1)$	$c(^3P_J)$	$c(^1S_0^{(p^2)})$	$c(^3S_1^{(p^2)})$
$W^+ Z$	$\frac{1}{2} c_W^2$	$\frac{1}{48}$	$\frac{2}{3} c_W^2$	$\frac{14}{3} c_W^2$	$-\frac{8}{3} c_W^2$	$-\frac{1}{9}$
$W^+ \gamma$	$\frac{1}{2} s_W^2$	0	$\frac{2}{3} s_W^2$	$\frac{14}{3} s_W^2$	$-\frac{8}{3} s_W^2$	0
$W^+ h^0$	0	$\frac{1}{48}$	0	0	0	$-\frac{1}{9}$
$u \bar{d}$	0	$\frac{1}{4}$	0	0	0	$-\frac{4}{3}$
$\nu l^+$	0	$\frac{1}{12}$	0	0	0	$-\frac{4}{9}$
$\sum X_A X_B$	$\frac{1}{2}$	$\frac{25}{24}$	$\frac{2}{3}$	$\frac{14}{3}$	$-\frac{8}{3}$	$-\frac{50}{9}$

Table 6:  $c(^{2s+1}L_J)$  expressions associated with the pure-wino NRMSSM Wilson coefficients in exclusive single charged  $\chi_1^0 \chi_1^+ \rightarrow X_A X_B \rightarrow \chi_1^0 \chi_1^+$  reactions. The last line is the inclusive result.

$\chi_1^+ \chi_1^+ \rightarrow \chi_1^+ \chi_1^+$ reactions						
physical final state $X_A X_B$	$c(^1S_0)$	$c(^3S_1)$	$c(^1P_1)$	$c(^3P_J)$	$c(^1S_0^{(p^2)})$	$c(^3S_1^{(p^2)})$
$W^+ W^+$	1	0	0	$\frac{28}{3}$	$-\frac{16}{3}$	0

Table 7:  $c(^{2s+1}L_J)$  factors related to the pure-wino NRMSSM Wilson coefficients in double charged  $\chi_1^+ \chi_1^+ \rightarrow X_A X_B \rightarrow \chi_1^+ \chi_1^+$  processes.

$\hat{h}_i$  always vanish in the pure-wino NRMSSM due to the complete mass-degeneracy of the  $\chi_1^0$  and  $\chi_1^\pm$  states.

We have already noted at the beginning of Sec. C that the pure-wino NRMSSM toy-scenario features massless SM gauge bosons and SM fermions. These can hence appear as possible  $X_A X_B$  final state particles in the  $\chi_{e1} \chi_{e2} \rightarrow X_A X_B \rightarrow \chi_{e4} \chi_{e3}$  reactions. As far as the Higgs-sector is concerned we present in this section results that refer to the decoupling limit [22] in the underlying MSSM scenario: we assume a SM-like  $CP$ -even Higgs boson  $h^0$  in the low-energy spectrum of the theory while the heavier Higgs states  $A^0, H^0, H^\pm$  are entirely decoupled ( $m_{A^0} \sim m_{H^0} \sim m_{H^\pm} \gg m_\chi \gg 0$ ). As generically  $m_{h^0} < m_Z$  at tree-level in the MSSM, the  $h^0$  is consequently treated as massless in the pure-wino NRMSSM. According to their overall charge the (co-)annihilation processes can be arranged into three charge-sectors: neutral, positive and double positive charged. The results for the corresponding (double) negative charged reactions are identical to the results for (double) positive charged processes. We collect our results for the factors  $c(^{2s+1}L_J)$  in Tables 5–7.

In case of inclusive leading-order  $^1S_0$  and  $^3S_1$  (co-) annihilations we find agreement between the results of Tables 5–7 and the corresponding expressions given in [12] for the

same scenario. In addition, we reproduce the leading-order  $^1S_0$  wave annihilation rates into the exclusive final states  $W^+W^-$ ,  $ZZ$ ,  $Z\gamma$  and  $\gamma\gamma$  given by the same authors in [11], apart from the  $W^+W^-$  off-diagonal rates, where our findings are a factor of 2 larger. The results for the  $P$ - and  $\mathcal{O}(v_{\text{rel}}^2)$   $S$ -wave Wilson coefficients are new.

## References

- [1] P. Gondolo, J. Edsjo, P. Ullio, L. Bergstrom, M. Schelke, *et al.*, *JCAP* **0407** (2004) 008, [arXiv:astro-ph/0406204](#) [astro-ph].
- [2] G. Belanger, F. Boudjema, P. Brun, A. Pukhov, S. Rosier-Lees, *et al.*, *Comput.Phys.Comm.* **182** (2011) 842–856, [arXiv:1004.1092](#) [hep-ph].
- [3] B. Herrmann and M. Klasen, *Phys.Rev.* **D76** (2007) 117704, [arXiv:0709.0043](#) [hep-ph].
- [4] B. Herrmann, M. Klasen, and K. Kovarik, *Phys.Rev.* **D79** (2009) 061701, [arXiv:0901.0481](#) [hep-ph].
- [5] B. Herrmann, M. Klasen, and K. Kovarik, *Phys.Rev.* **D80** (2009) 085025, [arXiv:0907.0030](#) [hep-ph].
- [6] N. Baro, F. Boudjema, and A. Semenov, *Phys.Lett.* **B660** (2008) 550–560, [arXiv:0710.1821](#) [hep-ph].
- [7] N. Baro, F. Boudjema, G. Chalons, and S. Hao, *Phys.Rev.* **D81** (2010) 015005, [arXiv:0910.3293](#) [hep-ph].
- [8] F. Boudjema, G. Drieu La Rochelle, and S. Kulkarni, *Phys.Rev.* **D84** (2011) 116001, [arXiv:1108.4291](#) [hep-ph].
- [9] A. Chatterjee, M. Drees, and S. Kulkarni, [arXiv:1209.2328](#) [hep-ph].
- [10] M. Drees and J. Gu, [arXiv:1301.1350](#) [hep-ph].
- [11] J. Hisano, S. Matsumoto, M. M. Nojiri, and O. Saito, *Phys.Rev.* **D71** (2005) 063528, [arXiv:hep-ph/0412403](#) [hep-ph].
- [12] J. Hisano, S. Matsumoto, M. Nagai, O. Saito, and M. Senami, *Phys.Lett.* **B646** (2007) 34–38, [arXiv:hep-ph/0610249](#) [hep-ph].
- [13] M. Cirelli, A. Strumia, and M. Tamburini, *Nucl.Phys.* **B787** (2007) 152–175, [arXiv:0706.4071](#) [hep-ph].
- [14] A. Hryczuk, R. Iengo, and P. Ullio, *JHEP* **1103** (2011) 069, [arXiv:1010.2172](#) [hep-ph].



- [15] A. Hryczuk and R. Iengo, *JHEP* **1201** (2012) 163, [arXiv:1111.2916 \[hep-ph\]](#).
- [16] M. Beneke, C. Hellmann and P. Ruiz-Femenia, *JHEP* **1303** (2013) 148 [[arXiv:1210.7928 \[hep-ph\]](#)].
- [17] J. Chen and Y. -F. Zhou, [arXiv:1301.5778 \[hep-ph\]](#).
- [18] See the `Mathematica` package “kinfactors.m” available with the arXiv source of this paper.
- [19] G. T. Bodwin, E. Braaten, and G. P. Lepage, *Phys.Rev.* **D51** (1995) 1125–1171, [arXiv:hep-ph/9407339 \[hep-ph\]](#).
- [20] J. Alwall, M. Herquet, F. Maltoni, O. Mattelaer, and T. Stelzer, *JHEP* **1106** (2011) 128, [arXiv:1106.0522 \[hep-ph\]](#).
- [21] M. Beneke, C. Hellmann, and P. Ruiz-Femenía. In preparation.
- [22] J. F. Gunion and H. E. Haber, *Phys. Rev. D* **67** (2003) 075019 [[hep-ph/0207010](#)].